5-2007

Mathematical Modeling of Reverse Flow Oxidation Catalysts

Barath Raghavan
University of Tennessee - Knoxville

To the Graduate Council:

I am submitting herewith a thesis written by Barath Raghavan entitled "Mathematical Modeling of Reverse Flow Oxidation Catalysts." I have examined the final electronic copy of this thesis for form and content and recommend that it be accepted in partial fulfillment of the requirements for the degree of Master of Science, with a major in Mechanical Engineering.

Ke Nguyen, Major Professor

We have read this thesis and recommend its acceptance:

David K. Irick, Rao V. Arimilli

Accepted for the Council:
Dixie L. Thompson

Vice Provost and Dean of the Graduate School

(Original signatures are on file with official student records.)

To the Graduate Council:

I am submitting herewith a thesis written by Barath Raghavan entitled "Mathematical Modeling of Reverse Flow Oxidation Catalysts." I have examined the final electronic copy of this thesis for form and content and recommend that it be accepted in partial fulfillment of the requirements for the degree of Master of Science, with a major in Mechanical Engineering.

Ke Nguyen

Dr. Ke Nguyen, Major Professor

We have read this thesis
and recommend its acceptance:

David K. Irick

Rao V. Arimilli

Accepted for the Council:

Anne Mayhew

Vice Provost and Dean of the Graduate School

(Original signatures are on file with official student records.)

MATHEMATICAL MODELING OF

REVERSE FLOW OXIDATION CATALYSTS

A

Thesis

Presented for the

Master of Science Degree

The University of Tennessee, Knoxville

Barath Raghavan

May 2007

DEDICATION

To my mom Mallika Raghavan
and my brother Kishore Raghavan
who have sacrificed a lot for my career.

ACKNOWLEDGEMENTS

I would like to thank my advisor, Dr. Ke Nguyen, for giving me the opportunity to widen my horizons though the course of this project. I would also like to thank my graduate committee members, Dr. David Irick and Dr. Rao Arimilli. I would like to express my appreciation to Dr. Jim Conklin of National Transport Research Corporation for spending his valuable time in educating me the basics of simulation. I would like to thank my laboratory colleagues, Vitaly Prikhodko, Scott smith, Ajit Gopinath, Scott Eaton, and Hakyong Kim, for their assistance and camaraderie throughout my project. I would like to thank the U.S. Department of Energy and the Advanced Reciprocating Engine Systems (ARES) program for their financial support and to Dr. Ming Zheng for obtaining funding for this project.

Lastly, I would like to thank my family for their love and guidance throughout the course of my life.

ABSTRACT

A theoretical model and a computer simulation on methane (CH_4) reduction in a simulated natural gas exhaust mixture are performed for a Reverse-Flow Oxidation Catalyst. This theoretical model is to predict the conversion of methane flowing through an oxidation catalyst with periodic reversal of flow direction. The model developed for this purpose is a transient, 1-Dimensional plug flow model with gas phase reactions and surface reactions. The derivation of the model resulted in the mole balance equation and the energy balance equation for the gas phase and the solid phase. The momentum equation for this model is neglected as it is assumed that there is no pressure drop across the catalyst.

A FORTRAN code was developed to simulate the forward flow and the reverse flow of the gas species through the catalyst. This code can have a symmetrical or an asymmetrical switching according to the user. It also gives an option of running the code either in the forward direction or with periodic switching to analyze the effect of switching. With this code, the optimum switching time for the maximum conversion of methane was found. The effect of various parameters such as the length of the catalyst, the concentration of the gas species, pre-exponential term and the activation energy was also analyzed.

The results show that the optimum switching frequency is 25 seconds for all space velocities for a 10 cm long catalyst with 2000 ppm of inlet methane. The increase in the

conversion of methane when compared to the unidirectional flow was found to be 47% at 450^{o}C for a gas hourly space velocity of 50,000 hr^{-1}. It was also found that, at 450^{o}C for a gas hourly space velocity of 50,000 hr^{-1}, the pre-exponential factor and the length of the catalyst had negligible effect on the conversion of methane. The activation energy and the inlet concentration had a significant effect on the methane conversion which is discussed in further chapters. It was also found that symmetric switching had increased solid temperature profile and methane conversion efficiency when compared to the asymmetric switching frequency.

TABLE OF CONTENTS

LIST OF TABLES

TABLE PAGE

LIST OF FIGURES

FIGURE PAGE

LIST OF SYMBOLS

ϕ……..equivalence ratio

a(x)……..……..……catalytic surface area per unit volume, cm^2/cm^3

A…….pre-exponential factor

Av……..…….frontal area of catalyst, cm^2

Al_2O_3…….……alumina

BFR……..…….bench-flow reactor

C……..……carbon atom

^oC……..…….degrees Celsius

cc/min……..cubic centimeters per minute

$C_{g,i}$ ……..concentration of species i in the bulk stream, mole fractions

CH_2……..…….methylene

CH_4……...……methane

CO……..……carbon monoxide

CO_2……...……..carbon dioxide

$C_{p,g}$……...……..specific heat of gas, J/gK

$C_{p,s}$……...……..…..specific heat of solid, J/gK

cpsi……..……..cells per square inch

CRS……..…… ……catalyst reactor section

$C_{s,i}$ ……..concentration of species i in the solid phase, mole fractions

DAC……..……data acquisition system

DC……..……..direct current

D_i……..……Diffusivity of species i in relative mixture, cm^2/s

E_a……..…..activation energy

FID…….flame ionization detector

g/ft^3……grams per cubic foot

GHSV……gas hourly space velocity

h……..heat transfer coefficient, J/cm^2sK

H……..……hydrogen atom

H_2……..……...…….hydrogen molecule

H_2O……..……...…water vapor

hr^{-1}…….……per hour

HTSV……..……..high temperature switching valve

I.D…….…..inner diameter

ICE……..internal combustion engine

k…….rate constant

$k_{m,i}$……...……..mass transfer coefficient, cm/s

kJ/mol…….…….kilojoules per mole

L/min……...liters per minute

N_2……..…nitrogen molecule

NO_x…….……oxides of nitrogen

O……..……...…oxygen atom

O.D…….outer diameter

Pd……..……palladium

PdO……..palladium oxide

$Pd(OH)_2$……palladium hydroxide

ppm……..parts per million

ppsi……..pores per square inch

psi…….pounds per square inch

Pt…….platinum

R_u……..…universal gas constant

Rh…….rhodium

R_h ……Hydraulic radius, cm

ST……..…….switching time

STP……..……..standard temperature and pressure

T……..…..temperature

t…….……time

THC…….……total hydrocarbon

CHAPTER 1

INTRODUCTION

1.1 Emission and emission regulations

All the countries are going through an environmental crisis due to the ever increasing air pollution and green house gases. Automotive emissions are one of the major contributors of air pollution. The common gas species in automotive emissions are hydrocarbons (HC), carbon dioxide (CO_2), carbon monoxide (CO), Oxides of nitrogen (NOx) and sulphur oxide (SOx). Due to the health hazards, lead, carbon monoxide and sulphur oxides are considered to be the most important pollutants. But the factor that goes unnoticed is the effect of green house gases like methane, carbon dioxide and oxides of nitrogen resulting in climatic changes and ozone holes.

1.1.1 History of emission regulations

In the 1950's and the 1960's, the number of vehicles on road was much less compared to present day, the automobile manufacturers were oriented towards engine power and efficiency without much consideration for the exhaust emissions. Realizing the importance of these gases on the effect of global environment, every country developed some kind of emission regulations and standards. The USA developed the US – EPA regulations while the European countries developed the EURO regulations because of the difference in their driving patterns. These regulations have become more stringent every year which makes the automobile designers to come up with new ideas to meet them.

The United States had the first emission standards and regulations in 1970. The first regulation had standards fixed for carbon monoxide, volatile organic compounds and oxides of nitrogen. It was to be effective from 1975, giving 5 years for the manufacturers to design and develop new emission control systems to keep up with this standard. These standards were mostly met with mere engine modifications. NOx was set at 3.1 grams/mile (gpm) and the total hydrocarbons (THC) were fixed at 5.5 gpm. The regulations became stringent in 1977 when NOx was set at 2.0 gpm and became more stringent in 1981 when the standard was set at 1.0 gpm. The THC was set to 1.2 gpm in 1981 and 0.25gpm in 1988. Light trucks and heavy duty trucks were also brought into standards in that year. In 1990, the NOx emission standards were set at 0.6 gpm, which is 40% more stringent than the previous regulations. In 1977, the THC was divided into 2 categories, namely total hydrocarbons and non-methane hydrocarbons. The THC was set to 0.25 gpm and the non-methane hydrocarbon was set to 0.16 gpm.

In 1999, the voluntary agreement for cleaner cars was started which was also called tier 1 standards. The NOx levels were set to 0.5 gpm, and by 2001 at 0.3 gpm. The standards in 2004 was called tier 2 and the NOx levels were set to 0.07 gpm. The average sulphur levers were also set to 30 ppm. Similar stringent standards have been set for carbon monoxide and particulate matter too. As of now methane does not have any standards set, but increasing use of natural gas and considering the greenhouse effect, it is expected to be included in the regulations very soon.

1.2 Lean burn natural gas engines

With stringent regulations, emission control has become very dramatic in present day automotive engine designs. Catalytic converters, fuel injection and engine controls have been rated in the top 100 significant developments in automotive industry in the past century. Due to the regulations and oil crisis, automotive companies have come up with various ideas like alternate fuels, hybrid vehicles, engine exhaust after treatment and much more. Of the alternate fuels, natural gas, being a cleaner fuel is one of the most commonly used fuels because of its abundance. Natural gas primarily consists of methane with a high octane number. It has less carbon in it when compared to gasoline resulting in reduced carbon monoxide and carbon dioxide emissions.

Although the carbon dioxide concentrations in the exhaust emissions in the lean burn engines are much lower when compared to other fuels, natural gas composes of 70 – 80% methane which is also a green house gas. Methane found in the exhaust emissions is around 5 – 10%. The disadvantage of this is, methane by mass is 15 – 25 times green house effect as compared to carbon dioxide [1]. Methane also has an adverse effect on human health. Though methane has not yet been proved cancerous, it causes dizziness, headache and breathing problems. In United States, present emission regulations do not regulate methane even though they regulate other hydrocarbons. On the other hand, European countries and Asian countries regulate methane emissions.

Natural gas engines are commanding more attention these days as they are preferred in industries for onsite power production because of the increased efficiency and are more environment friendly. Lean burn natural gas engines are a direct result of the above requirement where the engines use an air-fuel (AF) ratio with much more higher than that of stoichiometric mixture. Lean burn natural gas engines also have a high compression ratio with a low engine knock tendency due to the higher octane rating. The increased availability of air also reduces the amount of harmful CO present in the exhaust stream.

The drawback of natural gas engines is the presence of methane in the exhaust stream since methane is a very stable hydrocarbon with a strong C-H bond (bond energy of 414 J/mol).

1.3 Oxidation catalysts

The exhaust gas temperature is not sufficient enough to break down the C-H bond for the oxidation of methane at low temperatures for gas phase reactions, i.e. during idling and cruising. The exhaust gases have to be heated to higher temperatures for this oxidation to take place. In many cases preheating the exhaust gas to elevated temperatures is not a viable option. Catalytic converter with an oxidation catalyst is used in the downstream of exhaust gas to aid the oxidation of methane. The catalyst contains noble metal like platinum, palladium and rhodium. Palladium-based catalysts exhibit the greatest activity for oxidation of methane. The oxidation of methane leads to the formation of carbon dioxide, a relatively less harmful green house gas and water vapor. However, the temperature required for the catalyst

activity is also quite high and the present day research involves in reducing the temperature of the catalyst with an increased conversion. Some research includes either preheating the catalyst with supplement fuel or electrically heating the catalyst.

1.4 Reverse flow oxidation catalyst

The purpose of this research is to explore one such method in increasing methane conversions using a reverse flow oxidation catalyst. In a reverse flow catalyst, there is no fixed inlet side and outlet side. The inlet is periodically switched between the two sides of the catalyst. Thermal energy generated in a well insulated catalyst is often lost to the outlet stream. Reverse flow is a forced unsteady process of retaining this thermal energy of the inlet gas stream by the catalyst. Energy due to the exothermic reactions on the catalyst surface and the hot exhaust gases are captured and utilized by reverse flow. This allows the catalyst surface to maintain a higher temperature profile over its length in comparison to the unidirectional flow resulting in an increased methane conversion.

1.5 Theoretical model and computer simulation

Flow through a catalyst can be modeled in different ways depending on the considerations and assumptions. A modeling can be done by considering the changes in the physical properties along one, two or three spatial dimensions. This mainly depends on the symmetry of the object to be modeled. A simple model can be obtained by modeling in a single spatial dimension; where as complicated models require two or three dimensions. The present study considers a 1-dimensional model

with plug flow behavior. This model has mole balance equation and energy balance equation for both the gas phase and the solid phase.

Computer modeling and simulation can give a valuable insight of the performance of a process. In many situations, a computer modeling can be done more quickly and economical than the actual experiment. A lot of parameters for the actual design of the experiment can be obtained from the simulation since it is not feasible to vary all the physical properties to obtain the optimum design. This might make the experiment costly and waste of time. All these problems can be overcome by a computer simulation.

A computer simulation program using FORTRAN is developed to analyze the flow of the exhaust gas through a reverse flow oxidation catalyst. The effect of reverse flow on the conversion of methane and the optimum switching frequency are identified. The effect of various input parameters such as gas temperature, gas hourly space velocity, gas species concentration, length of the catalyst and the kinetics of reaction are studied. The effect of asymmetric switching (where the time period for the forward flow and the reverse flow are different) was also studied for the temperature profile and methane conversion efficiencies.

CHAPTER 2

LITERATURE REVIEW

Reverse flow reactor has been extensively investigated. It was patented in 1938 by Cottrell. But only few research studies have been carried out on reverse flow oxidation catalysts for lean burn natural gas engines. In this chapter, findings by other researchers on topics related to reverse flow oxidation catalyst modeling and simulation are shown. This chapter also shows the green house effect of the automotive exhaust emissions, lean-burn natural gas engines, oxidation catalysts, concept of reverse flow, reaction mechanisms, theoretical and computer simulation of the model.

2.1 Natural Gas as a Fuel

Climate change induced by global warming is a major issue in the world today. It has been suggested that excessive levels of greenhouse gases in the atmosphere contribute to global warming via greenhouse effect. The main greenhouse gases of concern with respect to lean burn engines include carbon dioxide, methane and other hydrocarbons, and oxides of nitrogen. Hydrocarbon emissions are a direct result of incomplete combustions. This may be either due to partial oxidation or no oxidation of hydrocarbons. Air contains 78% nitrogen and in lean engines where availability of air is in excess, NOx tends to form at higher temperatures. NOx mainly contains nitrogen oxide (NO) with traces of nitrogen dioxide (NO_2). NOx is a green house gas and also

aids in the formation of photochemical smog [1]. Carbon monoxide is also a result of incomplete combustion. When an engine is run fuel-rich, the level of carbon monoxide in the exhaust gases is high. Carbon monoxide is a very harmful pollutant. Apart from being a green house gas, CO is poisonous and causes death at high concentrations. However, CO is not a major concern for lean burn engines due to the excessive amounts of oxygen present.

Greenhouse gases are generally represented in terms of equivalent carbon dioxide emissions and methane has a global warming potential 23 times that of carbon dioxide [2]. The complete combustion of methane produced an equivalent amount of carbon dioxide. But when compared to other fuels, equal volume of methane produces 10 times lesser amount of carbon dioxide. Natural gas consists of 85 – 90% methane and it is the cleanest burning alternative fuel available today. Is has been used in a wide variety of applications ranging from producing electricity to heating houses, industrial engines and automotive engines. In addition to being a cleaner fuel, its abundance makes it more enticing. When natural gas is burnt, it produces far less amounts of CO_2 and NOx when compared to other standard fuels like gasoline [3]. It does not produce any sulphur, particulate matter or solid waste as in oil or coal. The oxidation of methane is expressed by the following chemical equation

$$CH_4 + 2\ O_2 \rightarrow CO_2 + H_2O + 819\ kJ/kmol \qquad (2.1)$$

The oxidation of methane produces enormous energy and is also more economic. Thus in the 1980's and the 1990's, industries started using natural gas for power

production [3]. The downside of using natural gas is the unburned methane found in the exhaust of natural gas engines. As mentioned before, natural gas being a more harmful green house gas when compared to CO_2 restricts its usage.

2.2 Lean-Burn Natural Gas Engines

As seen in the earlier section, natural gas emits increased levels of green house gases when compared to the gasoline engines. A number of ways have been employed to reduce the amount of methane from natural gas engines. Natural gas has a wide flammability range allowing it to work at relatively low equivalence ratio. Equivalence ratio is the ratio between actual fuel/air ratio to the stoichiometric fuel/air ratio. Figures 2.1 and 2.2 show the emission levels of hydrocarbons and carbon monoxide of a spark ignition engine as a function of equivalence ratio, respectively.

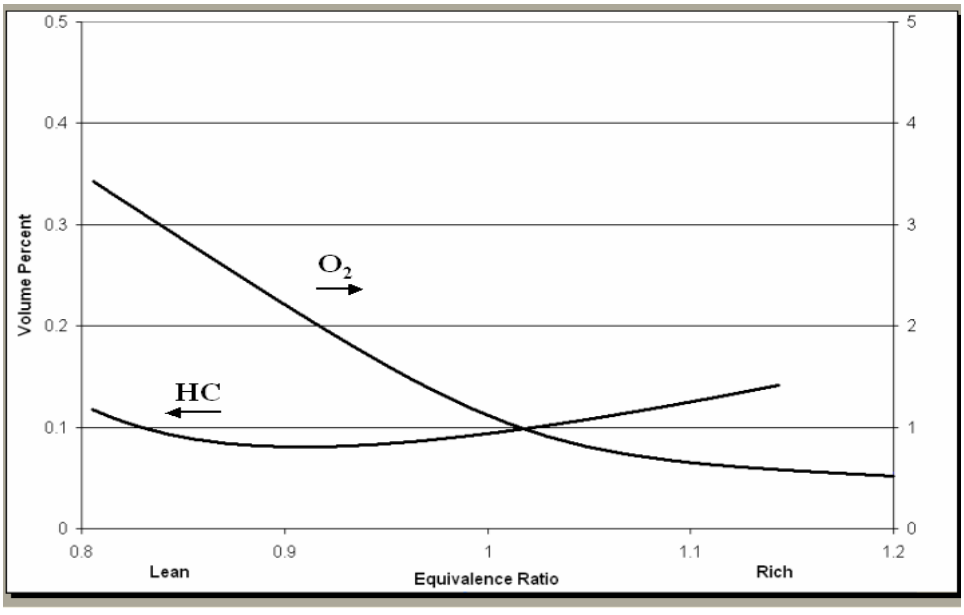

Figure 2.1. HC emission in SI engine as a function of equivalence ratio [1].

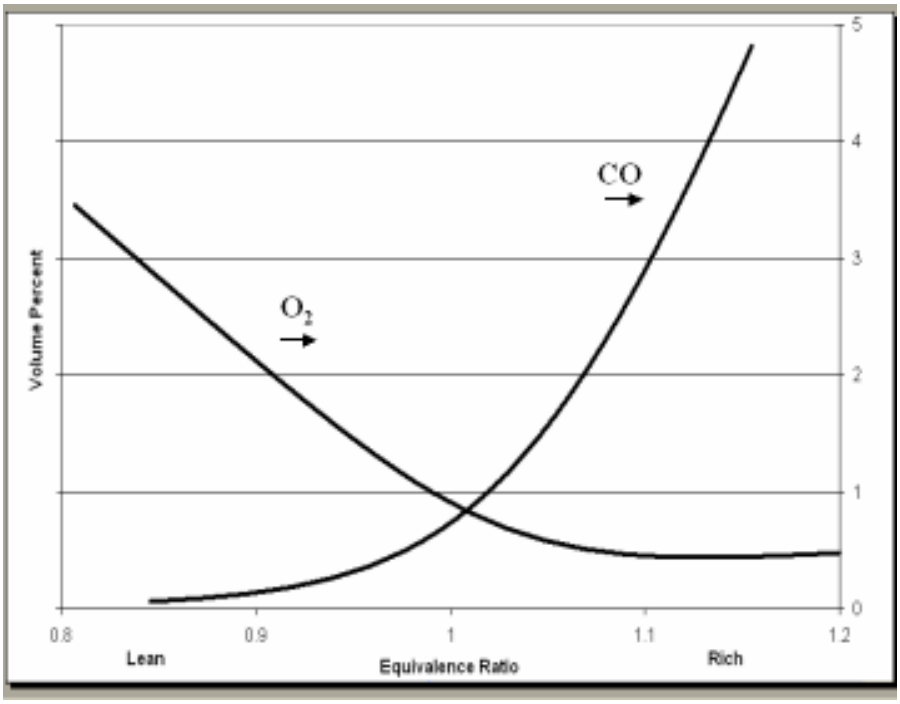

Figure 2.2. CO emission in a SI engine as a Function of equivalence ratio [1].

The above figures show that the emission levels of HC and CO strongly depend on the equivalence ratio [1]. When an engine is run in the lean condition, more oxygen is available for both HC and CO for oxidation process [4]. Thus, lean-burn natural gas engines contain relatively lower amounts of CO in the exhaust when compared to stoichiometric engines.

2.3 Methods of reducing methane emissions

Even in the lean-burn natural gas engines, the amount of methane in the exhaust stream is considerable. Thus different after treatment methods are used to reduce the amount of methane entering the atmosphere due to exhaust emissions.

2.3.1 Catalytic reduction of methane

Catalytic combustion is an environmentally friendly alternative to a conventional thermal combustion. In a catalytic combustion, the role of a catalyst is to assist the combustion of lean premixed fuel by increasing the temperatures high enough by preheating the gas to allow the reaction mixture to proceed to a complete combustion [5]. Catalytic combustion is a good alternative for the gas phase combustion. The catalytic combustion has a lower activation energy involved in the surface reactions. It has the ability to occur outside gas flammability limits of the fuel. This reduces the ignition temperature offering a wide range of fuel – air equivalence ratios and increased stability of operation. The lower temperature achieved prevent the formation of NOx to a great extent and also leads to the oxidation of CO and CH_4 by catalytic reaction [6]. The catalytic combustion is predominantly considered to work in a temperature range of 300 – 700 ^{o}C. Most of the catalysts has the best performance at a temperature around 400 ^{o}C [7]. Oxidation reactions are defined as chemical reactions in which compounds combine with oxygen to produce products. Combustion reactions are divided into two main types of reactions, complete and partial oxidation reactions. The intent of the complete oxidation reaction is to produce carbon dioxide and water, while the partial oxidation reaction produces intermediate compounds, such as carbon monoxide, which can be further oxidized to form carbon dioxide.

$$CH_4 + 2O_2 \rightarrow CO_2 + 2H_2O \qquad (2.2)$$

$$CH_4 + {}^{3}/_{2}\, O_2 \rightarrow CO + 2H_2O \qquad (2.3)$$

Examples of complete and partial oxidation reactions are shown in Equations 2.2 and 2.3. Furthermore, the remarkably strong C–H bond of the methane molecule makes CH_4 one of the most stable hydrocarbons and very resistant to dissociation. Due to the large energy barrier for the dissociation of methane (435 kJ/mol) a catalyst will be used to aid in the cracking of CH_4. The C-H bond in methane is very strong and hence very high temperatures are needed for the oxidation of methane. One way of overcoming this is to have a catalyst that aids the oxidation. One of the most effective abatement methods is the three-way catalyst. The three-way catalyst contains noble metals such as platinum (Pt) and rhodium (Rh). The results of the experiments using a three-way catalyst show considerable reduction of HC and CO. Figure 2.3 shows the conversion of a Pt-Rh three-way catalyst with an inlet temperature of 400^{o}C as a function of equivalence ratio for a compressed natural gas engine.

The subject of materials demonstrating high catalytic activity for methane is an extensively researched topic. Noble metals and metal-oxides have been shown to have a high affinity for dissociating methane. Generally the catalyst has an active noble metal such as platinum or palladium in a support like Al_2O_3. Palladium has been commonly employed as the most active catalyst for methane combustion. The sequence of the catalytic activity for methane oxidation has been reported as Pd > Rh > Pt [8].

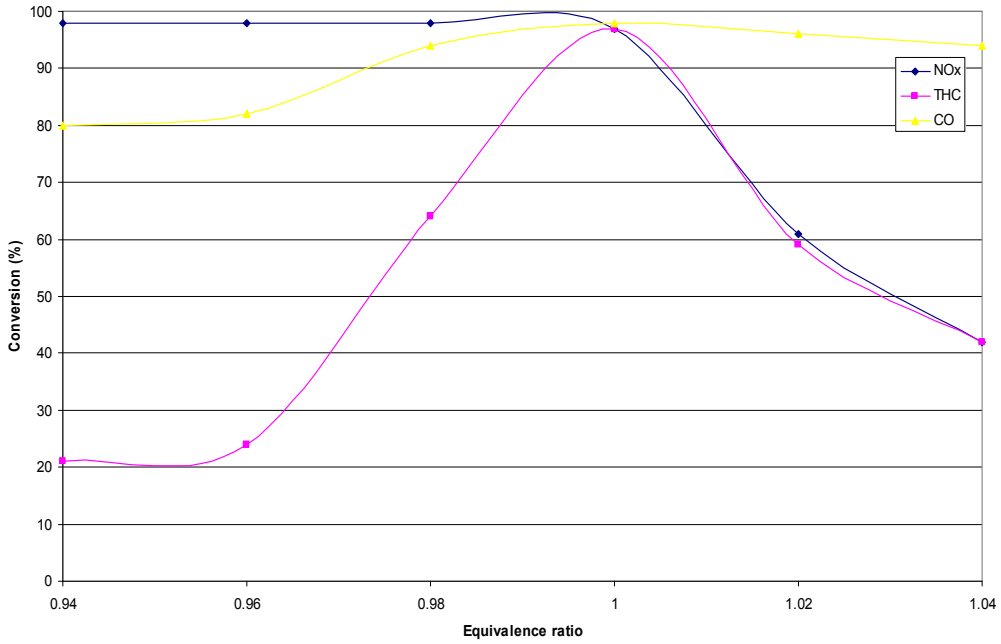

Figure 2.3. HC and CO conversion efficiency as a function of equivalence ratio for a Pt-Rh based three-way catalyst at an inlet temperature of 400^{o}C.

Lean-burn natural gas engines do not provide a good conversion efficiency even using catalysts because of their low exhaust temperature which is not sufficient for the oxidation of methane.

2.4 Reverse flow oxidation catalyst

It is very important to have a higher catalyst temperature in order to have a maximized conversion. Lots of methods have been proposed to increase the surface temperature. One such method is the flow reversal scheme where the direction of flow of the exhaust gas through the catalyst is altered at a predefined frequency. Periodic reversal of the direction of flow is an elegant way of combining the functions of heat transfer unit and catalytic reactor in one apparatus by using the thermal

storage capacity of the catalyst for regenerative heat transfer [10]. Thus reversing the flow has been shown as an effective method of increasing the catalyst temperature.

As shown in figure 2.4, the reversal of the flow is controlled by valves 1, 2, 3 and 4. When valves 1 and 4 are open and valves 2 and 3 are closed, the exhaust gas flows in the forward direction as marked by the arrows. When the flow is reversed, valves 2 and 3 are opened simultaneously with valves 1 and 4 closed. This causes a reversal in the flow direction.

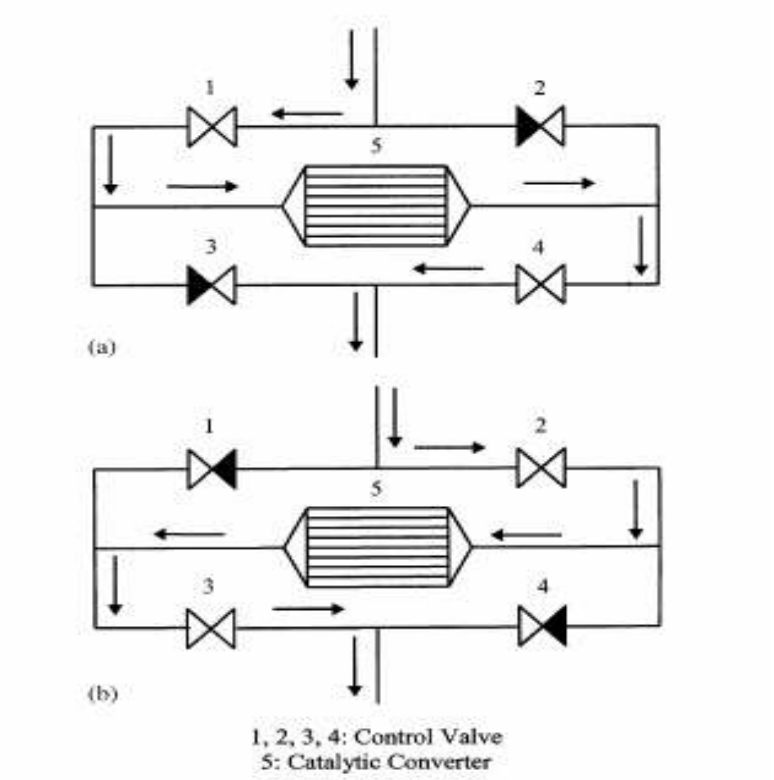

Figure 2.4. Schematic of a reverse flow reactor

The switching time is the time after which the flow is changed from forward to reverse, and vice versa. There are two different kinds of switching, namely the symmetric and the asymmetric switching. When the forward flow time is the same as the reverse flow time, it is called symmetric switching. If the two flow modes have different switching time, it is called asymmetric switching. For maximum performance, it is important to identify the optimum switching frequency. Figure 2.5 shows a typical catalyst surface temperature profile along the length of the catalyst. The green line in the graph represents the temperature profile for a unidirectional flow. The red and the orange lines indicate the temperature profile along the length of the catalyst for a reverse flow. It is seen that the temperature for a reverse flow is much higher than that of a unidirectional flow [11].

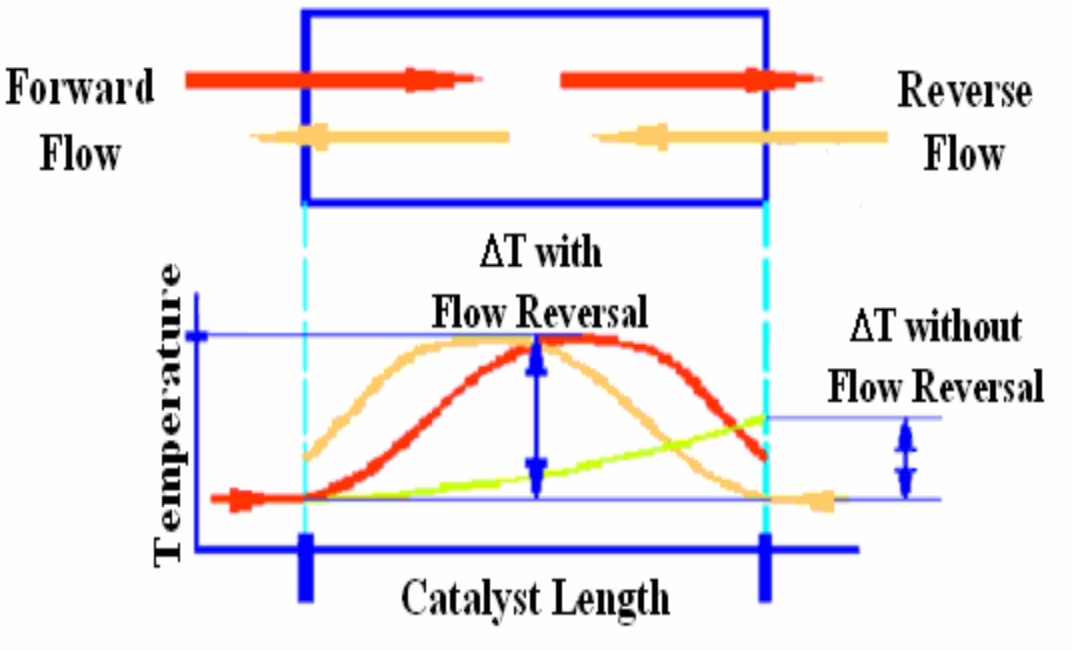

Figure 2.5. Temperature profile along the length of the catalyst for reverse flow

The reverse flow catalytic converter exhibits what is called a heat trap effect. The temperature profile for a standard unidirectional exothermic reaction is depicted in the figure 2.6. The shape of the curve is governed by its operating conditions, mainly the inlet temperature. For a lower inlet temperature the peak migrates towards the exit and for a higher inlet temperature the peak migrates towards the inlet. For a profile shown in Figures 2.6 a and b, the flow reversal can be implemented to increase the effectiveness of the catalytic converter. When the flow is reversed, the high temperature from the previous cycle can be used to preheat the feed exhaust stream to achieve higher temperature profile than the adiabatic temperature rise of the inlet exhaust stream at a relatively lower temperature. This effect is termed as heat sink [12]. Lie et. al.[11] called the same effect as heat trap. Hanamura et. al. found the effect of flow reversal on the catalyst temperature to be 13 times higher than the adiabatic temperature rise [13].

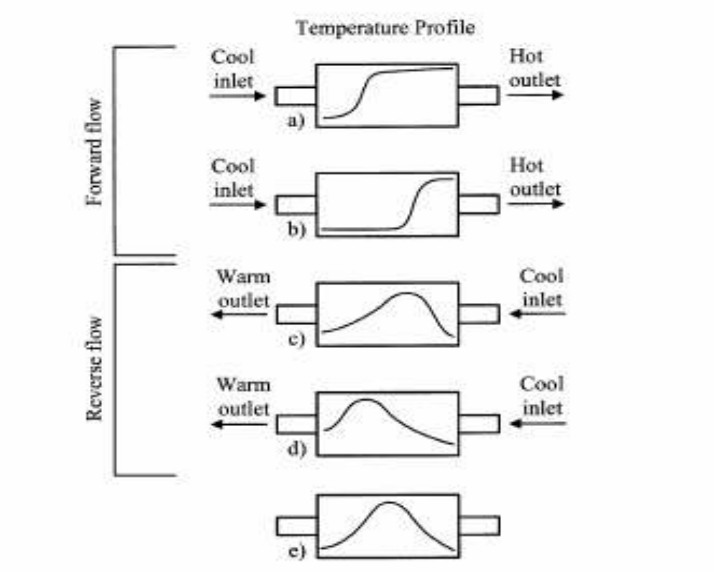

Figure 2.6. Temperature profiles at various stages in a reverse flow reactor [12]

2.5 Reaction mechanism in an oxidation catalyst

A catalyst provides an alternative pathway for a chemical reaction with lower activation energy, thereby increasing the rate of reaction for a particular species. Cullis and Willat studied the oxidation of CH_4 over palladium (Pd) in a pulse flow micro-reactor over a temperature range of 500 to 800 K and presented a proposed mechanism of the oxidation of methane over a palladium catalyst, shown in Figure 2.7 [14]. In figure 2.8 the proposed mechanism consists of the dissociation of CH_4 and the formation of new bonds with the active catalytic surface sites of palladium oxide (PdO). In addition O2 dissociates and bonds to an adjacent active PdO site. The methylene radical (CH_2) and oxygen atom (O) react with one another to form CO_2 and H_2O, for complete oxidization. H_2 from the dissociation of CH_4 reacts with O to form H_2O. However, the mechanisms for catalytic oxidation are very complex, and this proposed explanation is one possibility for the dissociation of methane over a palladium based catalyst.

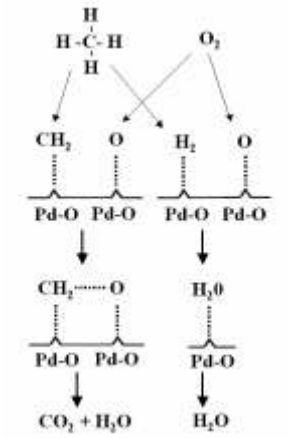

Figure 2.7. An outline mechanism of the oxidation of methane over a Pd catalyst.

The other proposed mechanism is the oxidation of methane on Pd site instead of PdO, which implies that metallic Pd is the active material. Zhu et. al. [15] conducted simulation and experimental studies for a periodic reverse flow oxidation catalyst reactor. They considered metallic Pd to be the active site and not PdO. The result from the model, Figure 2.8 shows that the surface temperatures were in close accordance to the experimental values. The mechanism used in this model, that the active material is metallic Pd seems to be acceptable [6].

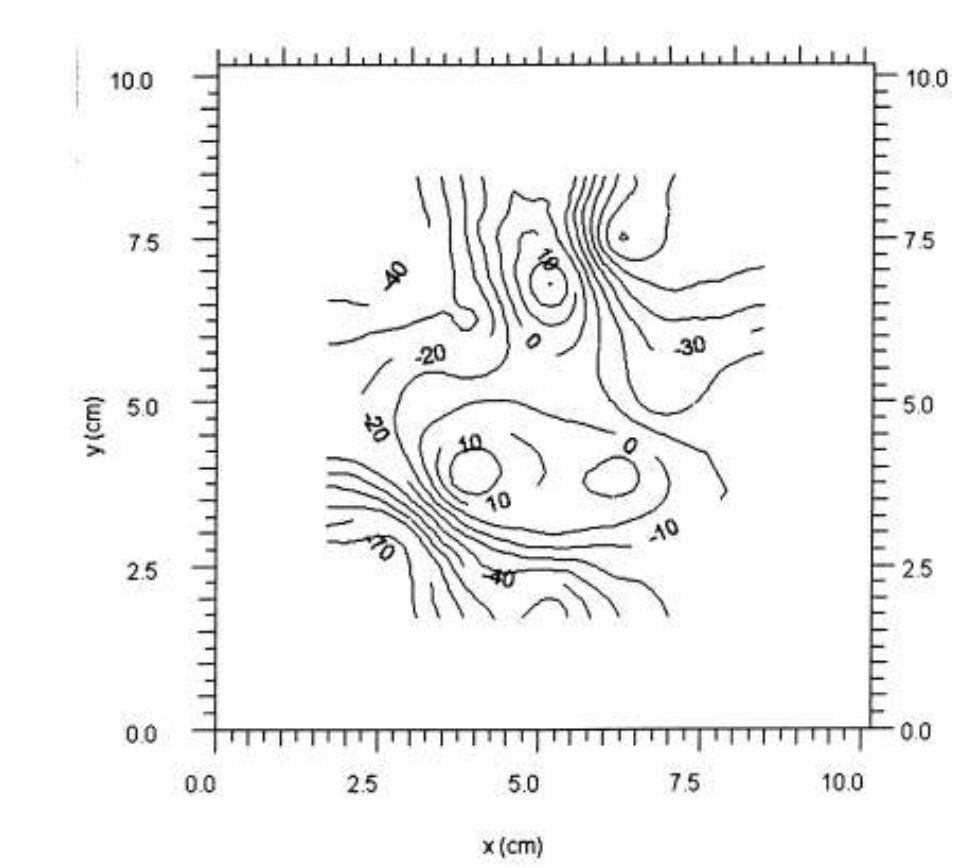

Figure 2.8. Difference between experimental temperature and modeling surface temperatures of a Pd catalyst with a flow rate of 40l/min.

2.6 Theoretical modeling

Modeling and simulation of a heterogeneous system requires the coupling of reactive flow with a gas – surface interaction. Catalytic combustion is a rapid transition from the kinetic controlled phase to the mass transfer controlled phase. Thus it is important to consider the complex interaction and the transport properties in the gas phase and the surface. The mathematical models are based on the numerical solution of the governing equations, considering the geometry of the problem [15].

The governing equations of an oxidation catalyst monolith mainly consist of the energy and the mass balance equations. The momentum equation need not be solved as it is assumed no pressure variation across the length of the catalyst. This further simplifies the modeling. Since catalyst mainly involves surface reactions it is important for us to consider these governing equations in both the gas phase and the surface [14].

There are a number of assumptions on which the model is built. This is mainly to simplify the complexity of the problem. These assumptions have negligible effect on the solution of the problem. When the simulation of a monolith reactor is done, it is based on the assumption that all the channels behave in a similar way, and hence it is enough if one of the channels is modeled. Hence it lies on a basic assumption that every channel is a representative of the entire honeycomb. The solution when compared between a two – dimensional model and a one dimensional model shows that there are not much difference, hence it is acceptable to assume that the model is

one dimensional which simplifies the model by a significant level [14]. Hayes et. al. [16] used a plug flow model, with a constant Nusselts number and Sherwood number over the entire length of the catalyst. They had a one dimensional model with values of Nusselts and Sherwood number for a non reacting fully-developed flow with constant physical properties. For the simplicity of the numerical simulations these numbers do not take into effect the entrance effect. The study also shows that there is negligible change when the entrance effect is considered though it increases the complexity of the problem manifold. The Nusselts and Sherwood numbers also show a perturbation when the light-off temperature (the temperature at which there is at least 50% conversion) is reached, but assuming a constant value is an acceptable solution to make the problem simpler [16].

Most of the previous reported modeling work follows a standard set of assumptions. When modeling a multi-channel monolith reactor, it is sufficient to simulate the flow in a single channel; it is assumed that there is no interaction between channels (Prasad 1984). The Nusselts number and the Sherwood number are the same throughout the entire length of the channel. A non-reacting fully-developed flow with constant physical properties is used to find the values of Nu and Sh (Heck and Oh). Results of previous study show that radiation does not have much effect because of the relatively low temperatures and hence conduction alone is considered in the solid phase. Hurtado et al. [18] proposed that the gas phase can be considered to be in a pseudo-steady state with the wall temperature because of the difference in their heat capacities and their high space velocities. Some of the researchers (Cullis et al., [19])

tend to consider the entrance effect and used different correlations for the Nusselts number and the Sherwood number, but these were more appropriate for gas turbines rather than automobile exhaust. Moreover they also found that the values of Nu and Sh have more impact when considering a two-dimensional model as we had radial deviations too. The effect of radiation is much more pronounced during the light-off point and might have a significant impact on the energy equation. But the addition of radiation further complicates the model and generally not considered in simple models.

The modeling of the flow of exhaust gas is based on the governing equations. To generate a model for a single channel of a multi-channel monolith reactor requires the catalyst to have a uniform flow distribution of exhaust gas across all channels, uniform catalyst distribution of active sites and an adiabatic system with no radiation. A simple 1-D model considers 4 basic equations, the mass balance equation and the energy balance equation for both the solid phase and the gas phase. The boundary conditions for the flow are symmetry, no slip at wall, flat velocity profile at inlet and zero normal shear stress at exit. The gas phase reactions may be neglected because of the gas temperatures considered and the short residence time [17].

One of the main objectives of the modeling and the simulation is to find the effect of reversing the flow. It is important to know the effect of the frequency of switching. Zufle et. al. [10] from their experimental results show that both the period of duration or the volumetric flow have a significant impact on the temperature profile. They also

show that an increasing reactant concentration causes an increase in the maximum temperature reached by the surface of the catalyst [10]. To do a computer simulation of the theoretical model, it is important to know the kinetics of the oxidation of methane over palladium. It is necessary to know the global reaction rate and the pre-exponential term and the specific rate constants. It is assumed in literature that a pseudo first order kinetic model provides a good fit for the kinetics of methane oxidation. Mechanistic models are preferred as they take account of the real phenomena that are considered to take place on the catalyst surface. The effect of partial pressure of methane oxygen and water can be effectively modeled using the Mars-Van Krevelen mechanism that considers the slow desorption of the reaction products. This model can also be used to find the inhibition effect of water vapor on the oxidation of methane [18]. The effect of Pt and Pd loading on the oxidation of methane were investigated by Cullis et. al. [19]. The oxidation rate of methane increased with increase in precious metals for conversions less than 10%, which is the kinetic-controlled regime. Though there was an increase in the oxidation of methane with increasing precious metals like Pt and Pd, the activity per unit area of the metal surface decreased with increase in loading [19].

The reaction order of methane was found approximately equal to 1. There was no effect oxygen on the reaction as oxygen concentration was very high when compared in lean-burn engines. Since water is produced during the oxidation of methane, it is important to know the effect of water on the global reaction rate. Water vapor has an inhibition effect and the order is found to be close to -1, whereas CO_2 has an order

close to – 1.3 [20]. For catalytic oxidation of methane over palladium, the activation energy varied from 139 kJ/mol at temperature less than 290 ^{o}C to 39 kJ/mol at temperatures above 290 ^{o}C. The rate of methane oxidation over Pd was found to be 0.45-0.8 order in CH_4 concentration and almost independent of oxygen, with an apparent activation energy of 71-100 kJ/mol. The kinetics of the catalytic oxidation is considered to be important only in the initial stages of the oxidation of methane. Once the process reaches a later state, it is mainly controlled by the heat and the mass transfer. The reaction on the catalyst surface is controlled by the intrinsic mass transfer limitation when the reaction rate is faster than the rate of reactant transported from the bulk stream to the catalytic surface. The reaction rate then becomes quite insensitive, which means an increase in the temperature has negligible effects on the catalytic activity [21].

Farrauto et. al. [22] examined the combustion of methane over Al_2O_3 supported PdO catalyst and reported a large hysteris between the heating cycle and the cooling cycle. They conducted experiments over a wide range of temperatures to find the decomposition of PdO and the reoxidation of Pd using gravimetric techniques. They also showed the higher activity of PdO at temperatures below 900 ^{o}C than Pd using high temperature X-ray diffraction methods. Their results clearly show the catalytic activity declined on the onset of transition from PdO to Pd [22].The kinetic results show that at temperatures below 750 ^{o}C, PdO is more active as compared to Pd metal, which, is in contrast for temperatures above 750 ^{o}C [23]. The mechanism of methane

oxidation over palladium has been in debate and the most acceptable one is the one mentioned above.

Many researchers have come up with different reaction mechanisms. In the case of Pt researchers have confirmed that the metallic pt is the active site where as in the case of a pd-based catalyst, there is no confirmed mechanism. Some researchers consider active Pd site to be the active material where as others consider the PdO as the active material at temperatures higher than 400^{o}C [8]. F. Moallemi et. al. [6] conducted experiments and modeling study on palladium and platinum-based catalyst monoliths used in methane combustors for heating purpose. In this modeling, they used metallic Pd as the active material for the oxidation of CO and CH_4. The reason for the researchers to use this method is that, in their study high temperatures of the order of 800 – 1000K is obtained. At these temperatures, the PdO formed is reverted back to Pd.

One more reason is the lack of availability of kinetic data for adsorption, oxidation and desorption of CO and methane over the PdO site. The third reason is that, even if PdO exists, its activity can be considered negligible when compared to the participation of active metallic Pd.

The activation energy for methane over a palladium catalyst was between 160 and 186 kJ/kmol. Liu et. al. [13] conducted experimental studies of a reverse flow catalytic reactor for natural gas. They used a 7mm internal diameter and 310 mm long

stainless steel reactor to find the kinetics of methane over palladium. The reactor was filled with 1g of crushed catalyst with an average particle size of 30μm. The methane mole fraction was kept at 3%, the flow rate was varied from 2.33 – 6 cm^3 /s and the temperature was varied from 250 to 500°C. Figure 2.9 below shows the conversion of CHG_4 at different temperatures. From the graph the authors found the activation energy of 92 kJ/ mol and a pre-exponential factor of 0.198 x 10^9 s^{-1}. The points show the experimental values and the lines from theoretical calculations [19].

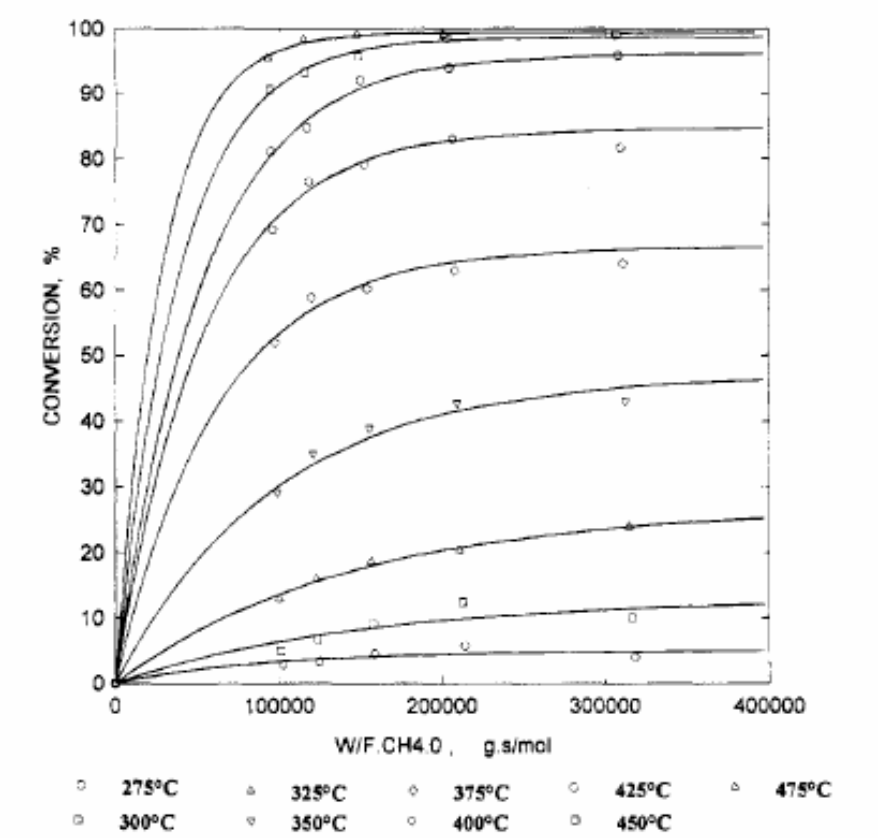

Figure 2.9. Conversion efficiency of methane over Pd/Al_2O_3 catalyst as a function of contact time [19].

C.R.F.Lund et. al. [20] from the State University of New York came up with the following reaction orders for the different components involved in the reactions. The reaction orders are given below in Table 2.1.

This table indicates that the concentration of oxygen does not affect the reaction as it is present in excessive amounts. Water vapor has an inhibition effect and carbon dioxide does not have any effect on the reaction at low concentrations [12]. Experimental work was done to find the effects of water vapor on the conversion of methane. Experiments on the Zirconia-supported and alumina-supported palladium catalyst with a dry feed and a wet feed of 3.4% water vapor were conducted [12]. The authors found similar effects on both the catalyst types.

Table 2.1 Reaction order of the components of natural gas exhaust stream

Component	Reaction Order
CH_4	1
O_2	0
H_2O	-1
CO_2	0 at low conc. -2 at high conc.

2.7 Computer simulation

Simulations have been done with a wide variety of softwares depending on the model. Some of the most common softwares are FEMlab, Matlab, Chemkin, CFDflow, Fortran etc. [17]. When the governing equations do not fall under a standard category, some of the standard softwares cannot be used. Fortran is a programming language used for mathematical purposes. It stands for formula translator. Fortran can handle a wide variety of mathematical operations very precisely. The governing equations are in the form of partial differential equations. It is first converted to ordinary differential equation and a standard solver is used to solve the equations. LSODE stands for Livermore Solver for Ordinary Differential Equations; it is a standard solver available in the ODEPACK that is available in the internet. This solver is used to solve the non linear ordinary differential equation.

A catalyst is divided into a number of sections and a forward progression method is used. The inlet temperatures and concentrations are known. The governing equations are solved at this point and the output is the condition at step 1. This now becomes the input condition for step 2 and thus the results are progressed till the exit of the catalyst. LSODE function uses adaptive numerical methods to a system of ordinary differential equation for one time step. Thus LSODE makes it a transient simulation program [24]. The input conditions include the concentration, gas and solid temperature, all physical properties of the catalyst like cell density, porosity and length. It also includes the subroutines to incorporate the reverse flow which will be discussed in appendix.

CHAPTER 3

THEORETICAL MODEL AND COMPUTER SIMULATION

3.1 Theoretical model

A theoretical model or a mathematical model is a system of equations which describe the relationship among the physical and chemical variables governing the behavior of the process. A theoretical model has a number of equations depending on the complexity of the model. The equations for catalytic combustion in general are the mass balance, the momentum and the energy balance equations. Since catalytic combustion is a transient process, these equations are mostly partial differential equations dependant on time, surface temperature and concentration. These governing equations have a set of input variables which mostly involve the inlet species concentration, the initial temperature and the physical constraints involved. There are different types of modeling with a wide range of criteria. It is necessary to identify the correct modeling conditions to get a close representation of the actual model.

3.2 Modeling criteria

In the present study, a theoretical model for the flow of exhaust gases through an oxidation catalyst is developed. The accuracy of the model depends on the considerations and the assumptions made. A complex model will be more accurate than a simplistic model, but if the difference is negligible or not considerable, a

simplistic model can be used, which saves both time and effort. The considerations for the developed model are stated below:

3.2.1 Phenomenological model

A modeling can be basically classified into empirical model and phenomenological model. An empirical model is a model developed based on experimental results. They mainly rely on the goodness of fit for the outcome of these models. Arbitrary equations are developed using the experimental values to get equations that are used to determine the outcome with in the experimental range. The main disadvantage of this method is the tendency to extrapolate outside the experimental range which often might not be the expected result. This kind of model is mainly for economic analysis where the past records are used to determine a forecast model for the future.

For a scientific model, researchers use phenomenological model which involves equations relating to fundamental physio-chemical process. It is possible to derive a theoretical modeling representing the actual process and can be used directly for design purposes without conducting experimental study. In most cases the phenomenological is supported with some experimental values as all the physical properties required for the theoretical model might not be available and experimental results have to be used. This model can be further classified into distributed parameter model and lumped parameter model. In a distributed parameter model, some of the physical properties have spatial property variations. In a lumped model, the physical properties are averaged over the entire spatial co-ordinate [Pulkrabek, 1].

3.2.2 1-Dimensional

Most modeling is done for a 1-dimensional flow owing to its simplicity. A 2-dimensional or a 3-dimensional model gives a closer prediction to the actual value but it complicates the problem manifold. In general a 3-dimensional model gives 98% closer to the actual value as compared to the 1-dimensional model which gives 91% [Pulkrabek, 1]. In the present study, the model involves heat transfer and mass transfer along with exothermic heat generation due to the oxidation of methane. Moreover to make it simpler, it is assumed that there is no variation in the radial direction making it a plug flow reactor; conveniently allow to use a 1-dimensional model. It is therefore a lumped parameter model in the radial and angular direction and a distributed parameter model in the axial direction.

3.2.3 Plug flow model

In a plug-flow model, it is assumed that the diffusion in the axial direction is negligible. The present model is assumed to be a plug flow model. Though no reactor can actually operate under this mode, it is a close enough assumption for modeling purposes. For a plug-flow model, concentration, velocity and temperature gradients exist in the axial direction but not in the radial direction.

3.2.4 Transient model

When the inlet conditions or the conditions inside the catalyst change as a function of time, the model is termed as transient model. In an automotive catalytic converter, in which energy generation mainly due to the surface reactions, the temperature profile

of the gas phase and the solid phase change as a function of time resulting in a transient model. Transient models are more complicated than the steady state models.

3.2.5 Pseudo-homogeneous model

The basic assumption in a pseudo-steady state is that the gas temperature is assumed to be a constant with respect to the solid temperature as the heat capacity of the solid is much more than the heat capacity of the gas. The temperature and the concentration are assumed to be the same as the fluid and the energy producing reactions in this phase are not considered. Thus in this model, it is assumed that there is no gas phase reactions and the governing equations of the gas phase are modeled as a pseudo-homogenous model. For pseudo-homogeneous model the wall temperature and the concentration are assumed to be the same as the fluid, and the reaction rate is incorporated into the conservation equations.

3.2.6 Heterogeneous model

The interface between the gas phase and the solid phase are assumed to be discontinuous and hence there are separate mole balance and energy balance equation for the solid phase. There are coupled to the fluid phase equations with the help of mass transfer coefficients and the heat transfer coefficients. Thus the solid phase in this model is considered to be a heterogeneous model.

3.3 Assumptions made while modeling

The accuracy of any model depends on the assumptions made. Any model that cannot justify its assumptions can be described as a hypothesis which might not be the actual case and which might not represent the actual model. The assumptions made should not have a strong influence on the model developed. The more the assumptions are made, the weaker the model is. Some of the assumptions that are made in modeling the reverse flow oxidation catalyst are listed below:

1. Radial variations of gas phase temperature, concentration and velocity within the individual channels are neglected. These variables are interpreted as cross sectional averages.
2. Negligible temperature gradient in solid phase in the transverse direction.
3. Negligible axial diffusion of mass and heat in gas phase.
4. Number of active sites is a constant.

   It is assumed that through out the process, the number of palladium sites participated in the reaction is a constant. This means that the entire palladium sites on the surface of the catalyst involve in the surface reactions. The deactivation of the active site due to thermal aging or poisoning is neglected.
5. Chemical reactions occur only on the surface of the catalytic surface.

   The model considered is a heterogeneous model and so the gas phase reactions are small and are neglected. Only the surface reactions are considered.

6. There is no pressure drop across the catalyst, and hence the momentum equation can be neglected. This is a very important assumption made as momentum equation is dependant on this assumption. Momentum equation is considered as one of the three important governing equations.
7. Thermo-physical properties are assumed to be a constant. This means that the thermal and the physical properties of the catalyst and the gases do not change during the course of the modeling and simulation.
8. The reactor is perfectly insulated with no heat loss from the inlet and exit sides. Thus the outer surface of the catalyst has no direct contact with the ambience. The radiation from the end surfaces is also neglected because of the relatively low temperature.
9. All channels behave similarly.

   Since all the channels in the catalyst have the same dimensions and properties, it is assumed to behave similarly. Because of this assumption, it is enough to model a single channel of the catalyst and the results can be extended to other channels because of similarity.

3.4 Governing equations

Governing equations define a model. Most models involve with 3 basic conservation equations, namely mass, momentum and energy. The accuracy of the model developed is highly dependent on these equations. The factors to be considered in the equations define the closeness of the theoretical model to the actual results.

3.4.1 Material balance equation

Material balance equation plays a very important role when there is a fluid flowing. In case of a non reacting flow, where the outcome of the model does not depend on the volume or the concentration of the inlet condition, this equation doesn't play a big role. But in catalytic converters, where the amount of flow of the reacting fluid plays a major role, it is important to properly derive the material balance equation or the mass balance equation.

Material balance equation gives an insight of the composition of the species involved and the concentration gradient inside the reactor. Material balance in this model defines the amount of methane available for combustion and thus the conversion efficiency of the catalytic converter. A simple material balance equation is shown below. This equation can also be extended to all other species in the gas flow.

$$\begin{bmatrix} Molar\ flow \\ of\ methane \\ in\ to\ system \end{bmatrix} - \begin{bmatrix} Molar\ flow \\ of\ methane \\ out\ of\ system \end{bmatrix} = \begin{bmatrix} Disappearance \\ of\ methane \\ due\ to\ reaction \end{bmatrix} + \begin{bmatrix} Rate\ of\ accumulation \\ of\ methane\ in\ to\ system \end{bmatrix} \quad (3.1)$$

3.4.2 Momentum balance equation

Momentum balance is important when there is a pressure drop across the system. Whenever there is variation of velocity and pressure profiles, momentum equation comes into play. A simple momentum equation is shown below

$$\begin{bmatrix} Rate\ of \\ momentum \\ in\ to\ the\ system \end{bmatrix} - \begin{bmatrix} Rate\ of \\ momentum \\ out\ of\ system \end{bmatrix} + \begin{bmatrix} Sum\ of\ forces \\ acting\ on\ system \end{bmatrix} = \begin{bmatrix} Rate\ of \\ accumulation\ of \\ momentum\ in\ system \end{bmatrix} \quad (3.2)$$

In this model it is assumed that there is no pressure drop across the catalyst and negligible viscous effect. Hence the momentum equation can be neglected.

3.4.3 Energy balance equation

Energy balance equation is one of the most important equations for any reacting flow. From the energy conservation equation the temperature profile across the catalyst can be obtained. The conversion of methane depends on the rate of the reaction, which in turn depends on the temperature profile. The energy equation gives how much of thermal energy is released for a given composition of inlet gas. A general form of the energy equation is shown below.

$$\begin{bmatrix} Rate\ of\ energy \\ flow\ in\ to\ system \end{bmatrix} - \begin{bmatrix} Rate\ of\ energy \\ flow\ out\ of\ system \end{bmatrix} = \begin{bmatrix} Rate\ of\ accumulation \\ of\ energy\ in\ the\ system \end{bmatrix} \qquad (3.3)$$

3.5 Derivation of governing equations

Thus this model considers the 2 basic equations, the material balance equation and the energy equation for the gas phase and the solid phase. The continuum model approach is used for deriving the governing equations, where the honeycomb structure is replaced with the homogeneous structure containing both the gas phase and the solid phase.

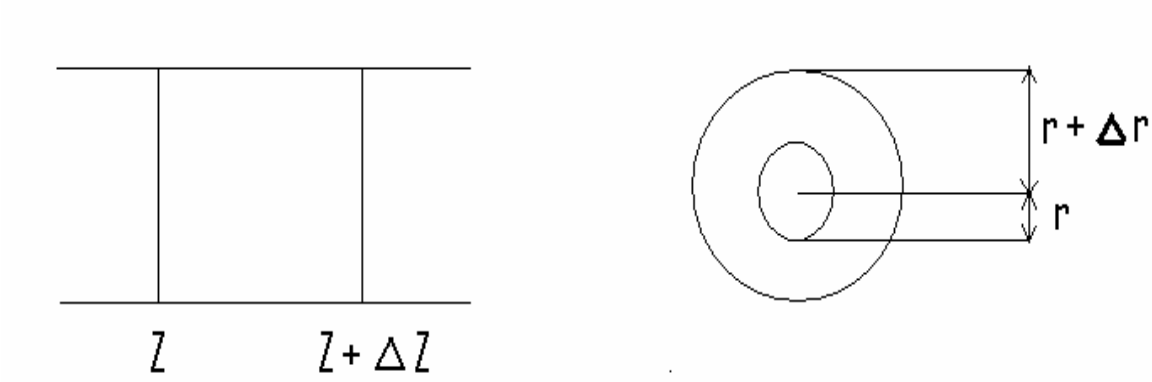

Figure 3.1. Differential control volume and cross sectional view

3.5.1 Mole Balance Equation in gas phase

Consider the differential volume as shown in figure 3.1,

Moles in – Moles out – Moles reacted in – Moles transported = 0

homogenous reaction to catalyst surface

Moles in – Moles out $= (F_A)_Z - (F_A)_{Z+\Delta Z} = -\Delta F_A$ (3.4)

Moles reacted in homogenous reaction = $(-R_A)_H \; \phi \; \Delta V$

Moles transported to the catalytic surface = $k_m \; C_b \left(Y_{A,B} - Y_{A,S}\right) A_S$

Thus the mole balance equation in gas phase becomes

$$-\Delta F_A \quad - \quad (-R_A)_H \; \phi \; \Delta V \quad - \quad k_m \; C_b \left(Y_{A,B} - Y_{A,S}\right) A_S \quad = \quad 0 \qquad (3.5)$$

Dividing the above equation by ΔV, $\Delta V = A_S \text{ X } \Delta Z$, we get

$$\frac{-\Delta F_A}{A_S \Delta Z} \quad - \quad (-R_A)_H \; \phi \quad - \quad k_m \; C_b \left(Y_{A,B} - Y_{A,S}\right) A_V \quad = \quad 0 \qquad (3.6)$$

Hence the mole balance equation becomes

$$-V_M C_{A,B} \frac{dY_{A,B}}{dZ} \quad - \quad \left(-R_A\right)_H \phi \quad - \quad k_m \; C_b \; A_V \left(Y_{A,B} - Y_{A,S}\right) \quad = \quad 0$$

(3.7)

3.5.2 Energy balance equation in gas phase

Energy accumulated in gas phase =

Heat added to gas from surface + Heat generated in gas phase due to reactions

Energy accumulated in gas phase

$$= \overset{o}{m} \; C_P \; \Delta T_{gas} \tag{3.8}$$

$$= \; Q_V \; \rho \; C_P \; \Delta T_{gas} \tag{3.9}$$

Heat added to the gas phase from the surface due to convection

$$= \; h \; A_S \left(T_s - T_{gas}\right) \tag{3.10}$$

Heat generated due to the chemical reactions in the gas phase

$$= \; -\Delta V \; \phi \left(-R_A\right)_H \; \Delta H_R \tag{3.11}$$

Therefore the energy balance in gas phase is

$$Q_V \; \rho \; C_P \; \Delta T_{gas} \quad = \quad h \; A_S \left(T_s - T_{gas}\right) \quad - \quad \Delta V \; \phi \left(-R_A\right)_H \; \Delta H_R \tag{3.12}$$

Dividing the above equation by ΔV

$$\frac{Q_V}{A_S} \rho \; C_P \; \frac{\partial T_{gas}}{\partial Z} \quad = \quad h \; A_V \left(T_s - T_{gas}\right) \quad - \quad \phi \left(-R_A\right)_H \; \Delta H_R \tag{3.13}$$

$$V_S \; \rho \; C_P \; \frac{\partial T_{gas}}{\partial Z} \quad = \quad h \; A_V \left(T_s - T_{gas}\right) \quad - \quad \phi \left(-R_A\right)_H \; \Delta H_R \tag{3.14}$$

A_V = Surface Area / Volume

V_S = Superficial Velocity

Therefore the energy balance equation in gas phase becomes

$$V_S \ \rho \ C_P \ \frac{\partial T_{gas}}{\partial Z} \ = \ h \ A_V \ \left(T_s - T_{gas}\right) \ - \ \phi \left(- R_A\right)_H \ \Delta H_R \tag{3.15}$$

$$h \ A_V \ \left(T_s - T_{gas}\right) \ - \ \phi \left(- R_A\right)_H \ \Delta H_R \ - \ \rho \ C_P \ V_S \ \frac{\partial T_{gas}}{\partial Z} \ = \ 0 \tag{3.16}$$

3.5.3 Mole Balance Equation for Solid Phase

The mole balance equation is obtained by equating the number of moles that is transported to the catalyst surface to the reaction rate.

$$\begin{bmatrix} Moles\ transported\ to \\ catalyst\ surface \end{bmatrix} = \begin{bmatrix} Moles\ reacted\ in \\ catalyst\ reaction \end{bmatrix} \tag{3.17}$$

Moles transported to the catalyst surface

= Mass transfer coefficient* Bulk concentration * Change in action * Incremental volume

$$= k_m \ C_{gas} \ \left(Y_s - Y_{gas}\right) \phi \ \Delta V \tag{3.18}$$

Reaction Rate = $\eta \left(- R_A\right)_S \ \phi \ \Delta V$ (3.19)

Dividing the equation 3.18 by $\phi \ \Delta V$

Mole Balance equation for Solid Phase

$$k_m \ C_b \ \left(Y_{surface} - Y_{gas}\right) \ = \ \eta \left(- R_A\right)_S \tag{3.20}$$

3.5.4 Energy balance equation is solid phase

The energy equation is developed for the solid phase considering an axisymmetric cylindrical monolith. The energy balance equation is a single partial differential equation involving the effective thermal conductivities.

$$\begin{bmatrix} Conduction \\ in-out \\ Z\ direction \end{bmatrix} + \begin{bmatrix} Conduction \\ in-out \\ r\ direction \end{bmatrix} - \begin{bmatrix} Heat\ loss\ by \\ convection \\ to\ gas \end{bmatrix} + \begin{bmatrix} Heat\ generated \\ by\ reaction\ in \\ the\ catalyst \end{bmatrix} = \begin{bmatrix} Energy \\ accumulation\ in \\ the\ solid\ phase \end{bmatrix} \quad (3.21)$$

Consider a differential volume as shown in the figure 3.1. The conduction occurs in the r and z directions.

Fourier's law of conduction

Heat transfer by conduction which is also known as thermal diffusion occurs at molecular level. Molecular energy is transferred in the direction of decreasing temperature. The amount of energy transferred per unit area per unit time is called heat flux and is directly proportional to the temperature gradient.

$$q = \left(-K_Z \frac{dT_S}{dZ} \right)_Z \quad (3.22)$$

The proportionality constant K_Z is called the thermal conductivity of the material. The heat flow rate is the product of the heat flux and the area through which it passes.

$$Q = \left(-K_Z A_Z \frac{\partial T_S}{\partial Z} \right)_Z \quad (3.23)$$

Change in conduction along the z direction

$$= \quad \text{Conduction a z} \quad - \quad \text{Conduction at z} + \Delta z$$

$$= \quad \left(-K_Z A_Z \frac{\partial T_S}{\partial Z}\right)_Z - \left(-K_Z A_Z \frac{\partial T_S}{\partial Z}\right)_{Z+\Delta Z} \qquad (3.24)$$

Change in conduction along the r direction

$$= \quad \text{Conduction at r} \quad - \quad \text{Conduction at r} + \Delta r$$

$$= \quad \left(-K_r A_r \frac{\partial T_S}{\partial r}\right)_r - \left(-K_r A_r \frac{\partial T_S}{\partial r}\right)_{r+\Delta r} \qquad (3.25)$$

Where $A_Z = 2\pi\, r\Delta r \quad A_r = 2\pi\, r\Delta Z \qquad (3.26)$

Porosity is the volume of void space in the catalyst. In this case, the porosity of the catalyst is considered to be 0.68 which means 68% of the entire volume of the catalyst is pores, which is considered as volume fraction of gas. The remaining 32% is the solid fraction which contains the washcoat and the substrate.

Let the fraction of gas in the total volume = ϕ

Therefore the fraction of the solid = 1 - ϕ

The effective thermal conductivity $K_Z = (1 - \phi)\, K_W \qquad (3.27)$

$_Z$ direction = $- \left((1-\phi) K_W\, 2\pi\, r\, \Delta r \frac{\partial T_S}{\partial z}\right)_Z - \left((1-\phi) K_W\, 2\pi\, r\, \Delta r \frac{\partial T_S}{\partial z}\right)_{Z+\Delta Z} \qquad (3.28)$

Expanding the above equation using Taylor's theorem and neglecting the higher order terms

$$\text{Z direction} = \Delta \left((1-\phi) K_W \; 2 \pi \; r \; \Delta r \frac{\partial T_S}{\partial z} \right) \tag{3.29}$$

Similarly conduction along the r direction is given by

$$\text{r direction} = \Delta \left((1-\phi) K_r \; 2 \pi \; r \; \Delta z \frac{\partial T_S}{\partial r} \right) \tag{3.30}$$

Energy due to the chemical reactions

The oxidation of methane over palladium is an exothermic reaction which generates energy. This is incorporated into the energy equation using the following equation.

$$Q_{generated} = \eta \; [\; \Delta H * \text{Reaction Rate} * \text{Incremental surface area}] \tag{3.31}$$

$$= \eta \; [\; \Delta H_R \; (-RA)_{surface} \; \Delta S \;] \tag{3.32}$$

Where η is the effectiveness factor, i.e., the fraction of the surface that is available for the reaction. The reactant concentration at the surface is C_S and the concentration at the base is 0 as the material is considered to impermeable. Thus at any point in the catalyst, the rate of reaction is given by intrinsic rate expression which is evaluated at the local temperature and pressure. Thus the effectiveness factor is used to quantify the effect of diffusion on the catalyst. For a flat catalyst slab, the effectiveness factor can be defined as

$$\eta = \frac{\tanh(\phi)}{\phi} \tag{3.33}$$

Where Φ is the Thiele modulus which is give by

$$\phi = L_C \sqrt{\frac{K_V}{D_{eff}}} \tag{3.34}$$

Where Kv is the reaction rate constant based on volume and D_{eff} is the effective diffusivity.

Convective heat transfer

Catalytic combustion results in surface temperature greater than the bulk temperature resulting in a convective heat transfer.

Q_{conv} = heat transfer coefficient * Incremental surface are * temperature difference

$$= h * \Delta S * (T_S - T_{gas}) \quad (3.35)$$

Where ΔS is the incremental surface area.

$$Q_{conv} = h \Delta S (T_S - T_{gas}) \quad (3.36)$$

$$\text{Accumulation of energy} = m C_p \Delta T \quad (3.37)$$

Expressing mass in terms of density and volume,

$$= \rho \Delta V (1-\phi) C_P \frac{\partial T_S}{\partial t} \quad (3.38)$$

Where Cp is the constant pressure heat capacity which is defined as the change in enthalpy due to the change in temperature at a constant pressure. In the above equation, the mass is written in terms of density and incremental volume. Therefore the energy balance equation in the solid phase is:

$$\Delta\left((1-\phi)K_W 2\pi r \Delta r \frac{\partial T_S}{\partial Z}\right) + \Delta\left((1-\phi)K_r 2\pi r \Delta Z \frac{\partial T_S}{\partial r}\right) - \eta [\Delta H_R (-RA)_s \Delta S]$$

$$- h \Delta S (T_S - T_{gas}) = \rho \Delta V (1-\phi) C_P \frac{\partial T_S}{\partial t} \quad (3.39)$$

The incremental volume is written in terms of incremental distance in the r and the z direction.

$$\Delta V = 2\,\pi\,\Delta r\,\Delta Z \tag{3.40}$$

Thus the energy equation can be written as

$$\left((1-\phi)\frac{\partial}{\partial Z}K_W\frac{\partial T_S}{\partial Z}\right) + \left((1-\phi)\frac{\partial}{\partial r}K_r\frac{\partial T_S}{\partial r}\right) - \eta\, A_v\, \Delta H_R\, (-RA)_s$$

$$- \; h\, A_v\, (T_S - T_{gas}) = \rho\,(1-\phi)\,C_P\,\frac{\partial T_S}{\partial t} \tag{3.41}$$

Where $\Delta S / \Delta V = A_v$, Therefore the energy balance equation becomes

$$\left((1-\phi)\frac{\partial}{\partial Z}K_W\frac{\partial T_S}{\partial Z}\right) + \left((1-\phi)\frac{\partial}{\partial r}K_r\frac{\partial T_S}{\partial r}\right) - \eta\, A_v\, \Delta H_R\, (-RA)_s$$

$$- \; h\, A_v\, (T_S - T_{gas}) = \rho\,(1-\phi)\,C_P\,\frac{\partial T_S}{\partial t} \tag{3.42}$$

<u>Gas Phase</u>

Mole Balance

$$-V_M C_{A,B}\frac{dY_{A,B}}{dZ} \quad - \quad (-R_A)_H\,\phi \quad - \quad k_m\, C_b\, A_V\,(Y_{A,B} - Y_{A,S}) = 0 \tag{3.43}$$

Energy Balance

$$h\, A_V\,(T_s - T_{gas}) \quad - \quad \phi\,(-R_A)_H\,\Delta H_R \quad - \quad \rho\, C_P\, V_S\,\frac{\partial T_{gas}}{\partial Z} = 0 \tag{3.44}$$

<u>Solid Phase</u>

Mole Balance

$$k_m\, C_b\,(Y_s - Y_{gas}) = \eta\,(-R_A)_S \tag{3.45}$$

Energy Balance

$$\left((1-\phi)\frac{\partial}{\partial Z}K_W\frac{\partial T_S}{\partial Z}\right) + \left((1-\phi)\frac{\partial}{\partial r}K_r\frac{\partial T_S}{\partial r}\right) - \eta\, A_v\, \Delta H_R\, (-RA)_s$$

$$- h\, A_v\, (T_S - T_{gas}) = \rho\,(1-\phi)\,C_P\frac{\partial T_S}{\partial t} \quad (3.46)$$

3.6 Boundary conditions

It is very important to define the boundary conditions properly as they are the ones that define the problem. Initially the model is considered to be insulated at the sides and no radiation is considered. The model can be extended to radiation once the solution for the simpler case is obtained. The initial temperature of the exhaust gas and the concentration of all the gas species at the inlet are known and these form the initial boundary conditions. The equation below shows the surface temperature profile. Initially, at t =0, the solid temperature through out the catalyst is the same.

$$T_S(X, 0) = T_{S0}(X) \quad (3.47)$$

The boundary conditions are defined below. The inlet concentration is always a constant. It does not change as time proceeds. Hence the concentration at time 0 is the same at any time t. As is the case for the gas temperature. The inlet gas temperature is always a constant.

$$C_{g,i}(0,t) = C_{g,i}^{in}$$

$$T_g(0,t) = T_g^{in} \tag{3.48}$$

$$\frac{\partial T_s}{\partial x}(0,t) = \frac{\partial T_s}{\partial x}(L,t) = 0$$

3.7 Reaction mechanism

3.7.1 Surface reaction principle

The oxidation of methane over palladium takes place on the surface of the catalyst. In this case the noble metal is palladium and hence the reaction takes place on palladium surface. There are basically two types of surface reactions that are common in most surface reactions. One is the Langmuir – Hinshelwood mechanism and the other is Eley – Rideal mechanism. The figure 3.2 illustrates the Langmuir – Hinshelwood mechanism. The first step in the mechanism is that the reactants in the gas phase are adsorbed onto the noble metal sites. Then they diffuse through the surface and react to form the product. Once the products are formed it is desorbed from the surface. Figure 3.3 below represents the Eley – Rideal mechanism. In this mechanism, one of the reactant is adsorbed to the surface. When the other reactant passes over the adsorbed reactant on the surface, product is formed and is desorbed from the surface. The oxidation of methane over palladium has been identified to follow the Langmuir – Hinshelwood mechanism [Pulkrabek, 1].

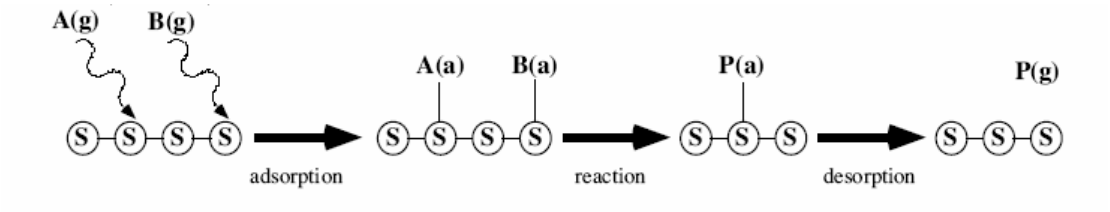

Figure 3.2. Langmuir – Hinshelwood mechanism

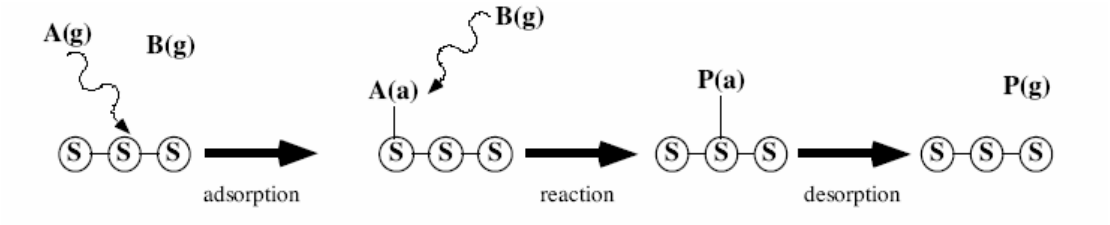

Figure 3.3. Eley – Rideal mechanism

The governing equation depends on the reaction mechanism and the rate of reaction of each species. The reaction mechanism, the surface reactions in this case can take place in a number of ways. Though in most cases one can only notice the overall reaction or the global reaction, the actual reaction takes place in a number of steps. The reaction mechanism clearly breaks the overall reaction into individual steps that is followed during the reaction. The transition of each chemical species involved in the reaction and the order in which the bonds break, everything can be found out using the reaction mechanism. Though this is not a very important factor for most cases, when modeling it is better to follow the reaction mechanism in order to obtain accurate results. The mechanism should also consider the order in which the molecules react. Often a single step reaction contains a series of micro level reactions making it a multi-step reaction.

A wide range of softwares are available to get a detailed elementary reaction mechanism. Some of the softwares are CHEMkin, KINALC, FLUXviewer can give accurate mechanisms. It also gives the kinetics involved with the mechanism. In general elementary reactions of hydrocarbons involve a dozen to hundreds of species and hundreds to thousands of reaction steps. The oxidation of methane is no simple process; it involves 23 species with 377 elementary reactions. It is extremely difficult to incorporate into the model a reaction mechanism like this. This not only makes the model complex, simulation of this model will take too much computation time without much difference in the accuracy.

Thus a simpler reaction mechanism can be considered for the oxidation of methane over palladium catalyst. One such mechanism is the Mars Van Krevelen mechanism [Kolaczkowzki et. al., 14] as shown in figure 3.4. This mechanism is one of the most common mechanisms used for the oxidation of methane over platinum and palladium. This mechanism has 7 intermediate steps. The steps are shown below.

$$O_2 + * \xleftrightarrow{K_1} O_2^* \qquad Step\ 1$$
$$O_2^* + * \xleftrightarrow{K_2} 2O^* \qquad Step\ 2$$
$$CH_4^* + * \xleftrightarrow{K_3} CH_4^* \qquad Step\ 3$$
$$CH_4^* + O^* \xleftrightarrow{K_4} CH_3^* + OH^* \qquad Step\ 4$$
$$2OH^* \xleftrightarrow{K_5} H_2O + O^* + * \qquad Step\ 5$$
$$CO_2^* \xleftrightarrow{K_6} CO_2 + * \qquad Step\ 6$$
$$CO_3^* \xleftrightarrow{K_7} CO_2 + O^* \qquad Step\ 7$$

Figure 3.4. Mars – Van Krevelen mechanism

The Mars – Van Krevelen mechanism is consistent with the reaction rates on O_2, CH_4, CO_2, CO and H_2O. The first step in the mechanism is the molecular adsorption of O_2 and the subsequent desorption of O atoms. The second step is assumed to be irreversible. There has not been any research to discern the second step even though it has been included in the reaction mechanism. The third step is also reversible which is the molecular adsorption of methane. The C – H bonds in methane are activated in step 4 using a vacant oxygen site pair. Step 5 is the one that produces water by recombining the surface hydroxyl. Steps 6 and 7 are reversible desorption of CO_2 adsorbed in vacant sites or lattice oxygen atoms. Applying a pseudo-steady approximation to the above mechanism, it leads to a Langmuir – Hinshelwood type reaction rate expression. The reaction rate is given by

$$Rate = \frac{K_1 k_2 P_{O_2}}{3\left(1 + \frac{K_1 k_2 P_{O_2}}{3K_3 k_4 P_{CH_4}} + K_1 P_{O_2} + K_3 P_{CH_4} + \left(\frac{K_1 k_2 |H_2O| P_{O_2}}{3K_4 k_5 P_{CH_4}}\right)^{1/2} + \frac{P_{CO_2}}{K_6} + \frac{K_1 k_2 P_{CO_2} P_{O_2}}{3K_7 K_4 k_3 P_{CH_4}}\right)^2} \quad (3.49)$$

When OH is abundant, the effect of H_2O increases and hence the reaction rate can further be simplifies to

$$r = \frac{K_3 k_4 K_5 P_{CH_4}}{P_{H_2O}} = k_{eff} P_{CH_4} / P_{H_2O} \quad (3.50)$$

If CO_2 is found to be abundant in the mixture, then it plays an important role in the reaction rate but since the formation of H_2O to CO_2 is always in the ratio 2:1, that is likely to happen and hence the latter reaction rate expression is used in most cases. In the model developed for this case only the global reactions are considered. This

further simplifies the model for the computer simulation. As seen in chapter 2, there is not much difference in the conversion and the temperature profile on the surface of the catalyst by using the global reaction rate instead of the Mars Van Krevelen mechanism. The global reaction rate contains 3 basic reactions which include the oxidation of methane, oxidation of CO and formation of water vapor. The equations are shown below

$$CO + (1/2)\ O_2 \rightarrow CO_2 \tag{3.51}$$

$$CH_4 + 2\ O_2 \rightarrow CO_2 + 2\ H_2O \tag{3.52}$$

$$H_2 + (1/2)\ O_2 \rightarrow H_2O \tag{3.53}$$

These are the three reactions that are considered in the model. The reaction rates are based on the above reaction. The rate equations are given below

$$\begin{aligned} \overline{R}_{CO} &= k_1 C_{CO} C_{O_2} / G && [mol\ CO / cm^2\ Pd.S] \\ \overline{R}_{CH_4} &= k_2 C_{CH_4} C_{O_2} / G && [mol\ CH_4 / cm^2\ Pd.S] \\ \overline{R}_{H_2} &= k_3 C_{H_2} C_{O_2} / G && [mol\ H_2 / cm^2\ Pd.S] \end{aligned} \tag{3.54}$$

Where $G = T\ (1 + K_1 c_{CO} + K_2 c_{CH_4})^2\ (1 + K_3 c^2_{CO} c^2_{CH_4})\ (1 + K_4 c^{0.7}_{NO})$

In the above equations k_1, k_2 and k_3 are the reaction rate coefficient. The reaction rate coefficients have a temperature dependency which is represented by Arrhenius equation.

$$k = Ae^{-\frac{E_a}{RT}} \tag{3.55}$$

In the above equation, A is the pre-exponential term, Ea is the activation energy, R is the universal gas constant and T is the temperature. To develop the model involving surface reaction between methane and oxygen over palladium, it is necessary to know

the kinetics. It is important to have the correct values of the decisive parameters like the activation energy, the specific rate constants and the pre-exponential term. The oxidation of methane over palladium takes place in the presence of CO_2 and water vapor. Thus it is necessary to find the effects of all these constituent gases on the reaction. From the literature and past work, activation energy was found to be 92 kJ/ mol and the pre-exponential factor was 0.198 x 10^9 s^{-1}. One of the other important factor is the reaction order involved with the species. The rate of the reaction depends on the concentration of the reacting species. The dependency of the species concentration on the reaction is termed as the reaction order. In the above reaction methane has a reaction order of 1. Since it is a lean mixture, excess oxygen is present and hence the reaction order of oxygen is 0. Water vapour has an inhibiting effect and carbon dioxide is 0 at low concentration and negative two at high concentrations.

3.8 Concept of reverse flow

Reverse flow catalyst has been a topic of research for last 50 years. One of the most important factor in the oxidation of methane over palladium is the surface temperature. The surface temperature thus governs the reaction rate and thus the methane conversion efficiency. Higher the surface temperature, higher the conversion. For a unidirectional flow, the surface temperature increases towards the exit due to the exothermic reactions of oxidation of methane. Thus for a reacting flow, the exit temperature is always higher than the inlet temperature. Thus when the flow of the direction of exhaust gas is reversed, the inlet temperature is higher thus

resulting in an increased surface temperature profile, thus resulting in increased conversion efficiency.

3.9 Computer simulation

It is important to validate the model developed to determine its accuracy. Computer programming has always been used to simulate models. The advantages of computer simulation have been explained in literature survey.

3.9.1 Programming language

There are many advanced softwares that are available which can perform complex model simulation. Models for simple non reacting flow and heat transfer models can be easily solved using those softwares. Some of the softwares are FEMlab, Matlab, CHEMKin. The model developed is more complex and hence do not fall under any of the standard modules available with these softwares. Hence a program had to be written specifically for the model. One of the main compilers used commonly for the mathematical purpose is Fortran. There are two main types, the visual Fortran with a user friendly interface like Compaq Visual FORTRAN Compiler and the command line based compiler like the Intel Fortran compiler, Linux based. The code would have a number of subroutines requires more linking and so a visual compiler was more suitable. It was easy to traverse between subroutines and had a simpler debugger. But the model developed did not require lots of subroutines and so the command line interpreter was chosen.

The advantage of a command line interpreter is that it gives more control to the user and is faster. Though it requires a number of syntax to be remembered, once familiar it has more control over the code compilation than the visual compilers. The current code has one main program and a solver for ordinary differential equation. So the Intel FORTRAN compiler for Linux was used. This compiler is used along with the VI editor.

3.9.2 Program Logic

The governing equation for the energy and the mass transfer for the gas and the solid phase are fully coupled. The first step in this process is to convert the partial differential equation to ordinary differential equation. Once that is done, the ordinary differential equations can be solved using a standard ordinary differential equation solver. Since there are 4 species considered (CO, CH_4, H_2, O_2) there are 4 mole balance equation in the gas phase and 4 mole balance equation at the surface. There is also an energy equation at the surface where the oxidation of methane takes place and an energy equation for gas phase. The energy equation for the gas phase is not very important as it is assumed that there is no gas phase reaction. The catalyst is also considered to be insulated. This leaves us with 10 equations that have to be solved simultaneously. The forward progression method is used to solve this kind of system. This is also known as backward difference method using space derivatives for governing equation. The catalyst is broken down into 200 nodes. It is assumed to be like a number of catalysts in series where the output of one becomes the input of the other. The reason for breaking down into nodes is to solve all the equations at the

same time. The input for the program involves the gas composition and the temperature of gas and catalyst surface. At the end of the node, the concentration at the surface is calculated at first. Then at that surface temperature the energy due to the reaction is calculated. All the other equations are solved at this point. The output at the end of this node becomes the input for the next node and it is proceeded this way till the end of the catalyst. The parameters to be defined are explained in detail as this chapter proceeds. For a unidirectional flow, once the gas flows to the next node from the inlet, node 1 is again recomputed with a fresh inlet gas at the same inlet temperature but with the solid temperature from the previous node. Thus the program keep tracks of the solid temperature profile and keeps updating as the reaction takes place. This makes the program transient and time dependent. For a reverse flow, the same logic is used but then after a particular switching time the surface temperature profile is reversed. This way the reversal of flow is simulated.

3.9.3 Input parameters

There are lots of parameters required for the program. They are described below.

3.9.3.1 Catalyst

Palladium-alumina (Pd-Al_2O_3) catalysts with a cordierite substrate support were selected for the reverse flow oxidation catalyst study based upon their strong affinity for methane (CH_4) oxidation. The dimensions and characteristics of a typical Pd-Al_2O_3 catalyst is shown in Table 3.1. The dimensions of the oxidation catalysts used are 10 cm long with a 2.2 cm diameter and a cell density of 46.5 cells/cm^2, and all oxidation catalysts received a precious metal loading of 100 g-Pd/ft^3.

Table 3.1. Physical properties of a catalyst

Length	10 cm
Diameter	2.2 cm
cpscm	46.5
Loading	100 g-pd/ft^3

3.9.3.2 Simulated Exhaust Gas Composition

Table 3.2. Simulated exhaust gas composition

NOx	500 ppm
H_2	0
CO	0.5 %
CH_4	2000 ppm
CO_2	6 %
H_2O	10 %
O_2	6 %
N_2	Balance

Based on a literature review the composition of a natural gas exhaust mixture, shown in Table 3.2, is selected for the reverse flow oxidation catalyst study.

3.9.3.3 Switching frequency

The program is capable of working both forward flow and reverse flow. The input screen has the option of selecting whether the reverse flow has to be incorporated. When the flag is set to 1 it incorporated reverse flow and when the flag is set to 0 it

runs as unidirectional flow. From previous research the switching frequencies of 10, 20, 25, 30 and 40 seconds are chosen for this study.

3.9.3.4 Temperature

The solid temperature is always set to 25^{o}C (398 K). The inlet gas temperature is varied for different runs. They are varied from 350^{o}C to 600^{o}C in steps of 50^{o}C.

3.9.3.5 Space velocity

Space velocity in a chemical reactor is defined as how fast the molecules move inside the reactor. The space velocity indirectly defines the residence time of the gas species inside the catalyst. For this study, 3 different space velocities of 20,000 Hr^{-1}, 50,000 Hr^{-1} and 80,000 Hr^{-1} are studied.

3.9.3.6 Length of the catalyst

The length of the catalyst plays a very important role in the surface temperature profile. If the length of the catalyst is too long, the peak of the surface temperature occurs away from the exit, resulting in a reduced exit temperature. If the length is too small, the peak if the surface temperature profile falls outside of the exit of catalyst, thus resulting in loss of useful surface temperature. Thus it is important to study the effect of length. Three different lengths, 8 cm, 10 cm and 12 cm are analyzed in this study. Also the effect of three different inlet concentrations of methane (1000 ppm, 1500 ppm and 2000 ppm) is analyzed.

CHAPTER 4

RESULTS AND DISCUSSION

This chapter presents the results obtained from the FORTRAN simulation program for the reverse flow oxidation catalyst. The simulations are mainly divided into two sections. The first section contains the results of methane conversion at various temperature, space velocity and reverse flow switching frequency. From these results the space velocity and the switching frequency for the lowest temperature with highest conversion efficiency is selected for further analysis in the second section. The effect of the length of the catalyst, methane concentration, pre-exponential term and asymmetric switching frequency on methane conversion efficiency is analyzed.

4.1 Reverse flow oxidation catalyst simulation results:

All simulations for the reverse flow oxidation catalyst are carried out for a time period of 300 seconds. The results showed that the temperature profile and the conversion profile over the length of the catalyst attain a steady state by that time. The simulation results show that the methane conversion is significantly improved by the flow reversal of the exhaust gas stream. Figure 4.1 shows methane conversion comparison between unidirectional flow and reverse flow at 450 ^{o}C with a space velocity of 50,000 hr^{-1}. The frequency of switching in this case is 25 seconds. As seen in the figure, methane conversion increased by 40.6 % with flow reversal as compared to the unidirectional flow.

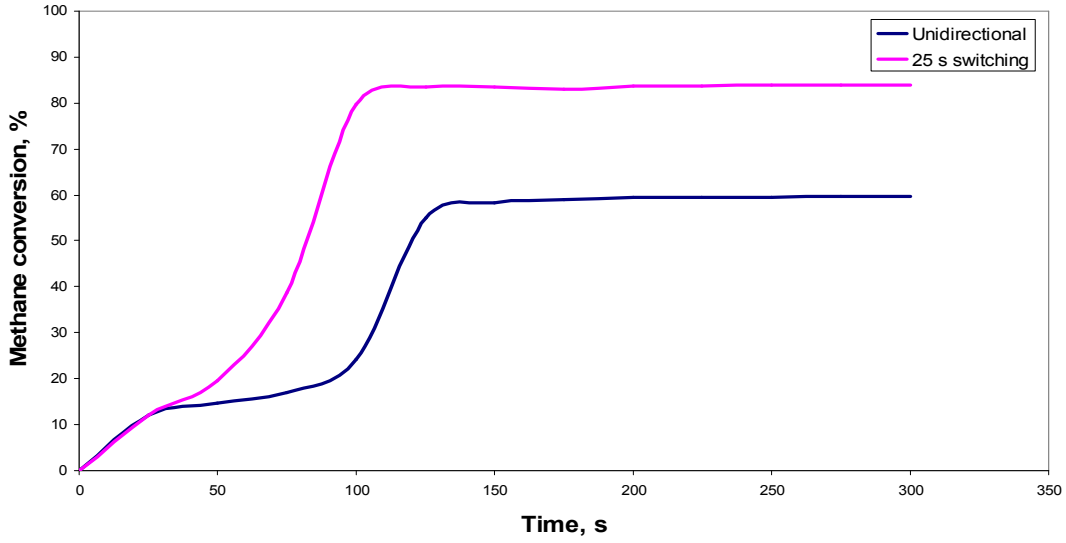

Figure 4.1. Methane conversion at an inlet gas temperature of 450^{o}C, initial surface temperature of 25^{o}C at a space velocity of 50,000 hr^{-1} and inlet methane concentration of 1500 ppm for unidirectional flow and 25 second switching flow

The increase in the conversion is due to the heat trap effect from the reaction of methane along the length of the catalyst. As seen in figure 4.1 for the solid temperature along the length of the catalyst for the unidirectional flow, the temperature keeps increasing due to the combustion of methane before it reaches steady state. Initially the surface temperature is lower than the gas temperature and is heated up by the flowing gases. The methane combustion during the initial period is very low which is evident from the conversion profile. But as time proceeds, the methane combustion in more resulting in higher surface temperature and increased conversion. Figure 4.2 and 4.3 shows the gas temperature profile along the length of the catalyst.

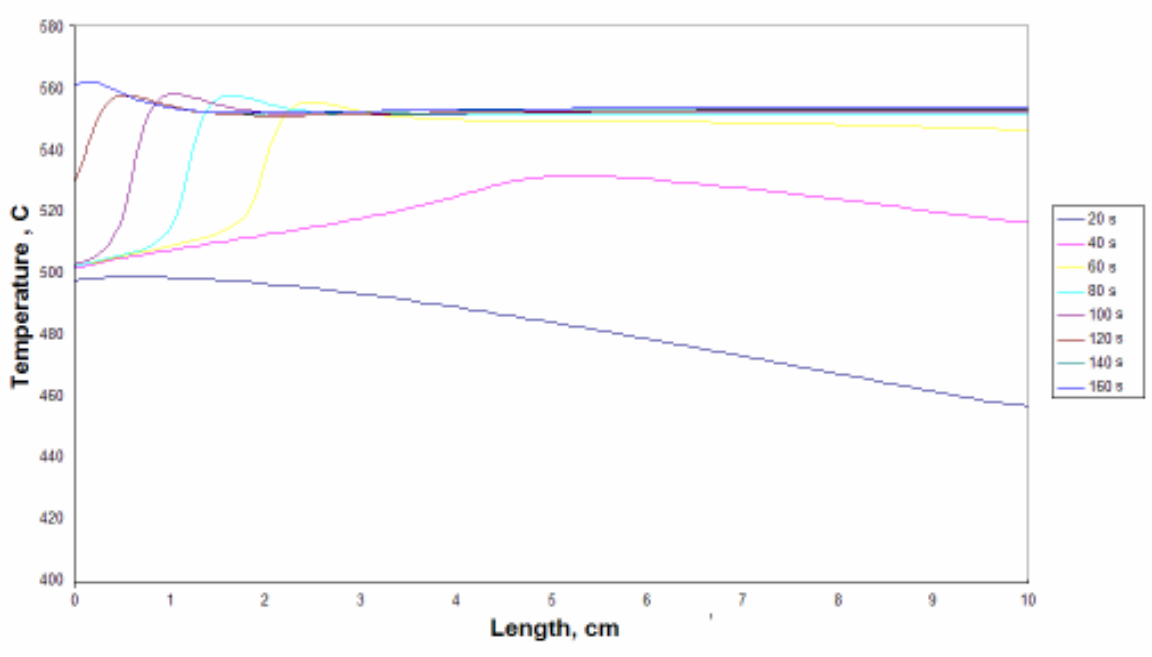

Figure 4.2. Solid temperature profile at an inlet gas temperature of 450°C at a space velocity of 50,000 hr^{-1} for unidirectional flow

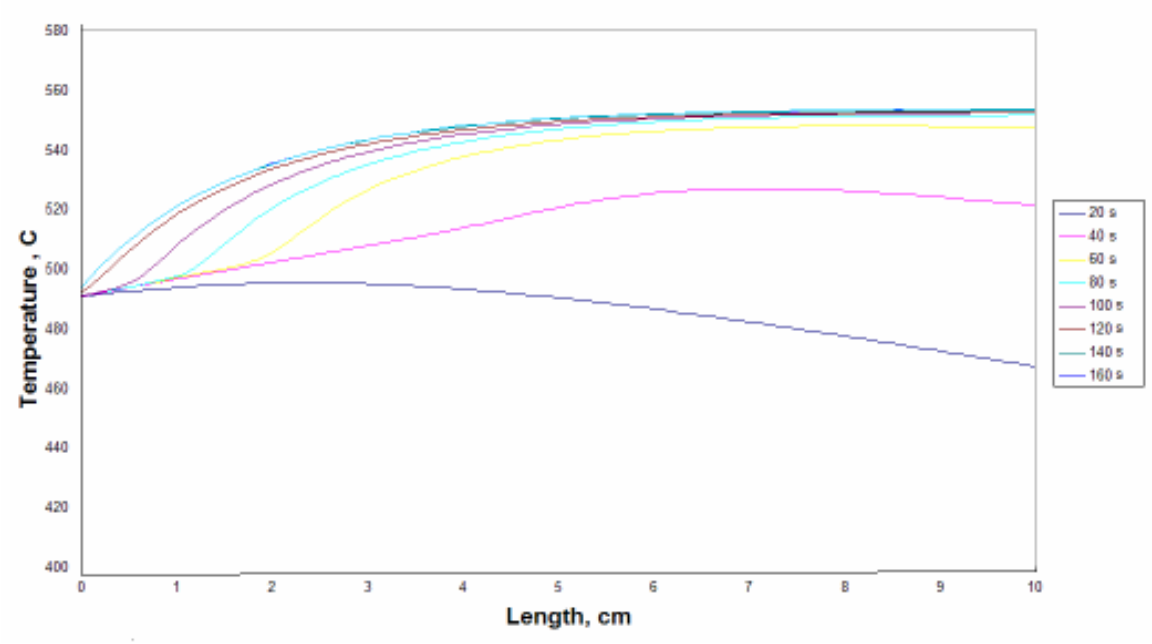

Figure 4.3. Gas temperature profile at an inlet gas temperature of 450°C at a space velocity of 50,000 hr^{-1} for unidirectional flow

Initially the gas temperature decreases as the gas temperature is used up to heat the catalyst surface which is at a lower temperature. Once the catalyst surface is heated up to the gas temperature, and once the combustion process starts, the gas temperature increases due to the increase in the catalyst temperature. The gas temperature reaches close to the solid temperature as it attains the steady state.

Figure 4.4 below shows the solid temperature along the length of the catalyst for the flow reversal case. We can see that the increase in the temperature is faster than that of the unidirectional flow. This is because during the flow reversal, the catalyst temperature which is higher at the exit becomes the inlet side and so the incoming gas is at a higher temperature than the unidirectional flow.

The solid temperature looks similar in both the cases at the 20 seconds as the flow reversal has not taken place but at 40 seconds, the inlet temperature is much more than the 40 second profile for the unidirectional flow. The peaks in the graph are the portion where the majority of the combustion takes place. As time progresses, the peak moves towards the inlet of the catalyst where the majority of the combustion takes place due to the high inlet temperature. Successive profiles also show an increased temperature profile in the case of reverse flow as to unidirectional flow.

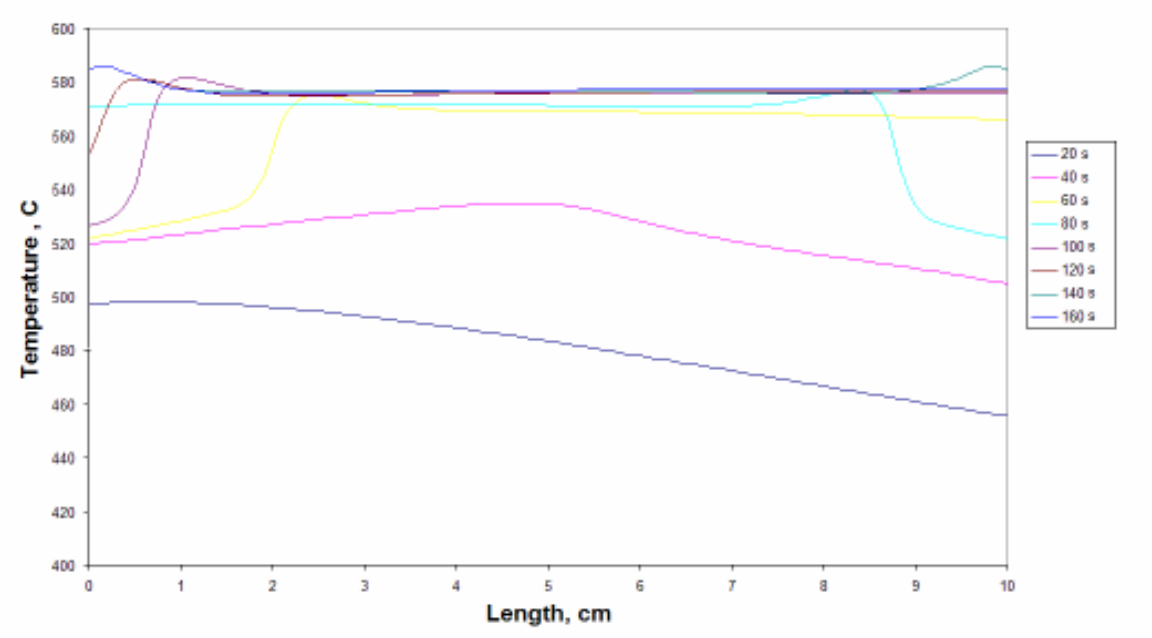

Figure 4.4. Solid temperature profile at an inlet gas temperature of 450°C at a space velocity of 50,000 hr^{-1} for 25 second switching flow

The simulations are carried over a wide range of temperatures with varying space velocities and reverse flow switching frequency. The space velocities considered are 20,000 hr^{-1}, 50,000 hr^{-1}, and 80,000 hr^{-1}. The switching duration were 10, 20, 25, 30, and 40 seconds and the temperatures were 350, 400, 450, 500, 550 and 600 °C. In the first section only symmetric switching was considered, where the time for the forward flow is the same as the time for the reverse flow. The second section considers asymmetric switching where the time for the forward flow and the time for the reverse flow are different. The results from the simulation for various cases are shown below in tables 4.1, 4.2 and 4.3 for different space velocities.

Table 4.1 Average methane conversion for the unidirectional and flow reversal regimes at reactor furnace temperatures of 350, 400, 450, 500, 550 and 600°C, switching frequencies of 10, 20, 25, 30, and 40 seconds, and a GHSV of 20,000 hr^{-1}

Temperature, C	Switching frequency, S	Methane conversion, %	Methane conversion, %
		Unidirectional flow	Reverse flow
350	10	9.2	11
	20	9.2	13.2
	25	9.2	14.6
	30	9.2	11.9
	40	9.2	11.4
400	10	21.6	24.6
	20	21.6	27.4
	25	21.6	29.3
	30	21.6	26.4
	40	21.6	23.4
450	10	78.3	84.6
	20	78.3	89.8
	25	78.3	94.6
	30	78.3	93.4
	40	78.3	89.5
500	10	97	99.8
	20	97	100
	25	97	100
	30	97	100
	40	97	100
550	10	100	100
	20	100	100
	25	100	100
	30	100	100
	40	100	100
600	10	100	100
	20	100	100
	25	100	100
	30	100	100
	40	100	100

Table 4.2 Average methane conversion for the unidirectional and flow reversal regimes at reactor furnace temperatures of 350, 400, 450, 500, 550 and 600°C, switching frequencies of 10, 20, 25, 30, and 40 seconds, and a GHSV of 50,000 hr^{-1}

Temperature, C	Switching frequency, S	Methane conversion, %	Methane conversion, %
		Unidirectional flow	Reverse flow
350	10	8.6	10.2
	20	8.6	11.9
	25	8.6	13.6
	30	8.6	14.2
	40	8.6	13.1
400	10	14.9	15.6
	20	14.9	21.4
	25	14.9	23.1
	30	14.9	23
	40	14.9	19.4
450	10	59.6	72.8
	20	59.6	77.9
	25	59.6	83.8
	30	59.6	81.5
	40	59.6	77.7
500	10	73.1	88.9
	20	73.1	91.4
	25	73.1	96.4
	30	73.1	91.5
	40	73.1	89.2
550	10	81.4	94.7
	20	81.4	98.2
	25	81.4	100
	30	81.4	100
	40	81.4	99.2
600	10	100	100
	20	100	100
	25	100	100
	30	100	100
	40	100	100

Table 4.3 Average methane conversion for the unidirectional and flow reversal regimes at reactor furnace temperatures of 350, 400, 450, 500, 550 and 600°C, switching frequencies of 10, 20, 25, 30, and 40 seconds, and a GHSV of 80,000 hr^{-1}

Temperature, C	Switching frequency, S	Methane conversion, % Unidirectional flow	Methane conversion, % Reverse flow
350	10	2.1	6.9
	20	2.1	7.2
	25	2.1	7.6
	30	2.1	8.1
	40	2.1	7.1
400	10	6.7	9.2
	20	6.7	11.2
	25	6.7	12.9
	30	6.7	14.1
	40	6.7	10.8
450	10	19.6	25.6
	20	19.6	28.9
	25	19.6	33.5
	30	19.6	28.6
	40	19.6	26.9
500	10	43.6	54.6
	20	43.6	57.8
	25	43.6	59.3
	30	43.6	56.2
	40	43.6	54.7
550	10	68.7	78.2
	20	68.7	79.8
	25	68.7	82.4
	30	68.7	79.8
	40	68.7	77.4
600	10	91.6	94.6
	20	91.6	97.8
	25	91.6	100
	30	91.6	99.4
	40	91.6	98.1

4.2 Effect of space velocity

The variation of space velocity had a significant effect on the methane conversion efficiency. Graphs were plotted for different space velocities as a function of methane conversion percentage and inlet gas temperature. The graphs 4.5 to 4.9 below show the effect of space velocity on the methane conversion efficiency at various switching frequency.

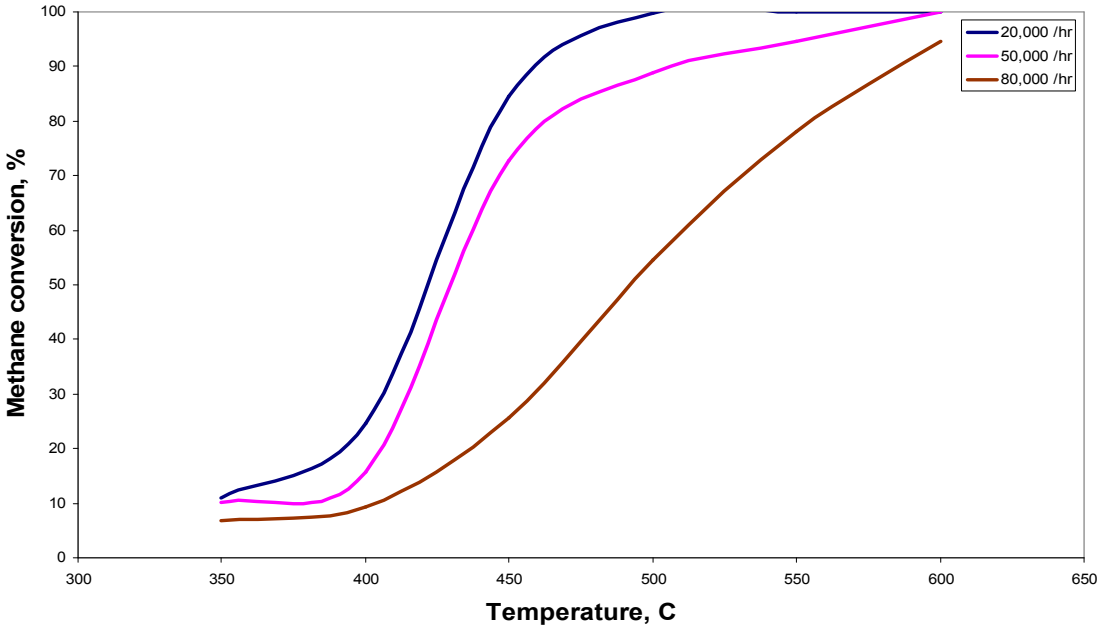

Figure 4.5. Methane conversion at an inlet gas temperature of 450^{o}C, with a 10 second switching frequency as a function of space velocity.

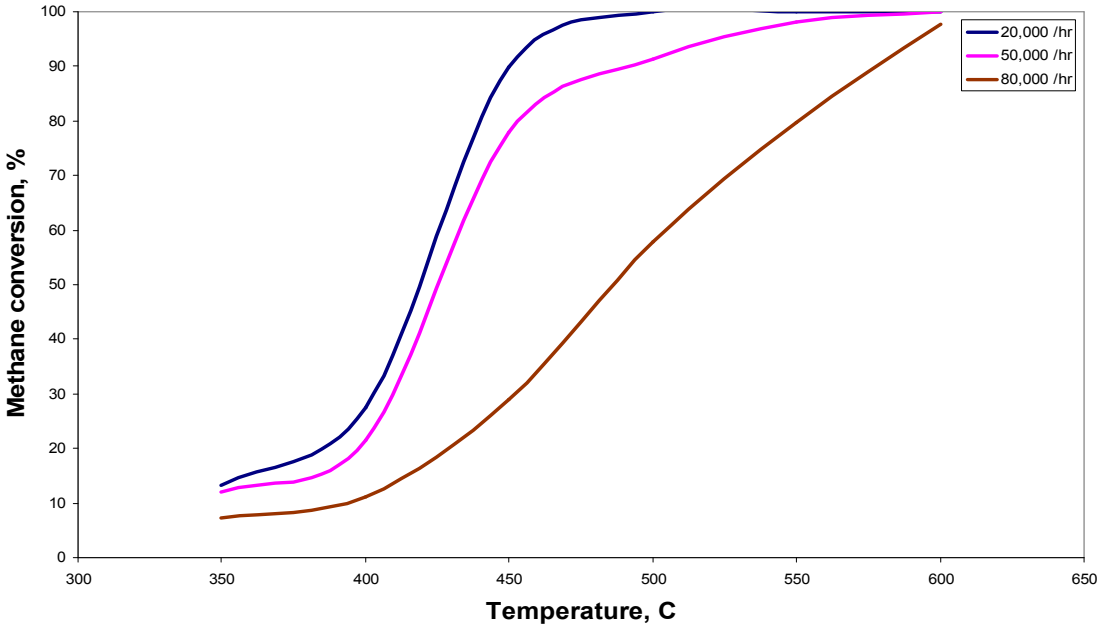

Figure 4.6. Methane conversion at an inlet gas temperature of 450°C, with 20 second switching frequency as a function of space velocity.

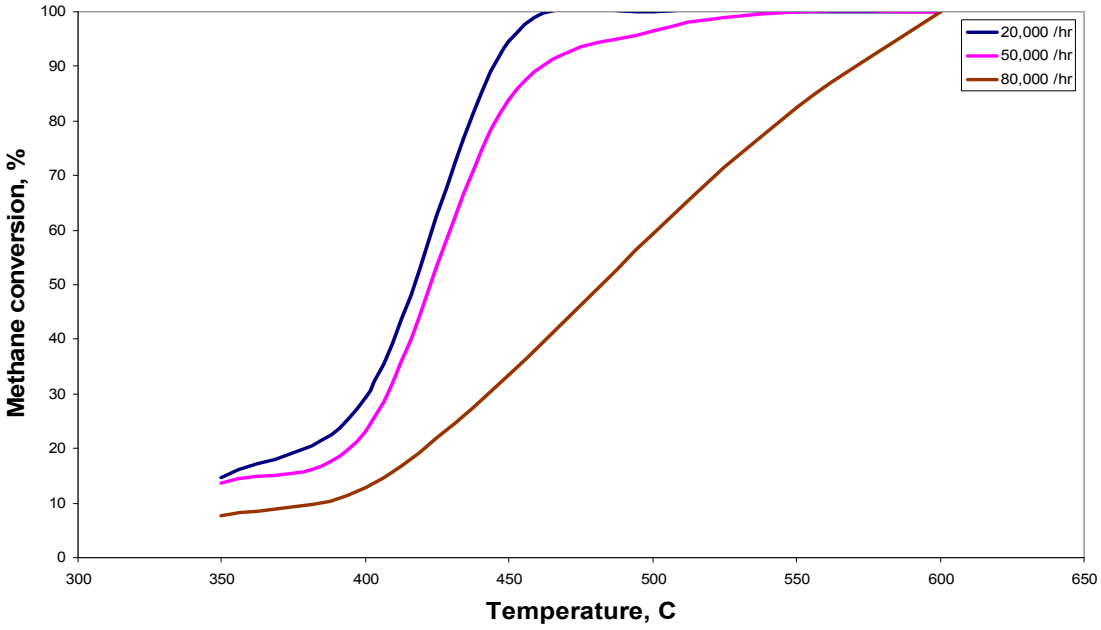

Figure 4.7. Methane conversion at an inlet gas temperature of 450°C, with 25 second switching frequency as a function of space velocity.

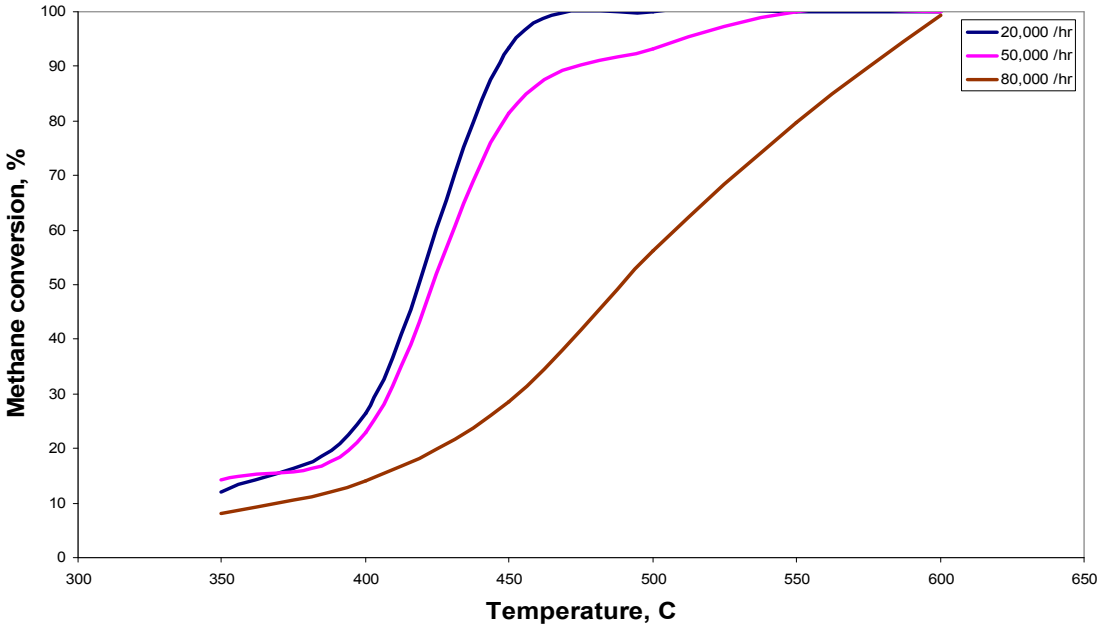

Figure 4.8. Methane conversion at an inlet gas temperature of 450°C, with 30 second switching frequency as a function of space velocity.

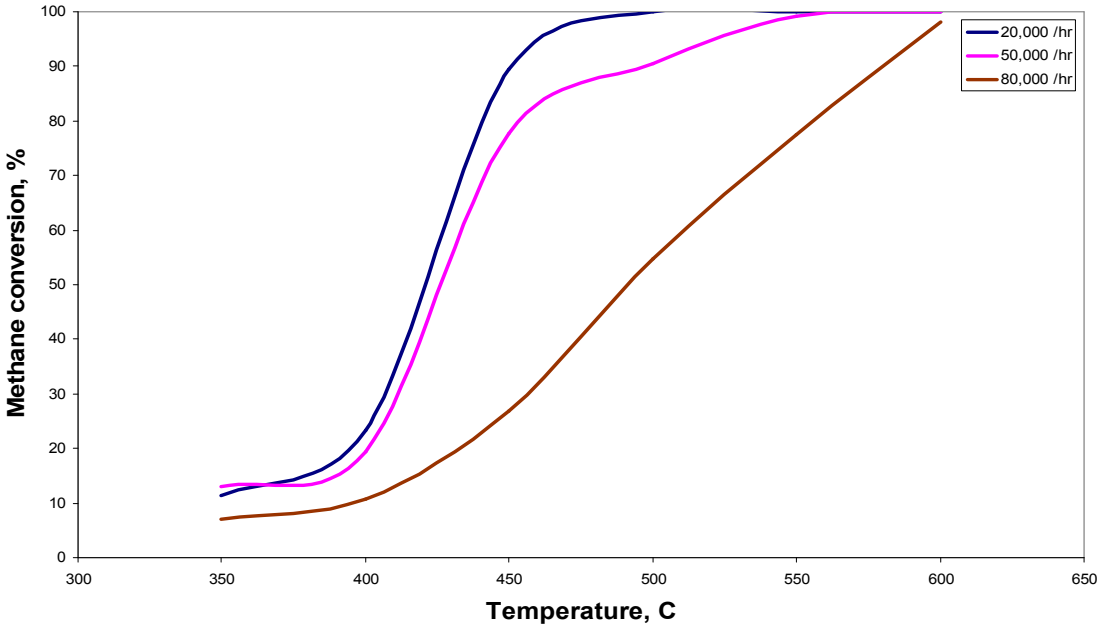

Figure 4.9. Methane conversion at an inlet gas temperature of 450°C, with 40 second switching frequency as a function of space velocity.

It is evident from the graphs 4.5, 4.6, 4.7, 4.8 and 4.9 that the conversion efficiency is higher at lower space velocities. The graphs for 10, 20 and 25 second switching frequency exhibit similar effects. The gas hourly space velocity defines the residence time. It is the time the exhaust gas has inside the catalyst. At lower space velocities, methane in the exhaust gas has relatively more time to find the palladium sites than at higher temperatures. Thus at lower space velocities, the conversion is higher.

4.3 Effect of switching time

Figures 4.10, 4,11 and 4.12 show the effect of switching time on the methane conversion at different inlet gas temperature for various space velocities.

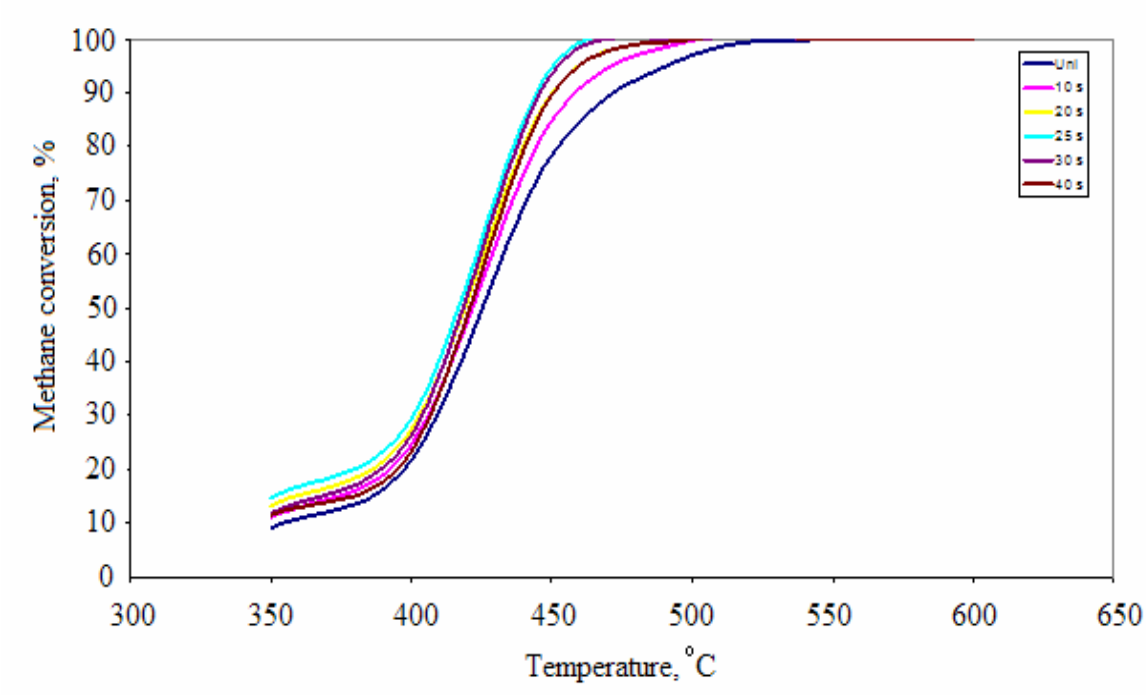

Figure 4.10. Effects of switching time on CH_4 conversion with a space velocity of 20,000 hr^{-1} as a function of inlet gas temperature.

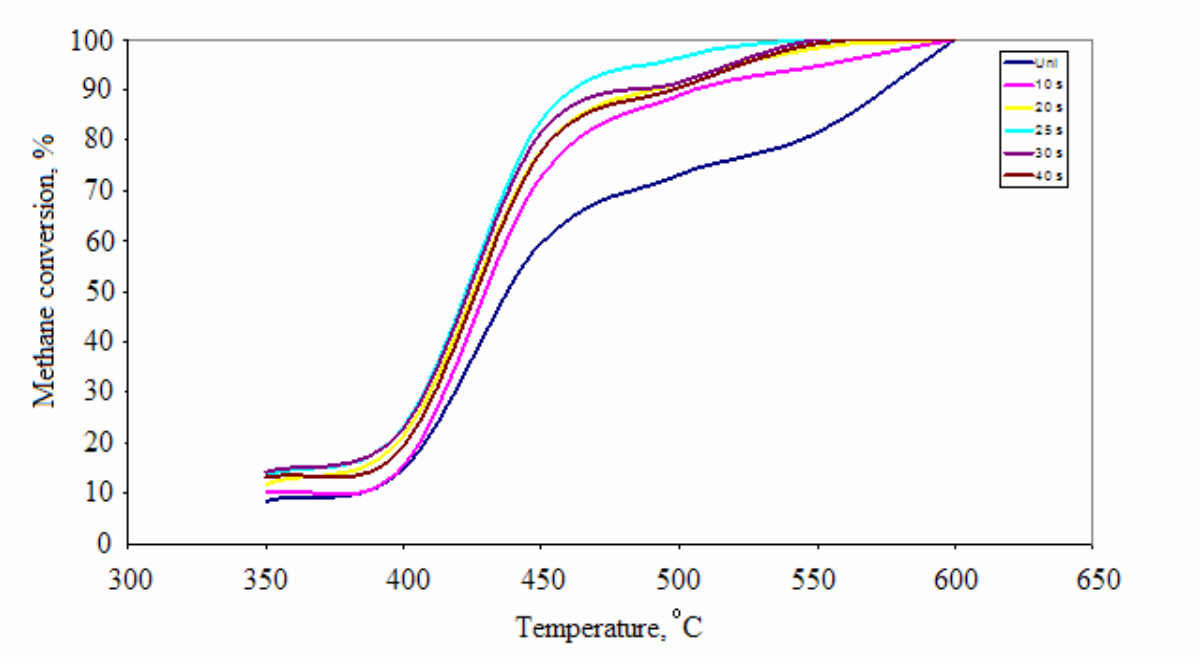

Figure 4.11. Effects of switching time on CH_4 conversion with a space velocity of 50,000 hr^{-1} as a function of inlet gas temperature.

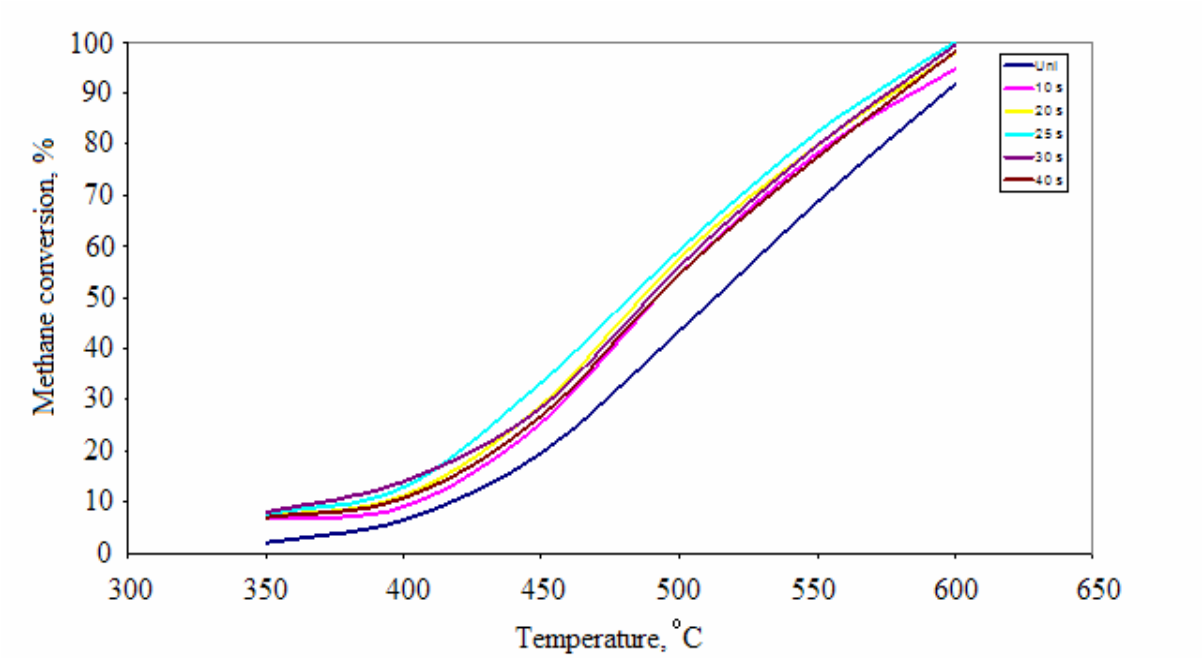

Figure 4.12. Effects of switching frequency on CH_4 conversion with a space velocity of 80,000 hr^{-1} as a function of inlet gas temperature.

It is evident from the graphs that the conversion is maximum at 25 seconds switching followed by 20 seconds, 30 seconds, 40 seconds and then 10 seconds. For a switching time of 10 seconds and 20 seconds, the methane conversion is lower because of the premature switching. The maximum conversion is attained when the peak in the solid temperature profile is at the centre of the catalyst. At lower switching times, the peak in the solid temperature profile is closer to the exit when compared to the higher switching times. Figure 4.13 shows for a switching frequency of 30 and 40 seconds, the peak in the temperature profile is closer to the entrance of the catalyst when compared to lower switching times and the temperature reduces towards the exit of the catalyst resulting in a reduced conversion. For a switching time of 25 seconds, the peak surface temperature occurs at the centre of the catalyst resulting in maximum conversion.

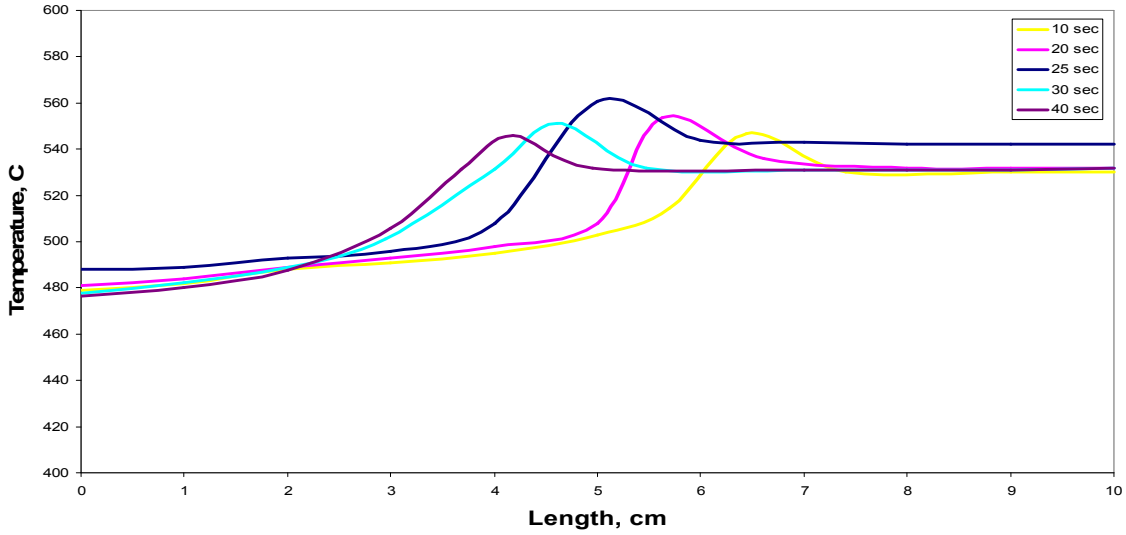

Figure 4.13. Effects of switching frequency on CH_4 conversion profile with a space velocity of 50,000 hr^{-1} at an inlet gas temperature of 450°C.

4.4 Effect of inlet gas temperature

The effect of inlet gas temperature on the conversion of methane is shown in graphs 4.14 to 4.16. The conversion of methane is plotted for different inlet gas temperatures for different switching frequency.

From figures 4.14 to 4.16, it is seen that the methane conversion is directly proportional to the inlet gas temperature. At lower temperatures, there is about 10% methane conversion. The light-off temperature for the unidirectional flow at a space velocity of 20,000 hr^{-1} is approximately 430 ^{o}C. The light of temperature at a space velocity of 50,000 hr^{-1} is approximately 450 ^{o}C and it is 510 ^{o}C at a space velocity of 80,000 hr^{-1}.

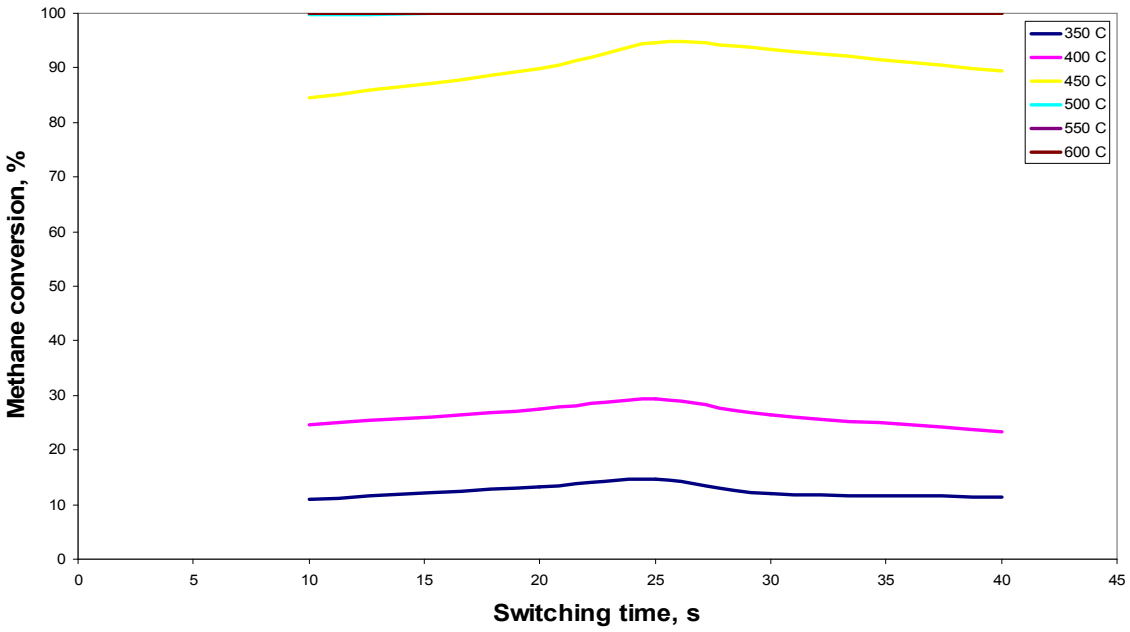

Figure 4.14. Effects of inlet gas temperature on CH_4 conversion with a space velocity of 20,000 hr^{-1} for various switching frequencies.

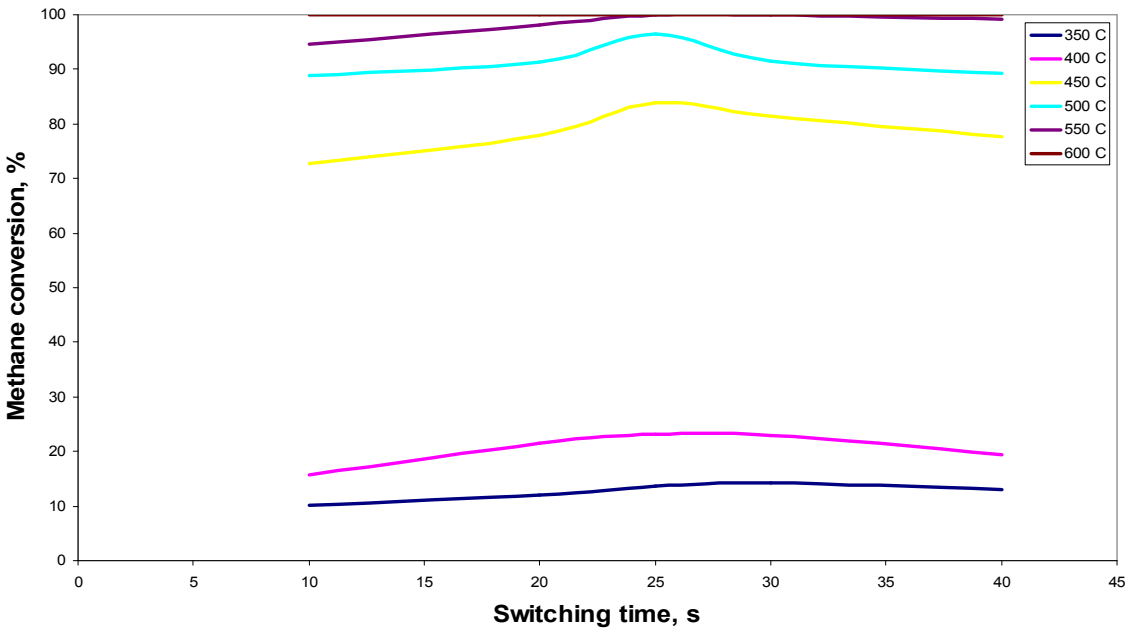

Figure 4.15. Effects of inlet gas temperature on CH_4 conversion with a space velocity of 50,000 hr^{-1} for various switching frequencies.

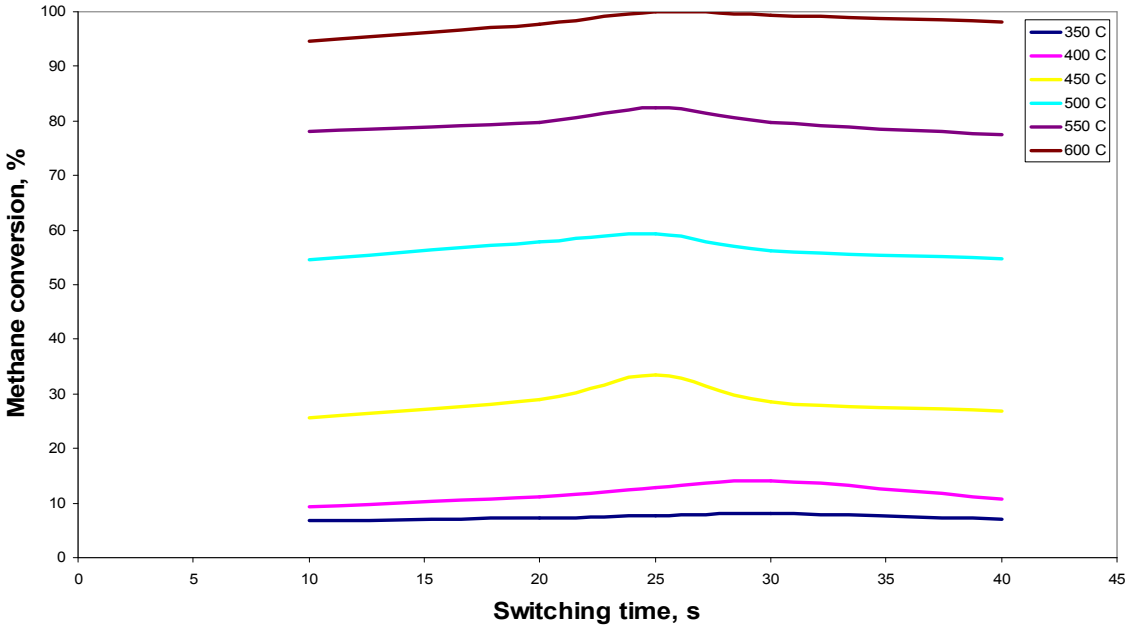

Figure 4.16. Effects of inlet gas temperature on CH_4 conversion with a space velocity of 80,000 hr^{-1} for various switching frequencies.

From the above simulation results, it is evident that periodical flow reversal increases the methane conversion percentage due to the increase in the catalyst surface temperature. As the space velocity increases, the residence time for the exhaust gases in the catalyst reduces resulting in lower conversion. The maximum conversion increase of 40.6% is found at a space velocity of 50,000 hr^{-1} for 450 ^{o}C. At lower space velocities with a higher inlet temperature, the unidirectional flow by itself achieves 100% conversion and at lower temperatures it is too low to be considered for further analysis.

The switching time has a slight effect on the methane conversion efficiency; it varied from 2 to 13%. At a space velocity of 80,000 hr^{-1}, the residence time is so low that switching time has very less effect. This is because the methane conversion is relatively less and hence there is not much heat generated on the surface of the catalyst to trap it by flow reversal. At these space velocities the variation in methane conversion due to different switching frequency is less than 5%. At higher switching frequency of 10 and 20 seconds there is not enough time to trap the heat effect due to prematured flow reversal. This is evident from the graphs 4.14 to 4.16 where the methane conversion is lower at low switching time. At higher switching time of 30, 40 seconds the switching occurs past the peak temperature resulting in a loss of useful temperature. A switching frequency of 25 seconds is found to be the best as maximum methane conversion is achieved for this case.

The prematured switching frequency does allow the temperature profile to peak within the catalyst resulting in a reduced conversion. The initial rise in the temperature shown in figure 4.17 is due to exothermic reaction of methane oxidation. After the temperature increase due to kinetics, the further temperature increase is diffusion limited. Thus the switching time affects the diffusion limited increase in temperature as shown in the above plot by Hayes and Kolaczkowski.

Simulations are carried out for further analysis at a temperature of 500 ^{o}C for a space velocity of 50,000 hr^{-1} and a switching time of 25 seconds since the methane conversion efficiency was maximum for these conditions.

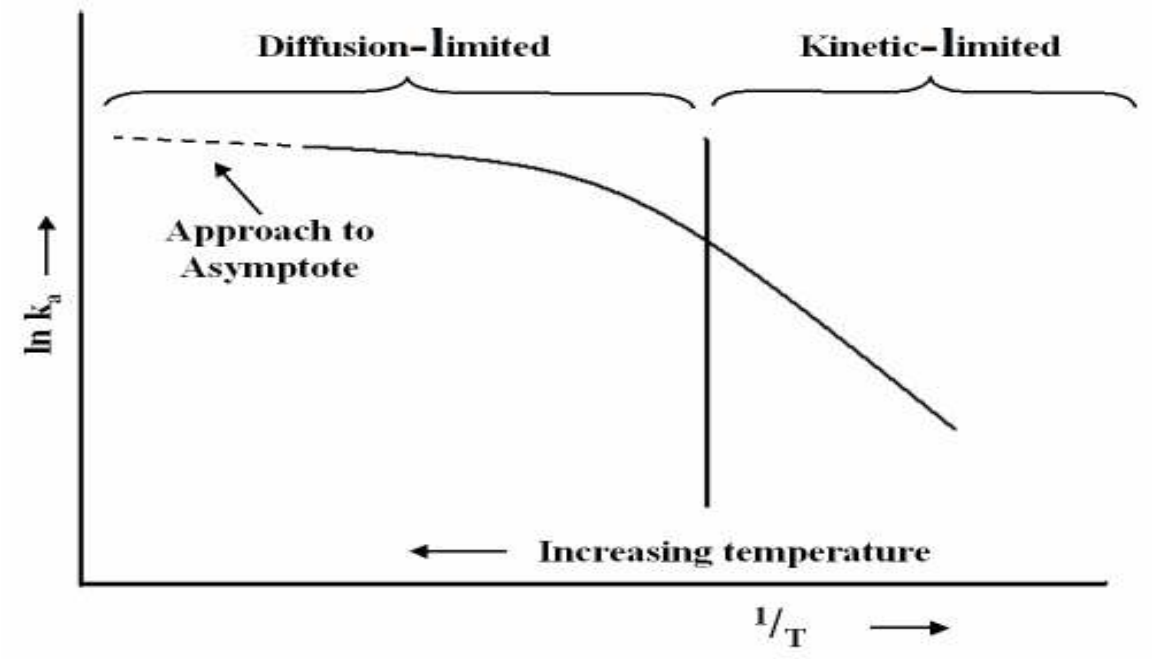

Figure 4.17. Different regimes in conversion profile

4.5 Effect of length of catalyst

Length of the catalyst plays an important role in the conversion efficiency of methane. Length of the catalyst defines the residence time of the exhaust gases inside the catalyst at a particular space velocity. For all the above simulations the length of the catalyst was 10cm. For further analysis, four different lengths have been chosen (7.5, 8.75, 10, 11.25 and 12.5 cm). The table 4.4 below gives the methane conversion efficiency at various lengths for an inlet gas temperature of 500^{o}C at different space velocities for a unidirectional flow and a reverse flow with 25 second switching frequency. Figure 4.18 and 4.19 below represent the conversion efficiency of methane for a unidirectional flow and for a reverse flow with 25 second switching.

Table 4.4. Effect of length of catalyst on methane conversion

Temperature, C	Length, cm	Switching, s	Methane conversion, %		
			20000hr^{-1}	50000 hr^{-1}	80000 hr^{-1}
500	7.5	uni	96.9	72.6	32.1
	8.75	uni	97	72.8	36.8
	10	uni	97	73.1	43.6
	11.25	uni	96.9	73.9	48.6
	12.5	uni	96.8	74.1	50.2
500	7.5	25	100	94.1	50.3
	8.75	25	100	95.2	54.7
	10	25	100	96.4	59.3
	11.25	25	99.8	97.2	60.8
	12.5	25	99.7	97.9	61.4

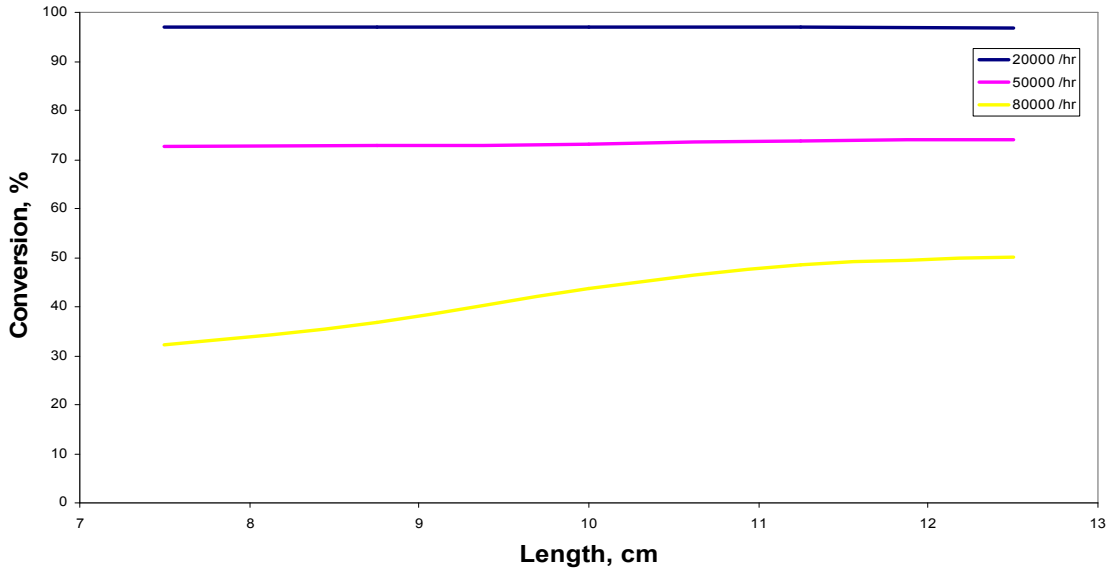

Figure 4.18. Effects of length of the catalyst on CH_4 conversion with an inlet gas temperature of 500^oC for a unidirectional flow.

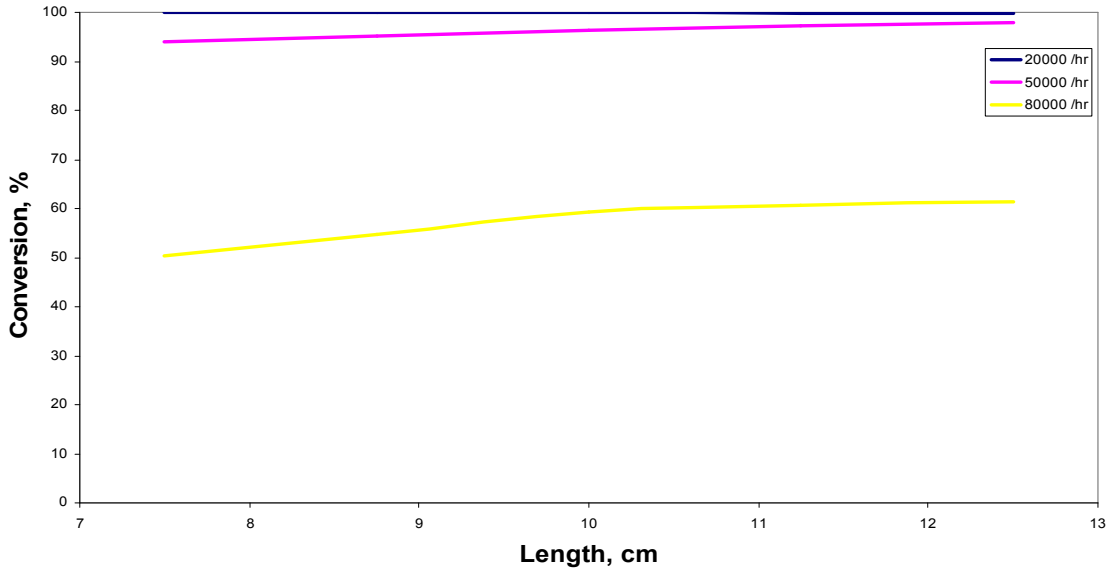

Figure 4.19. Effects of length of the catalyst on CH_4 conversion with an inlet gas temperature of 500^oC for a 25 second switching frequency.

As seen in figure 4.18, there is not much effect on the conversion efficiency due to the variation in length of the catalyst at lower space velocities. At a space velocity of 20,000 hr^{-1}, there is not much effect as the space velocity is very low and the conversion is high. At a space velocity of 50,000 hr^{-1}, the conversion efficiency goes down at lower lengths because the reduced length results in a lower residence time and the conversion goes up at increased lengths because of the increased residence time.

Much variation is seen at a space velocity of 80,000 hr^{-1} because at this high space velocity, the conversion is mainly diffusion controlled because of the low residence time available. So at increased lengths, the residence time increases resulting in an increased methane conversion. Table 4.5 below gives the residence times for the exhaust gas species inside the catalyst for different space velocities. At higher space velocities, the residence time drastically reduces resulting in a reduced methane conversion.

Table 4.5. Residence time for various space velocities at different temperature

Reactor inlet gas Temperature, C	Residence time, ms		
	20,000 hr^{-1}	50,000 hr^{-1}	80,000 hr^{-1}
400	207	93	61
450	188	87	58
500	171	80	55

4.6 Effect of pre-exponential term

From Lund et. al. [20] the pre-exponential factor for the oxidation reaction of methane over palladium catalyst was found to be 0.198 x 10^9 s^{-1} for Pd/Al_2O_3 catalyst with 0.2 wt % palladium loading. This value could not be compared to other literature as they were not present and so the effect of this value on the conversion and the temperature profile was analyzed. The pre-exponential factor was analyzed by increasing and decreasing the factor by an order of magnitude i.e., 0.198 x 10^8 s^{-1} and 0.198 x 10^{10} s^{-1}. The simulations are carried at 500 ^oC for a space velocity of 50,000 hr^{-1}. Figure 4.20 show results of this simulation. The solid temperature profile show an increase of 4^oC when it is increased by an order of magnitude where as the temperature is decreased by 11^oC when it is reduced by an order magnitude.

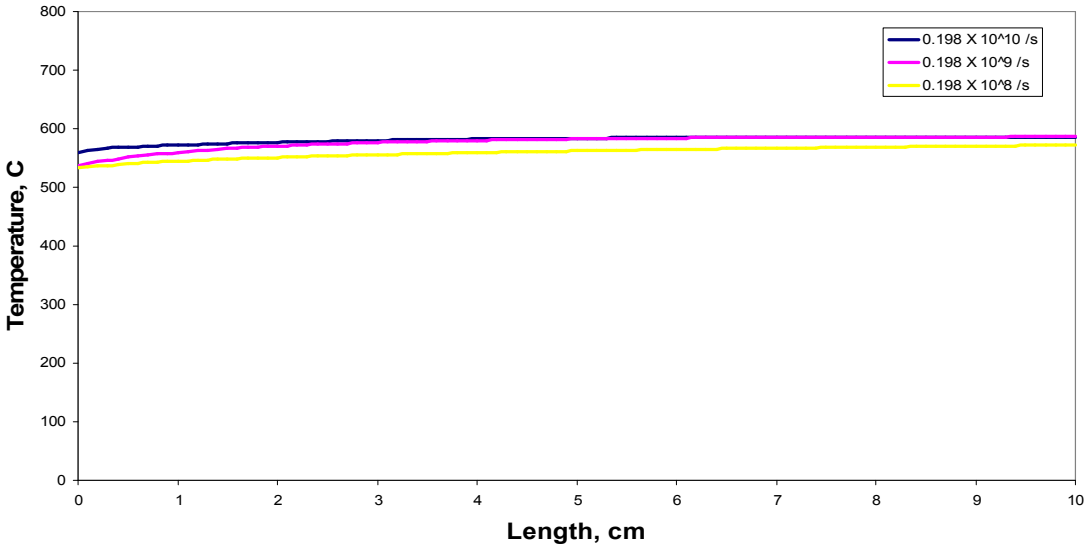

Figure 4.20. Effects of pre-exponential term with an inlet gas temperature of 500^oC at a space velocity of GHSV hr^{-1} for a unidirectional flow.

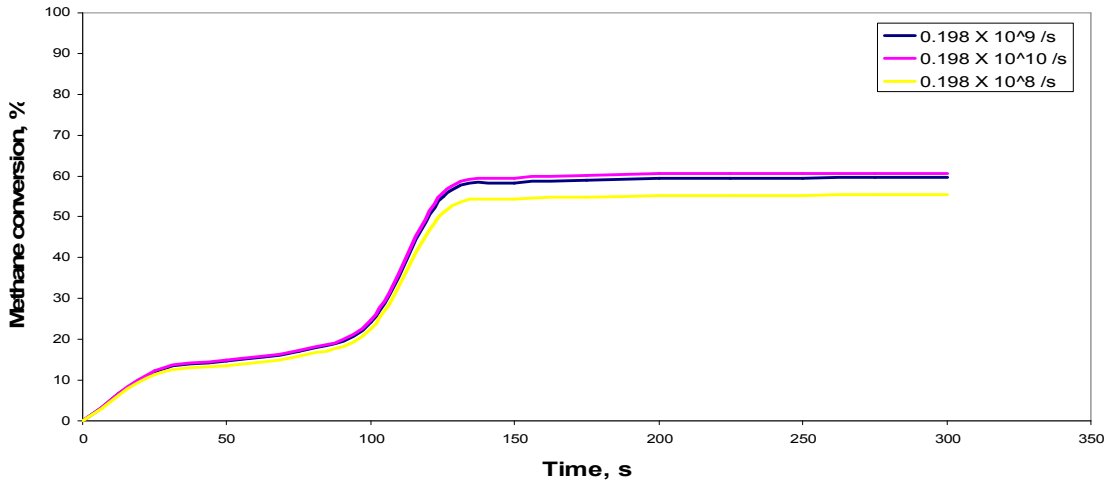

Figure 4.21. Effects of pre-exponential term on CH_4 conversion with an inlet gas temperature of 500^{o}C at a GHSV of 50,000 hr^{-1} for a unidirectional flow.

Figure 4.21 shows methane conversion increases by 1% when the pre-exponential factor is increased by an order magnitude and decreases by 4% when the pre-exponential factor is decreased by an order magnitude. Thus from the graphs it can be said that the pre-exponential factor does not have a strong effect on the conversion efficiency of methane.

4.7 Effect of concentration of methane

The effect of methane concentration on the conversion of methane is analyzed in this section. Three different concentrations 1500, 2000 and 2500 ppm of methane are used with inlet gas temperature of 450^{o}C and a space velocity of 50,000 hr^{-1}. All the other parameters are kept constant. Table 4.6 gives the various conversions for the three different concentrations of methane at various switching times.

Table 4.6. Effect of concentration of methane on methane conversion

Switching Frequency, s	Methane conversion, %		
	1500 ppm	2000 ppm	2500 ppm
unidirectional	89	59	32
10	100	72	41
20	100	77	43
25	100	83	47
30	99	81	46
40	98	77	44

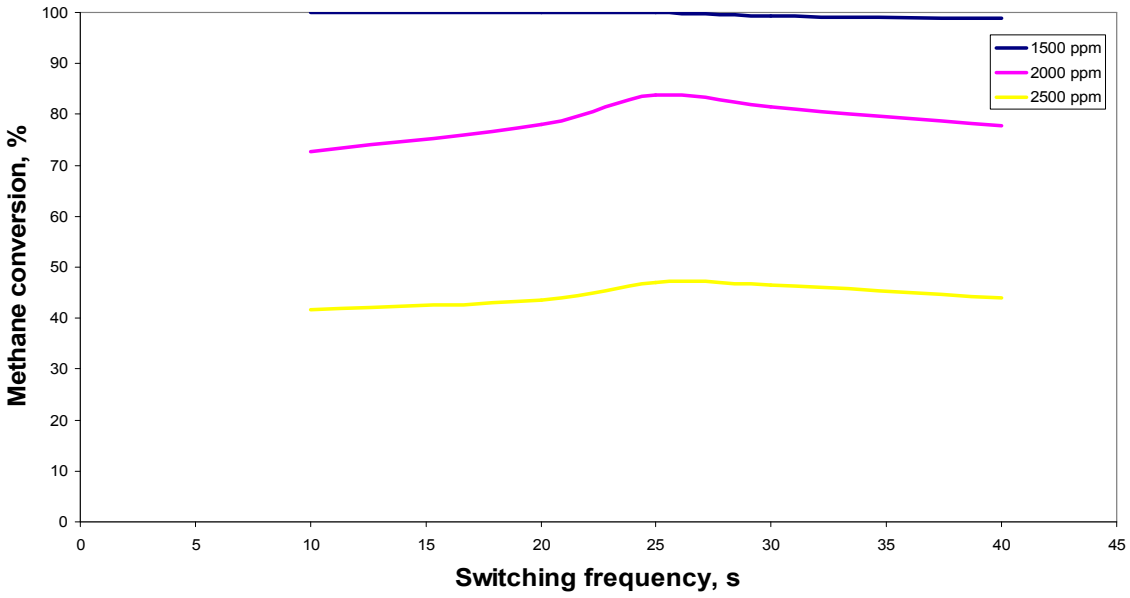

Figure 4.22. Effects of concentration of CH_4 on CH_4 Conversion with an inlet gas temperature of 500^{o}C at a GHSV of 50,000 hr^{-1} for different switching freq.

From figure 4.22 it is found that the conversion of methane goes up by reducing the methane concentration to 1500 ppm. The conversion reaches 100% at around 3cm from the inlet of the catalyst for a 25 second switching frequency as seen in the figure 4.23.

This can be explained from the solid temperature profile where the temperature reaches the peak close to the inlet as the majority of the conversion takes place close to the entrance of the catalyst. The temperature profile when compared between 1500 ppm and 2000 ppm in figure 4.24 shows that there is considerable difference in the average temperature but the peak has moved towards the entrance of the catalyst.

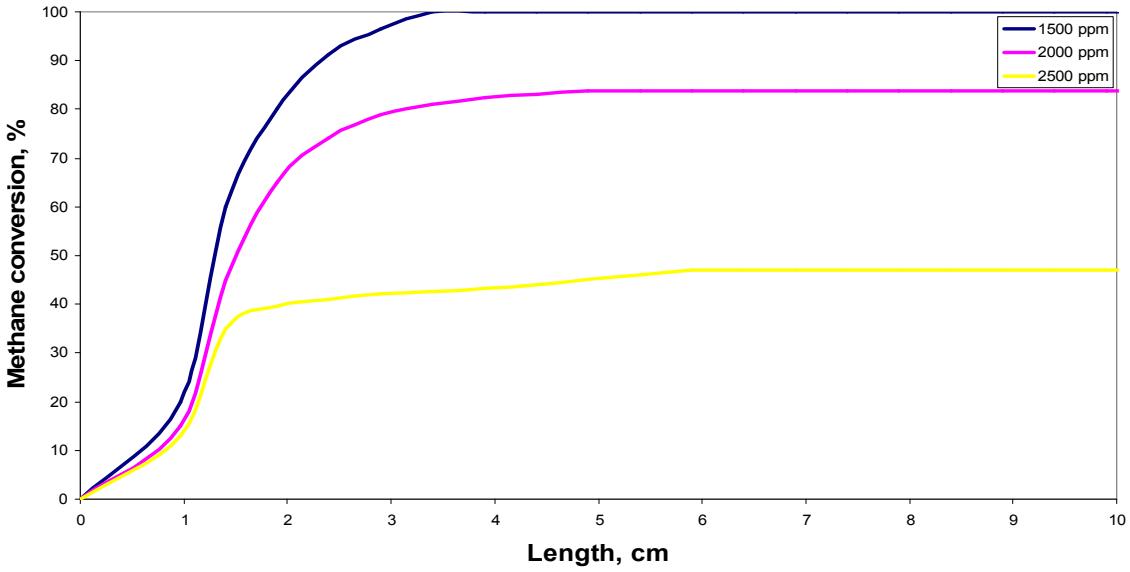

Figure 4.23. Effects of concentration of CH_4 on CH_4 conversion with an inlet gas temperature of 500^oC at a space velocity of 50,000 hr^{-1}

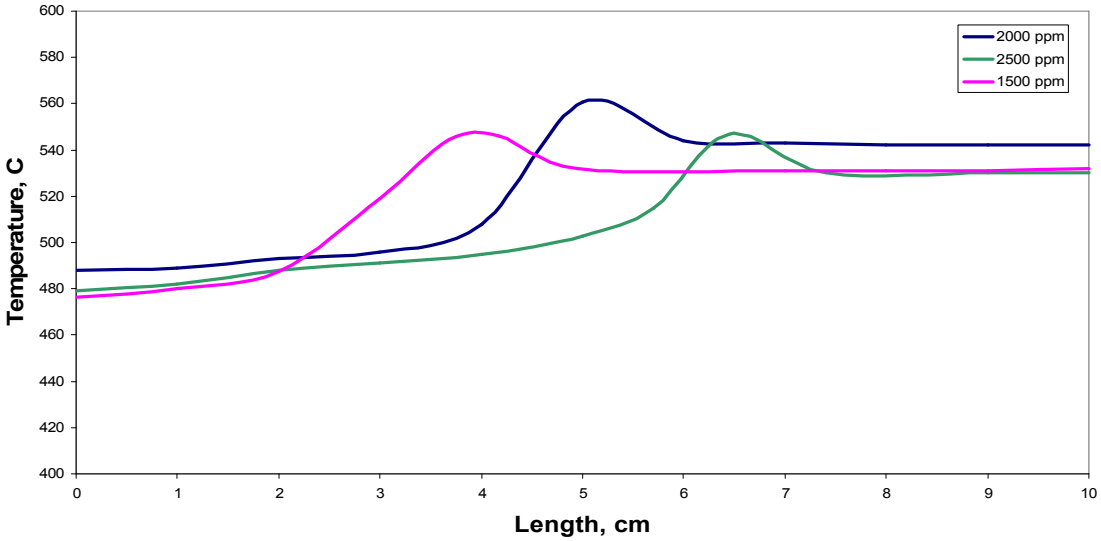

Figure 4.24. Effects of concentration of CH_4 on surface temperature with an inlet gas temperature of 500^oC at a space velocity of 50,000 hr^{-1}

On comparison with the 2000 ppm and 2500 ppm methane concentration solid temperature profile, it is seen that there is not much decrease in the temperature profile though there is a considerable decrease in the conversion. It is also found that the peak of the temperature profile shifts towards the exit as compared to the other cases. In this case the conversion is more diffusion controlled than kinetic control because of the high methane concentration.

4.8 Effect of asymmetric switching

All the previous simulations are done with a symmetric switching time, i.e., the time for the forward flow is the same as the time for the reverse flow. In this section the effect of having different switching time for the forward flow and the reverse flow on

the conversion of methane is analyzed. From the previous results, it was found that the best switching frequency was 25 seconds which is 25 seconds of forward flow and 25 seconds of reverse flow. Simulations were done for asymmetric switching frequency of 25 – 20 and 25 – 30 seconds, which means 25 seconds of forward flow and either 20 or 30 seconds of reverse flow.

Table 4.7 shows the conversion of methane at 450^{o}C and 500^{o}Cfor 2000 ppm methane at a space velocity of 50,000 hr^{-1} for the asymmetric and symmetric switching. The table shows that the conversion efficiency is maximum for symmetric switching with a switching frequency of 25 seconds. The asymmetric switching conversions are lesser than the symmetric switching. The reason for this can be seen from the solid temperature profile for different switching frequencies as shown in figure 4.25.

Table 4.7. Methane conversion for symmetric and asymmetric switching freq.

Temperature, C	Switching freq, s	Methane conversion, %
450	25-25	83.8
	25-20	79.1
	25-30	82.1
500	25-25	96.4
	25-20	92.5
	25-30	93.6

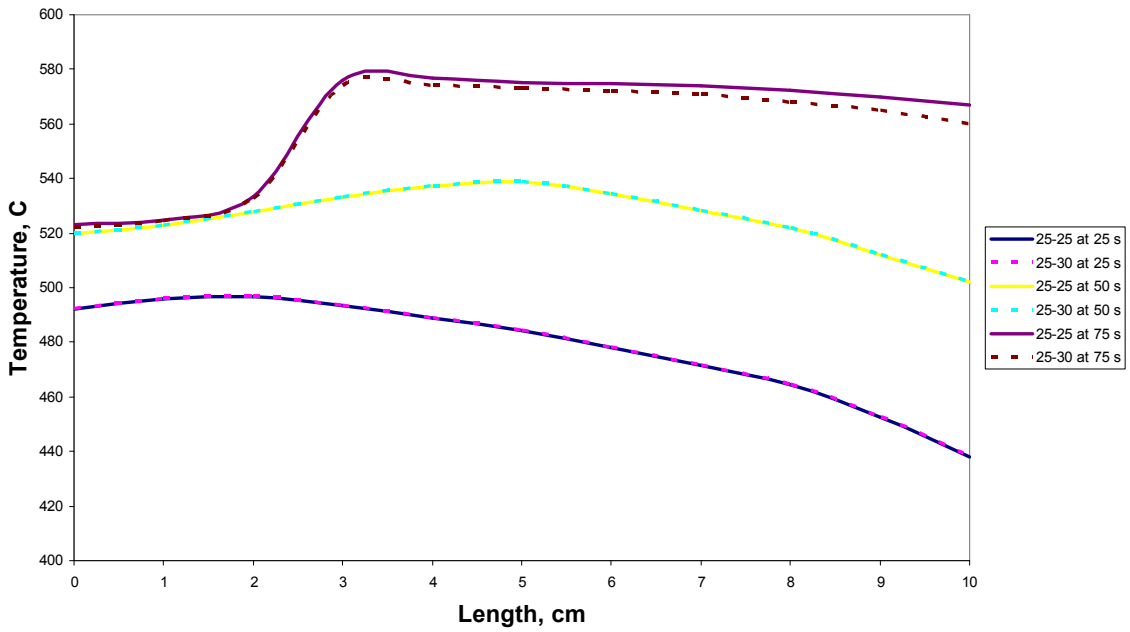

Figure 4.25. Effects of asymmetric switching on surface temperature with an inlet gas temperature of 500^{o}C at a space velocity of 50,000 hr^{-1}.

The solid profile at 25 seconds is similar for both symmetric and asymmetric switching cases as it is forward flow in both the cases. At 50 seconds, the solid temperature is same for both the cases as the effect of asymmetric switching has not yet taken place. At 75 seconds the temperature for the symmetrical switching is slightly more than the asymmetric switching case. This is because at 55 second, the symmetric switching case would have been reversed 5 seconds ago and attained more temperature where as the asymmetric case would have just reversed resulting in a lower temperature as compared to the symmetric switching. Thus the subsequent temperature profiles are lower resulting in a reduced conversion.

CHAPTER 5

CONCLUSIONS AND RECOMMENDATION

This research was targeted towards finding the effects of different important parameters like space velocity, inlet temperature and switching frequency on reverse flow oxidation catalyst. In addition, this research investigates the effect of methane concentration, pre-exponential term, length of catalyst and asymmetric switching on the methane conversion efficiency. The goal of this research is to find the optimum characteristics and settings to maximize the methane conversion efficiency.

The results from the simulation program developed for the flow of exhaust gases from natural gas engines through a reverse flow oxidation catalyst indicate that the flow reversal increases the methane conversion efficiency to a considerable level. At low inlet gas temperature and low space velocity (20,000 hr^{-1}), the effect of reversing the flow through the catalyst is negligible. But at higher space velocities, reverse flow has a significant effect on the methane conversion. Methane conversion increased by 40.6% at an inlet gas temperature of 450^{o}C for a space velocity of 50,000 hr^{-1} with a 25 second switching frequency. Short switching times of 10 seconds and 20 seconds do enhance the methane conversion efficiency. A switching time of 25 seconds is found to be the optimum switching time. Switching times of 30 seconds and 40 seconds are effective at higher space velocities (80,000 hr^{-1}).

It is also found that the length of the catalyst plays an important role in the methane conversion. The optimum length is found to be 10 cm. Shorter lengths resulted in reduced residence times resulting in a reduced conversion. At higher lengths, the surface temperature is lower towards the exit and hence reduces conversion. Ideally the peak in the surface temperature profile should be at the centre of the catalyst as in the case of 10 cm long catalyst. The pre-exponential term appears not to have any appreciable effect on the methane conversion. Even an order of magnitude difference results in a couple of percentage difference in methane conversion. The concentration of methane also plays a very important role in the methane conversion. Increased concentration (2500 ppm) yields very low conversion percentage as compared to nominal value (2000 ppm). Asymmetrical switching results in a reduced methane conversion. This is due to the fact that 25 second switching is the ideal and any variation to it results in a reduced conversion.

References

1. Willard W. Pulkrabek, “Engineering Fundamentals of the Internal Combustion Engine”, 2nd Edition, Pearson, Prentice Hall.
2. S. Salamons, R.E. Hayes, M. Poirier and H. Sapoundjiev, “Flow Reversal Reactor of the Catalytic Combustion of Lean Methane Mixtures”, Catalysis Today, Vol. 83, pp. 50-69, 2003.
3. Naturalgas.org maintained by natural gas supply organization, “Electric Generation Using Natural Gas”, 12/14/05, http://naturalgas.org/overviews/uses_electrical.asp
4. Jordan K. Lampert, M. Shahjahan Kazi, Robert J. Farrauto, “Palladium catalyst performance for methane emissions abatement from lean burn natural gas vehicles”, Applied Catalysis B: Environmental 14 (1997) 211-223.
5. R.A. Dalla Betta and T. Rostrup-Nielson, “Application of catalytic combustion to a 1.5 MW industrial gas turbine”, Catalysis Today, Vol. 47, pp. 369, 1999.
6. F. Moallemi, G. Batley, V. Dupont, T.J. Foster, M. Pourkashanian and A. Williams, “Chemical Modeling and Measurement of the Catalytic Combustion of CH4/air mixtures on Platinum and Palladium Catalysts.
7. I. Stambler, Gas Turbine World, May-June, 1993, p. 32.
8. R.F. Hicks, H. Qi, M.L. Young and R.G. Lee, “Structure sensitivity of methane oxidation over platinum and palladium” J. Catal., Vol. 122, pp 280, 1990.
9. Alan Janbey, Wayne Clark, Ehan Noordally, Sue Grimes, Saad Tahir, “ Noble metal catalysts for methane removal”, *Chemosphere 52 (2003) 1041-1046*.

10. H. Zufle and T. Turek, " Catalystic Combustion in a reactor with Periodic Flow Reversal : experimental results", Chemical Engineering and Processing, Vol. 36, pp. 327-340, 1997.
11. Liu, B., Checkel, M.D., Hayes, R.E., Zheng, M., and Mirosh, E., "Experimental and Modeling Study of Variable Cycle Time for a Reversing Flow Catalytic Converter for Natural Gas/Diesel Dual Fuel Engines," SAE Paper 2000-01-0213, 2000.
12. Matros yu. Sh. And G.A. Bunimovich, " reverse-flow operation in fixed bed catalytic reactors", catal. Rev. sci. eng, 38(1), 1-68, 1996.
13. B. Liu, M.D. Checkel, R.E. Hayes, M. Zheng and E. Mirosh, "Experimental and modeling study of variable time for a reversing flow catalytic converter for natural gas / diesel dual fuel engines", Society of Automotive Engineers, 2000 – 01 – 0213.
14. Stan T. Kolaczkowski, W. John Thomas, and James Titiloye, "Transient Experiments and Modeling of the Catalytic Combustion in a Monolith Reactor", Industrial Engineering and Chemistry Research, Vol. 35(2), pp. 406-414, 1996.
15. G. Zhu, J. Han, R.S. Monteiro, D. Zemlyanov and F.H. Ribiero, " Complete Methane Oxidation on Palladium Model Catalyst", Worcester Polytechnic Institute, MA.
16. R.H. Hayes, J. Wei and J.R. Katzer, "Transient response of Monolith Catalyst Support", Chemical Reaction Engineering: Adv. Chem. Ser., Vol. 133, pp. 34, 1974.

17. Robert E. Hayes, Stan T. Kolaczkowski, W. Thomas and James Titiloye, "Transient experiments and modeling of the catalytic combustion of methane in a monolith reactor", Ind. Eng. Chem., Vol. 35(2), pp. 406 – 414, 1996.
18. Paloma Hurtado, Salvador Ordóñez, Herminio Sastre, Fernando V. D´ıez, "Development of a Kinetic Model for the Oxidation of Methane over Pd/Al2O3 at Dry and Wet Conditions", Applied Catalysis B: Environmental Vol. 51, pp. 229–238, 2004.
19. CF. Cullis, and B.M. Willatt, "Oxidation of methane over supported precious metal catalysts', Journal of Catalysis, Vol. 83: pp. 267-285, 1983.
20. C. R. F. Lund, S. S. Peri and S. Harou-Kouka, "Changes in Reaction Kinetics During Activation of Supported Pd", Chemical Engineering Department, SUNY-Buffalo.
21. Joo H. Lee, David L. Trimm, "Catalytic combustion of methane", Fuel Processing Technology, Vol. 42, pp. 339-359, 1995.
22. R.J. Farrauto, M.C. Hobson, T. Kennelly and E.M. Waterman, "Catalytic chemistry of supported palladium for combustion of methane", Appl. Catal. A: General, Vol. 81, pp. 227, 1992.
23. G. Zhu, J. Han, R.S. Monteiro, D. Zemlyanov and F.H. Ribiero, " Complete Methane Oxidation on Palladium Model Catalyst", Worcester Polytechnic Institite, MA.
24. Alan C. Hindmarsh, Serial fortran solvers for oridianry initial value problems. www.llnl.gov/CASC/odepack/download.htm

Appendix

A.1 Main and Subroutines used in this program code

A.1.1 Driver

This is the main program which is executed first. This is where the variables are defined and the memory allocations are done. We can see that most of the variables are defined as common. This is to define it as a global variable so that its values are available for all the subroutines for further calculations. The main program is where we input all the values. This is the program that accepts the input values for the variables used. After accepting the input parameters, it divides the catalyst into 200 nodes for computing the concentration and the temperature along the length of the catalyst. All input boundary conditions are assigned to node zero. The main program is where all the subroutines are called from. After going through all subroutines, the results are displayed using a print statement.

A.1.2 c1solver

This subroutine is called from the main program. The purpose of this subroutine is to find the terms required for the mass balance equation. It calculates the mass transfer coefficients from Sherwood number and hydraulic radius. The Sherwood number is found to 3.608 in our case. From c1solver the control is transferred to node1 subroutine at node 1 and to nleqs subroutine for the remaining nodes.

A.1.3 node1

This is the subroutine where the parameters for the first node are found. Node1 subroutine computes the reaction rate, temperature and concentration of different species at the point. It uses a subroutine called Hybrd.

A.1.4 nleqs

This subroutine is called from c1solver and this is used for computing the values at the remaining 79 nodes. This solves fully coupled non linear algebraic equations. The complex species conservation and mass conservation equations are broken to non linear algebraic equation using the finite difference method. The values that are obtained at the end of the subroutine is sent back to c1solver which in turn does calculation and send it back to the main program.

A.1.5 lsode

Lsode stands for Livermore solver for ordinary differential equation. LSODE is the basic solver of the collection, and solves explicitly given systems. It solves stiff and nonstiff systems of the form dy/dt = f, where y is the vector of dependent variables and t is the independent variable. In the stiff case, it treats the Jacobean matrix df/dy as either a

dense (full) or a banded matrix, and as either user-supplied or internally approximated by difference quotients. It uses Adams methods (predictor-corrector) in the nonstiff case and Backward Differentiation Formula (BDF) methods (the Gear methods) in the stiff case. The linear systems that arise are solved by direct methods (LU factor/solve). LSODE supersedes the older GEAR and GEARB packages, and reflects a complete redesign of the user interface and internal organization, with some algorithmic improvements. This program is called from the main program.

When using LSODE, some important inputs are:

- Number of first-order Ode's
- Array of initial values
- Initial value of independent variable
- First point where output is desired
- Tolerance
- Name of subroutine for Jacobean matrix (optional)
- Method flag (can choose between BDF or Adams methods, user-supplied or internally generated Jacobean, banded or full Jacobean, etc.)

In addition, the expected output includes:

- The y(t) vector of computed values

- Corresponding value of independent variable
- A state flag (indicates if program was successful or not and why)

A.1.6 hybrd1

The purpose of the entire HYBRD system of subroutines is to solve the nonlinear algebraic equations. The hybrd1 subroutine is to find a zero of a system of N nonlinear functions in N variables by a modification of the Powell hybrid method. The user must provide a subroutine which calculates the functions. The Jacobean is then calculated by a forward difference approximation. It requires the physical variables to be renamed as mathematical variables and be used. In our model we have a total of 9 equations and 9 unknowns. Hybrd solves these 9 equations and it gives us the concentration of the various species and the catalyst temperature at all those nodal points. This subroutine is called from both node1 and nleqs. It returns the main program with newly computed values at the nodal points.

A.2 Input screen

The program runs of a batch file. The input screen has all the variables that can be modified for different runs. If ireverse is set to 0 then it runs as a unidirectional flow. If it is set to 1 then it runs as a reverse flow. The time step for output gives the profiles at the chosen intervals. The total time for transient gives the

total time for which the simulation is run and time step for reversal gives the switching frequency. The next part gives the thermodynamic property and the catalyst properties. Then the input table has the concentrations of different species and the heat of formation. The tolerance for the Livermore solver (LSODE) is set to 1 X 10^{-5} which is in the acceptable range.

```
#! /bin/csh -f
#---------------------------------------------------------------
echo '------> cat.x started\!'
./cat.x << EOF
#------  output control  ------------------------------------
10.0     ![10] dt: time step for output (s)
300.0     ![240] totaltm: total time for transient (s)
25.0    ![10] rt: time step for reversal (s)
1        !ireverse: reverse flow direction in intervals of dt [0=no;
1=yes]
#------  thermodynamic, material and flow properties  ----------
300.0     ![550] tsin: initial solid temp (K)
773.0     ![600] tgin: inlet gas temp (K)
36.4      !mdottot:  total mass flow rate(g/s) (36.4,40.2,44.0)
0.1013    !press: inlet gas pressure (MPa or Nt/mm^2 to cancel
units)
1.089     !cpg:  specific heat of gas (J/gK)
2.5       !rhos: solid density (g/cm^3)
0.01675   !thcons: thermal conductivity of solid (W/cmK)
#------  catalyst properties  ---------------------------------
10.0      !alen: flow length in cat (cm)(10)
60.0      !facearea: face area of cat (cm^2)(60)
268.95    !ax: catalyst surface area per unit reactor volume
(/cm)(268.95)
0.6836    !eps:  "hole" fraction
46.5      !chandens: channel openings per cm**2(46.5)
#------  inlet mole fractions  --------------------------------
0.005      !ygin(1): CO inlet mole frac(0.02)
2000.0d-6  !ygin(2): C3H6(450)
0.0001     !ygin(3): H2(.00667)
0.06       !ygin(4): O2(0.05)
500.0d-6  !ygin(5): NO (500)
#------  heats of formation (J/g-mol)  ------------------------
2.832d5   !deltah(1) [2.432d6]: CO  + 0.5 O_2 -> CO_2
1.928d6   !deltah(2) [1.928d6]: CH_4+  2O_2 -> CO_2 + 2H_2O
2.420d5   !deltah(3) [2.420d5]: H_2 + 0.5 O_2 -> H_2O
0.0       !deltah(4) [0.0]
0.0       !deltah(5) [0.0]
#------  other parameters -------------------------------------
3.608      !sherw [3.608]: Sherwood number
3.608      !anuss [3.608]  Nusselt number
```

```
1.0d-5    ![1.0d-5] rtol: relative tolerance for LSODE
1.0d-5    ![1.0d-5] atol: absolute tolerance for LSODE
#-------------------------------------------------------------
EOF
exit
```

A.3 Common block comblock.i

This is common block that used in all routines and sub routines. It has the entire global variable with their corresponding values.

```
      parameter (neqn=101)  !# of nodes (= #intervals+1)
c      parameter (lrw=22+13*neqn)
      parameter (lrw=20+16*neqn)
      parameter (liw=20+neqn)
c      common/intdata/deltah(5),ygin(5)
      common/intdata/deltah(5),ygin(5),tgin,tsin

common/variables/cg(5,0:neqn),cs(5,neqn),rate1(5,neqn),tg(0:neqn)
      common/one/sherw,ax,rhos,eps,flarea,press,thcons
      common/node/ts,tga,heat,rate(5)
      common/constant/rgas,sigma
      common/two/anuss,dhyd,mdot,cpg,s,dx
      common/critparm/tc(5),pc(5),xmolw(5),air_mw,air_tc,air_pc

common/jacob/denom(neqn),tsdot(neqn),dtgdts(neqn),dheatdts(neqn),
     &             heatsum(neqn),solidcnd,heatcon
      common/jacob1/dratedts(5),nfun
      common/radterms/drdti(neqn),drdtim1(2:neqn),drdtip1(neqn-1),
     &             viewfac(0:neqn+1,0:neqn+1)
      real*8 mdot
```

A.4 Cat_conv.f

This is the main program that is called by the executable file. It has all the main routines and the sub routines. This program also calls the Livermore Solver for ordinary differential equations (LSODE). The program also reads the data from the jcat input file. The output is in the form of four files. The first file contains all the

conversion and temperature data. The second file has the gas temperature as a function of length at various times and the third file has the surface temperature as a function of length at various times. The fourth file contains the conversion data as a function of time.

```
ccc*******Driver routine********
      program cat_converter
      implicit real*8(a-h,o-z)
      external fex,jex
      include 'comblock.i'
c      real*8 outdat(neqn,9)
      real*8 mdottot
cfxt1_output
      real*8 gasfrac(5)
cfxt2_output
      dimension y(neqn),rwork(lrw),iwork(liw)
      dimension depth(0:neqn)
c      call cpu_time(start_time)
cfxt0_linux      call timer(istart)  ! start runtime clock for Lahey
c input parameters
      read(5,*) !------- output control  --------------
      read(5,*) dt       ! time step for output (s)
      read(5,*) totaltm  ! total time for transient (s)
      read(5,*) ireverse ! reverse flow direction [0=no; 1=yes]
      read(5,*) !------- thermodynamic, material and flow properties
--
      read(5,*) tsin     ! initial solid temp (K)
      read(5,*) tgin     ! inlet gas temp (K)
      read(5,*) mdottot  ! total mass flow (g/s)
      read(5,*) press    ! inlet gas pressure (MPa or Nt/mm^2 to
cancel units)
      read(5,*) cpg      ! specific heat of gas (J/gK)
      read(5,*) rhos     ! solid density (g/cm^3)
      read(5,*) thcons   ! thermal conductivity of solid (W/cmK)
      read(5,*) !------- catalyst properties  ---------
      read(5,*) alen     ! flow length in cat (cm)
      read(5,*) facearea ! face area of cat (cm^2)
      read(5,*) ax       ! catalyst surface area per unit reactor
volume (/cm)
      read(5,*) eps      ! "hole" fraction
      read(5,*) chandens ! channel openings per cm**2
      read(5,*) !------- inlet mole fractions  ---------
      read(5,*) ygin(1)  ! CO inlet mole frac
      read(5,*) ygin(2)  ! C3H6
      read(5,*) ygin(3)  ! H2
      read(5,*) ygin(4)  ! O2
      read(5,*) ygin(5)  ! NO
      read(5,*) !------- heats of formation (J/g-mol)  ----
```

```
      do i=1,5
        read(5,*) deltah(i) !heat of formations (J/g-mol)
      enddo
      read(5,*) !------- other parameters -------------
      read(5,*) sherw    ! Sherwood number
      read(5,*) anuss    ! Nusselt number
      read(5,*) rtol     ! relative tolerance for LSODE
      read(5,*) atol     ! absolute tolerance for LSODE
      read(5,*) !------- empty line -------------------
c  end input parameters
      s=4.*sqrt(chandens*eps)  ! ht area / total vol (cm^-1)
      flarea=facearea*eps
      dhyd=4.*eps/s  !sqrt(eps/chandens)  ! hydraulic diameter
      nchannel=facearea*chandens
      mdot=mdottot/nchannel
cfxt      dx=alen/dfloat(neqn)
      dx=alen/(dfloat(neqn)-1.0)  !neqn is # nodes (not intervals)
      call viewfact
      nprint=ifix(totaltm/dt)
      cg(1,0)=ygin(1)
      cg(2,0)=ygin(2)
      cg(3,0)=ygin(3)
      cg(4,0)=ygin(4)
      do i=1,neqn
        y(i)=tsin
        tg(i)=tsin
        do k=1,5
          cg(k,i)=ygin(k)
          cs(k,i)=ygin(k)
        enddo
      enddo
c  compute the mesh points
cfxt      depth(0)=0.0
      depth(1)=0.0
      do i=2,neqn
        depth(i)=depth(i-1)+dx
c       outdat(i,1)=depth(i)
      enddo
      tg(0)=tgin
      neq=neqn  !# nodes
      t=0.0     !initial value of independent variable
      tout=dt   !first point where output is desired (>t)
      itol=1    !=1 if atol is a scalar; =2 if atol is array
      itask=1   !=1 for normal computation of output values of y at
tout
      istate=1  ![=1] integer flag (input and output)
      iopt=0    !=0 if no optional inputs used
      mf=24     !method flag: =24 (stiff method) user-supplied
banded Jacobian
      iwork(1)=1  !input upper and lower bandwidths
      iwork(2)=1
      dtmin=1000.
      dtmax=0.
      tmin=0.
      tmax=0.
```

```
cfxt1_output
      write(13,'(a)')'#Gas Conversion Fractions at Channel Exit'
      write(13,'(a)')'#       Time          CO        Fuel'//
     &               '          H2          O2'
cfxt2_output
      do 40 iout=1,nprint
        call lsode(fex,neq,y,t,tout,itol,rtol,atol,itask,istate,
     &             iopt,rwork,lrw,iwork,liw,jex,mf)
cfxt       print*,t,tout,istate
cfxt            print *
        write(10,*)
cfxt         write(10,10100) t,depth(0),tg(0),(ygin(k),k=1,4)
        write(10,10100) t,depth(1),tgin,(ygin(k),k=1,4)
        write(11,'(a,f6.2)') '& Gas Temperature at Time [s] = ',t
        write(12,'(a,f6.2)') '& Solid Temperature at Time [s] = ',t
        do i=1,neqn
          write(10,10110)depth(i),tg(i),y(i),
c     &       (cg(k,i),cs(k,i),k=1,4)
     &       (cg(k,i),cs(k,i),rate1(k,i),k=1,4)
c          outdat(i,iout+1)=y(i)
          write(11,'(f10.2,1pe12.5)') depth(i),tg(i)
          write(12,'(f10.2,1pe12.5)') depth(i),y(i)
        enddo !do i=1,neqn
c        write(10,fmt="(5f8.3)") t,(1.-cg(k,neqn)/cg(k,0),k=1,4)
cfxt1_output
cfxt         write(10,10101)(1.-cg(k,neqn)/cg(k,0),k=1,4)
        do k=1,4
          gasfrac(k)=1.-cg(k,neqn)/ygin(k)
        enddo
        write(10,10101)(gasfrac(k),k=1,4)
        write(13,'(f12.2,4(1pe12.5))') t, (gasfrac(k),k=1,4)
cfxt2_output

        if(istate.ne.2) then  !if lsode successful then istate=2
          write(10,10090)istate
          go to 100
        endif
        dtminmax=rwork(11)
        if(dtminmax.lt.dtmin) then
          dtmin=dtminmax
          tmin=tout
        elseif(dtminmax.gt.dtmax) then
          dtmax=dtminmax
          tmax=tout
        endif
        tout=tout+dt
cfxt1_reverse
        if(ireverse.eq.1) then
          call reversearray(2,neqn+1,tg)
          call reversearray(1,neqn,y)
c          call reversearray(21,20+neqn,rwork) !used if istate=2
          call reversematrix(5,2,neqn+1,cg)
          call reversematrix(5,1,neqn,cs)
          istate=1   !istate=1 then lsoded.f does initializations
again
```

```
c        stop
        endif !if(ireverse.eq.1)
cfxt2_reverse
40    continue
c      do 50 i=1,neqn
c            write(10,fmt="(9f7.1)") (outdat(i,j),j=1,9)
c50    continue
cfxt      print *,' dtmin @ ',dtmin,tmin
      write(10,*) 'dtmin @ ',dtmin,tmin
cfxt      print *,' dtmax @ ',dtmax,tmax
      write(10,*) 'dtmax @ ',dtmax,tmax
100   write(10,10060) iwork(11),iwork(12),iwork(13)
cfxt      print *,' concentration function evaluations ',nfun
      write(10,*) 'concentration function evaluations ',nfun
c      call cpu_time(end_time)
c      print *,' cpu time ',end_time-start_time
cfxt0_linux     call timer(istop)
cfxt      print *,' elapsed time (s)',(istop-istart)/100.
      write(10,*) 'elapsed time (s)',(istop-istart)/100.
      stop
10060 format(/,' no. LSODE steps =',i4,' function evaluations=',i4,
     &      ' jacobian evaluations=',i4)
10090 format(///22h error halt.. istate=,i3)
10100 format( ' Time ',f6.0,/,' Position',' Tgas',' Twall',2x,
c     &      ' Gas CO',13x' Gas C3H6',11x,' Gas H2',13x,' Gas O2',/,
c     &      1x,f6.3,1x,f5.1,8x,4(e10.3,10x))
     &      ' Gas CO   Wall CO   Rate CO   ',
     &      ' Gas C3H6 Wall C3H6 Rate C3H6 ',
     &      ' Gas H2   Wall H2   Rate H2   ',
     &      ' Gas O2   Wall O2   Rate O2',/,
     &      1x,f6.3,1x,f5.1,8x,4(e10.3,20x))
10101 format(' gas conversion frac ',4(e10.3,20x))
c10110 format(1x,f6.3,1x,f5.1,1x,f6.1,1x,8d10.3)
10110 format(1x,f6.3,1x,f5.1,1x,f6.1,1x,12d10.3)
      end
cfxt ------------------------------------------------------------------
---
      subroutine reversearray(nstart,nend,aa)
      implicit real*8(a-h,o-z)
      real*8 aa(*)
      do i=nstart,(nstart+nend-1)/2
        store=aa(i)
        aa(i)=aa(nend-i+nstart)
        aa(nend-i+nstart)=store
c        print*,store,aa(i)
      enddo
      return
      end
cfxt ------------------------------------------------------------------
---
      subroutine reversematrix(nvec,nstart,nend,aa)
      implicit real*8(a-h,o-z)
      real*8 aa(nvec,*)
      do k=1,nvec
        do i=nstart,(nstart+nend-1)/2
```

```
          store=aa(k,i)
          aa(k,i)=aa(k,nend-i+nstart)
          aa(k,nend-i+nstart)=store
c          print*,store,aa(k,i)
        enddo
      enddo
      return
      end
cfxt ----------------------------------------------------------------
---
      subroutine fex(n,t,y,ydot)
      implicit real*8(a-h,o-z)
      dimension y(*),ydot(*)
      include 'comblock.i'
      real*8 radheat(neqn)
      cps(arg)=1.071+3.12d-04*arg+3.435d+04/(arg*arg) ! specific
heat of the solid
      data kn/0/
      call radiant(n,y,radheat)
      call gastemp(n,y)
cfxt0      tga=0.5*(tg(0)+tg(1))
      tga=0.5*(tgin+tg(1))
      call heatgen(1,y(1),tga,t)
cfxt      print*,t, y(1),tga
      solidcnd=(1.-eps)*thcons/dx**2
      heatcon=s*mdot*cpg/(4.*dhyd*dx)
      denom(1)=(1.-eps)*rhos*cps(y(1))
cfxt0      ydot(1)=(2.*solidcnd*(y(2)-y(1))+heatcon*(tg(0)-
tg(1))+radheat(1)
      ydot(1)=(2.*solidcnd*(y(2)-y(1))+heatcon*(tgin-
tg(1))+radheat(1)
     &      + heatsum(1))/denom(1)
      do 10 i=2,n-1
            tga=0.5*(tg(i)+tg(i-1))
            call heatgen(i,y(i),tga,t)
            denom(i)=(1.-eps)*rhos*cps(y(i))
            ydot(i)=(solidcnd*(y(i+1)+y(i-1)-2.*y(i))+radheat(i)
     &          + heatcon*(tg(i-1)-tg(i)) + heatsum(i))/denom(i)
10    continue
      tga=0.5*(tg(n)+tg(n-1))
      call heatgen(n,y(n),tga,t)
      denom(n)=(1.-eps)*rhos*cps(y(n))
      ydot(n)=(2.*solidcnd*(y(n-1)-y(n))+heatcon*(tg(n-1)-tg(n))
     1  + radheat(n) + heatsum(n))/denom(n)
c load jacobian array
      do 20 i=1,n
            tsdot(i)=ydot(i)
20    continue
      kn=kn+1
      return
      end
c----------------------------------------------------------------------
----
      subroutine jex(n,t,y,ml,mu,pd,nrowpd)
c computes Jacobian matrix (if mf=21 or mf=24)
```

```
      implicit real*8(a-h,o-z)
      dimension y(n),pd(nrowpd,n)
      include 'comblock.i'
c derivative of solid specific heat term
      dcps(arg)=(1.-eps)*rhos*(3.12d-04-2.*3.435d+04/arg**3)
      pd(1,2)=(2.*solidcnd+drdtip1(1))/denom(1)
      pd(2,1)=(-2.*solidcnd-heatcon*dtgdts(1)+dheatdts(1)+drdti(1)
     &            -tsdot(1)*dcps(y(1)))/denom(1)
      do 10 i=2,n-1
            pd(1,i+1)=(solidcnd+drdtip1(i))/denom(i)
            pd(2,i)=(-2.*solidcnd-
heatcon*dtgdts(i)+dheatdts(i)+drdti(i)
     &            -tsdot(i)*dcps(y(i)))/denom(i)
            pd(3,i-1)=(solidcnd+drdtim1(i)
     &                +heatcon*dtgdts(i)*dtgdts(i-1))/denom(i)
10    continue
      pd(3,n-1)=(2.*solidcnd+drdtim1(n)
     &          +heatcon*dtgdts(n)*dtgdts(n-1))/denom(n)
      pd(2,n)=(-2.*solidcnd-heatcon*dtgdts(n)+dheatdts(n)
     &            -tsdot(n)*dcps(y(n)))/denom(n)
      return
      end
c-----------------------------------------------------------------------
----
      subroutine viewfact
      implicit real*8(a-h,o-z)
      include 'comblock.i'
      real*8 pi/3.141592654d0/
      s1(j,i)=(abs(j-i)-1)*dx/dhyd !separation distance, C-16, pg104
      f(z)=2.*(sqrt(z*z+1.)*atan(1./sqrt(z*z+1.))-z*atan(1./z))
     &      +z*z/2.*log((z*z+1.)**2/(z*z*(z*z+2.))) ! C-16, pg104
      f1_2(w)=1./(pi*w)*(w*atan(1./w)+pi/4.-sqrt(1.+w*w)*
     &      atan(1./sqrt(1.+w*w))+0.25*log(2.*(1.+w*w)/(2.+w*w)*
     &
(w*w*(2.+w*w)/(w*w+1.)**2)**(w*w)*(w*w+2.)/(2.*(w*w+1.))))!C-13, pg
98
      do 10 i=1,neqn
            if(i.eq.1) then
                viewfac(0,1)=f1_2(dx/dhyd)
            else
                viewfac(0,i)=i*f1_2(i*dx/dhyd)-(i-1)*f1_2((i-
1)*dx/dhyd)
            endif
            viewfac(i,0)=viewfac(0,i)
            viewfac(i,i)=1.-2.*viewfac(0,1) ! allow for node to see
itself
            if (i.eq.neqn) then
                viewfac(neqn+1,neqn)=f1_2(dx/dhyd)
            else
                viewfac(neqn+1,i)=(neqn-i+1)*f1_2((neqn-
i+1)*dx/dhyd)-
     &                  (neqn-i)*f1_2((neqn-i)*dx/dhyd)

viewfac(i+1,i)=dhyd/(2.*pi*dx)*(f(s1(i+1,i)+2.*dx/dhyd)-
     &                  2.*f(s1(i+1,i)+dx/dhyd)+pi/2.)
```

```
            endif
            viewfac(i,neqn+1)=viewfac(neqn+1,i)
            viewfac(i,i+1)=viewfac(i+1,i)
            do 15 j=i+2,neqn

viewfac(j,i)=dhyd/(2.*pi*dx)*(f(s1(j,i)+2.*dx/dhyd)-
     &                 2.*f(s1(j,i)+dx/dhyd)+f(s1(j,i)))
                  viewfac(i,j)=viewfac(j,i)
15          continue
10    continue
check viewfactor sum to unity
      do 20 i=1,neqn
            viewsum=0.
            do 25 j=0,neqn+1
                  viewsum=viewsum+viewfac(j,i)
25          continue
            if (viewsum.gt.1.001.or.viewsum.lt.0.999) then
                  print *,' i,viewsum',i,viewsum
                  stop
            endif
20    continue
c
      return
      end
c-----------------------------------------------------------------------
----
      subroutine radiant(n,y,radheat)
      implicit real*8(a-h,o-z)
      include 'comblock.i'
      dimension y(n),radheat(n)
      real*8 t4(0:neqn+1)
      do 5 i=1,n
            t4(i)=y(i)**4
5     continue
cfxt      t4(0)=tg(0)**4
      t4(0)=tgin**4
      t4(n+1)=tg(n)**4
      do 10 i=1,n
            temp=0.
            dtempdti=0.
            do 15 j=0,n+1
                  temp=temp+viewfac(j,i)*(t4(j)-t4(i))
                  dtempdti=dtempdti-viewfac(j,i)
15          continue
            radheat(i)=s*sigma*temp
            drdti(i)=4.*s*sigma*dtempdti*t4(i)/y(i)
10    continue
      do 20 i=2,n
            drdtim1(i)=4.*s*sigma*viewfac(i-1,i)*t4(i)/y(i)
20    continue
      do 30 i=1,n-1
            drdtip1(i)=4.*s*sigma*viewfac(i+1,i)*t4(i)/y(i)
30    continue
      return
      end
```

```
c-----------------------------------------------------------------------
----
      subroutine gastemp(n,y)
      implicit real*8(a-h,o-z)
      include 'comblock.i'
      dimension y(n)
      real*8 lambda,ntu,nu
      lambda(arg)=2.269d-6*arg**0.832 ! gas thermal conductivity
      nu(arg)=-0.89d-1+arg*(6.108d-4+arg*6.542d-7)
c kinematic viscosity from Jeong & Kim, eqn 21 (mult by 10^4 for
cm^2/s)
      do 10 i=1,n
            ntu=anuss*lambda(0.5*(tg(i)+tg(i-1)))*dx*4./(mdot*cpg)
            tg(i)=((1.-0.5*ntu)*tg(i-1)+ntu*y(i))/(1.+0.5*ntu)
            dtgdts(i)=ntu/(1.+0.5*ntu)
            re=mdot*rgas*tg(i)/(dhyd*press*air_mw*nu(tg(i)))
            if(re.gt.2000.) print *,' turbulent flow, i,re',i,re
            if(ntu.gt.2.) then
                  print *,' node too long. ntu,i,ts,tg',
     &                  ntu,i,y(i),tg(i)
                  stop
            endif
10    continue
      return
      end
c-----------------------------------------------------------------------
----
      subroutine heatgen(node,tsolid,tgas,time)
      implicit real*8(a-h,o-z)
      include 'comblock.i'
      double precision x(4),f(4),a(4,4)
      integer ipvt(4)
      real*8 deltacsi(4)/4*0.d0/
      data tol/1.d-7/
      integer*4 nn/4/
      save deltacsi
      do 10 m=1,nn
            x(m)=cg(m,node)+deltacsi(m) ! guess for start of Newton
iteration
10    continue
      ts=tsolid
      tga=tgas
      do 20 iter=1,15
            call fcn(node,nn,x,f,a,nn)
            call dgefa(a,nn,nn,ipvt,info)
            if(info.ne.0) print *,' singular matrix at ',info
            call dgesl(a,nn,nn,ipvt,f,0)
            iflag=0
            do 25 m=1,4
                  x(m)=x(m)+f(m)
                  error=abs(f(m)/x(m))
                  if(error.gt.tol)iflag=m
25          continue
            if(iflag.eq.0) go to 30
20    continue
```

```
      print *,' newton iteration failure at time',time
      print *,' node,iflag,error',node,iflag,error
      print *,' x,dx',x(iflag),f(iflag)
      print *,' ts,tgas',ts,tga
      stop
30    continue
      heat=0.
      dheat=0.
      do 90 m=1,nn
            deltacsi(m)=x(m)-cg(m,node)
            cg(m,node)=x(m)
            heat=heat+deltah(m)*rate(m)
            dheat=dheat+deltah(m)*dratedts(m)
            rate1(m,node)=rate(m)
90    continue
      heatsum(node)=ax*heat
      dheatdts(node)=ax*dheat
      return
      end
c-----------------------------------------------------------------------
----
      subroutine fcn(i,n,x,f,a,ldfjac)
      implicit real*8(a-h,o-z)
      include 'comblock.i'
      double precision x(*),f(*),a(ldfjac,*)
      real*8 ka(2)/6.699d9,1.392d11/
      real*8 kb(2)/-12556.d0,-14556.d0/
      real*8 kka(4)/65.5d0,2080.d0,3.98d0,4.79d5/
      real*8 kkb(4)/961.d0,361.d0,11611.d0,-3733.d0/
      real*8 k,kk,km(5)
      real*8 csi(5),dcsi(5)
      k(j)=ka(j)*exp(kb(j)/ts)
      dkdts(j)=-kb(j)*k(j)/(ts*ts)
      kk(j)=kka(j)*exp(kkb(j)/ts)
      dkkdts(j)=-kkb(j)*kk(j)/(ts*ts)
      d(j,t)=2.745d-4*(t/sqrt(tc(j)*air_tc))**1.823*
     &      (pc(j)*air_pc)**(1./3.)*(tc(j)*air_tc)**(5./12.)*
     &      sqrt(1./xmolw(j)+1./air_mw)*(patm/press)  ! diffusion
coef (cm2/s), BSL pg 505
      data csi(5)/5.d-4/
      data patm/0.101d0/
c atmospheric pressure in MPa (N/mm^2) to be consistent with input
variable PRESS
      csi(5)=cg(5,i) ! set NO mol concentration constant for now
(JCC 2/2/99)
      do 10 m=1,4
            km(m)=sherw*d(m,tga)/dhyd
            coef=rgas*tga*mdot/(km(m)*4.*press*dhyd*dx*air_mw)
            if(coef.lt.0.5) then
                  print *,' nodes too big, coef,m,i',coef,m,i
                  stop
            endif
            dcsi(m)=coef+0.5
            csi(m)=dcsi(m)*x(m)-(dcsi(m)-1.)*cg(m,i-1)
c exponential approach, instead of algebraic mean
```

```
c             coef=km(m)*4.*p*dhyd*dx*air_mw/(rgas*tga*mdot)
c             dcsi(m)=1./(1.-exp(-coef))
c             csi(m)=dcsi(m)*(x(m)-exp(-coef)*cg(m,i-1))
c
            cs(m,i)=csi(m)
10    continue
      g1term = (1.+kk(1)*csi(1)+kk(2)*csi(2))**2
      g2term = (1.+kk(3)*(csi(1)*csi(2))**2)*(1.+kk(4)*csi(5)**0.7)
      gterm = ts*g1term*g2term
      nfun=nfun+1
      rate(1)=k(1)*csi(1)*csi(4)/gterm
      f(1)=-(ax*rate(1)+eps*mdot/(dhyd**2*air_mw*dx)*(x(1)-cg(1,i-
1)))
      rate(2)=k(2)*csi(2)*csi(4)/gterm
      f(2)=-(ax*rate(2)+eps*mdot/(dhyd**2*air_mw*dx)*(x(2)-cg(2,i-
1)))
      rate(3)=k(1)*csi(3)*csi(4)/gterm
      f(3)=-(ax*rate(3)+eps*mdot/(dhyd**2*air_mw*dx)*(x(3)-cg(3,i-
1)))
      rate(4)=0.5*(rate(1)+9.*rate(2)+rate(3))
      f(4)=-(ax*rate(4)+eps*mdot/(dhyd**2*air_mw*dx)*(x(4)-cg(4,i-
1)))
      if(ts.ge.1650.)print *,' surface temp>1650, NO oxidation not
done'
              rate(5) = 0.0
c        endif
      dg1tdc1=2.*(1.+kk(1)*csi(1)+kk(2)*csi(2))*kk(1)*dcsi(1)

dg2tdc1=(kk(3)*2.*csi(1)*csi(2)**2*dcsi(1))*(1.+kk(4)*csi(5)**0.7)
      dg1tdc2=2.*(1.+kk(1)*csi(1)+kk(2)*csi(2))*kk(2)*dcsi(2)

dg2tdc2=(kk(3)*2.*csi(2)*csi(1)**2*dcsi(2))*(1.+kk(4)*csi(5)**0.7)
      dgtrmdc1 = ts*(g1term*dg2tdc1+g2term*dg1tdc1)
      dgtrmdc2 = ts*(g1term*dg2tdc2+g2term*dg1tdc2)
      dr1dc1=k(1)*csi(4)/gterm*(dcsi(1)-csi(1)*dgtrmdc1/gterm)
      a(1,1)=ax*dr1dc1+eps*mdot/(dhyd*dhyd*air_mw*dx)
      dr1dc2=-k(1)*csi(1)*csi(4)*dgtrmdc2/gterm**2
      a(1,2)=ax*dr1dc2
      a(1,3)=0.d0
      dr1dc4=k(1)*csi(1)*dcsi(4)/gterm
      a(1,4)=ax*dr1dc4
      dr2dc1=-k(2)*csi(2)*csi(4)*dgtrmdc1/gterm**2
      a(2,1)=ax*dr2dc1
      dr2dc2=k(2)*csi(4)/gterm*(dcsi(2)-csi(2)*dgtrmdc2/gterm)
      a(2,2)=ax*dr2dc2+eps*mdot/(dhyd*dhyd*air_mw*dx)
      a(2,3)=0.d0
      dr2dc4=k(2)*csi(2)*dcsi(4)/gterm
      a(2,4)=ax*dr2dc4
      dr3dc1=-k(1)*csi(3)*csi(4)*dgtrmdc1/gterm**2
      a(3,1)=ax*dr3dc1
      dr3dc2=-k(1)*csi(3)*csi(4)*dgtrmdc2/gterm**2
      a(3,2)=ax*dr3dc2
      dr3dc3=k(1)*dcsi(3)*csi(4)/gterm
      a(3,3)=ax*dr3dc3+eps*mdot/(dhyd*dhyd*air_mw*dx)
      dr3dc4=k(1)*csi(3)*dcsi(4)/gterm
```

```
      a(3,4)=ax*dr3dc4
      dr4dc1=0.5*(dr1dc1+9.*dr2dc1+dr3dc1)
      a(4,1)=ax*dr4dc1
      dr4dc2=0.5*(dr1dc2+9.*dr2dc2+dr3dc2)
      a(4,2)=ax*dr4dc2
      dr4dc3=0.5*dr3dc3
      a(4,3)=ax*dr4dc3
      dr4dc4=0.5*(dr1dc4+9.*dr2dc4+dr3dc4)
      a(4,4)=ax*dr4dc4+eps*mdot/(dhyd*dhyd*air_mw*dx)
            dg1dts=2.*(1.+kk(1)*csi(1)+kk(2)*csi(2))*
     &            (dkkdts(1)*csi(1)+dkkdts(2)*csi(2))

dg2dts=(1.+kk(3)*(csi(1)*csi(2))**2)*(dkkdts(4)*csi(5)**0.7)
     &         +
(dkkdts(3)*(csi(1)*csi(2))**2)*(1.+kk(4)*csi(5)**0.7)
            dgtrmdts=g1term*g2term+ts*(dg1dts*g2term+g1term*dg2dts)
          dratedts(1)=(dkdts(1)-
k(1)*dgtrmdts/gterm)*csi(1)*csi(4)/gterm
          dratedts(2)=(dkdts(2)-
k(2)*dgtrmdts/gterm)*csi(2)*csi(4)/gterm
          dratedts(3)=(dkdts(1)-
k(1)*dgtrmdts/gterm)*csi(3)*csi(4)/gterm
            dratedts(4)=0.5*(dratedts(1)+9.*dratedts(2)+dratedts(3))
        return
        end
c-----------------------------------------------------------------------
----
      block data
      implicit real*8 (a-h,o-z)
      common/intdata/deltah(5),ygin(5)
      common/constant/rgas,sigma
      common/critparm/ tc(5),pc(5),xmolw(5),air_mw,air_tc,air_pc
      common/jacob1/dratedts(5),nfun
c  1=CO, 2=C3H6, 3=H2, 4=O2, 5=NO
      data tc/133.d0,365.d0,33.3d0,154.4d0,180.d0/ ! critical temps
(K)
      data pc/34.5d0,45.5d0,12.8d0,49.7d0,64.d0/ ! critical
pressures (atm)
      data xmolw/28.01d0,42.d0,2.016,32.d0,30.01d0/ ! molecular
weights
      data air_mw/28.97d0/,air_tc/132.d0/,air_pc/36.4d0/ ! air
critical parms
      data rgas/8.314d0/ ! ideal gas constant, (J/g-mole K)
      data sigma/5.669d-12/     ! Stefan-Boltzman const, W/(cm^2
K^4)
cfxt      data deltah/2.832d5,1.928d6,2.42d5,0.,0./ ! heats of
formation (J/g-mol)
      data nfun/0/
      end
```

A.4 Linpack

Linpack is a group of subroutines that come along with the Livermore solver. It contains a list of common subroutines that is used by solvers and is publicly available. Subroutines include dgefa which factors the matrix for double precision Gaussian elimination. Dges solves the double precision system and dgbfa factors a double precision band matrix by elimination. All these subroutines are used by the Livermore solver. Linpack also has the LSODE.f which is the Livermore solver. The code has not been added here as it is too big and is also available in the internet.

```
c Linpack subroutines
dgefa,dgesl,dgbfa,dgbsl,daxpy,dscal,idamax,&ddot  JCC 12/2/98
      subroutine dgefa(a,lda,n,ipvt,info)
      integer lda,n,ipvt(n),info
      double precision a(lda,n)
      info = 0
      nm1 = n - 1
      if (nm1 .lt. 1) go to 70
      do 60 k = 1, nm1
         kp1 = k + 1
         l = idamax(n-k+1,a(k,k),1) + k - 1
         ipvt(k) = l

         if (a(l,k) .eq. 0.0d0) go to 40

            if (l .eq. k) go to 10
               t = a(l,k)
               a(l,k) = a(k,k)
               a(k,k) = t
   10       continue

            t = -1.0d0/a(k,k)
            call dscal(n-k,t,a(k+1,k),1)

            do 30 j = kp1, n
               t = a(l,j)
               if (l .eq. k) go to 20
                  a(l,j) = a(k,j)
                  a(k,j) = t
   20          continue
               call daxpy(n-k,t,a(k+1,k),1,a(k+1,j),1)
   30       continue
         go to 50
   40    continue
            info = k
```

```
   50    continue
   60 continue
   70 continue
      ipvt(n) = n
      if (a(n,n) .eq. 0.0d0) info = n
      return
      end
c-----------------------------------------------------------------------
----
      subroutine dgesl(a,lda,n,ipvt,b,job)
      integer lda,n,ipvt(n),job
      double precision a(lda,n),b(n)
      double precision ddot,t
      integer k,kb,l,nm1
c
      nm1 = n - 1
      if (job .ne. 0) go to 50
         if (nm1 .lt. 1) go to 30
         do 20 k = 1, nm1
            l = ipvt(k)
            t = b(l)
            if (l .eq. k) go to 10
               b(l) = b(k)
               b(k) = t
   10       continue
            call daxpy(n-k,t,a(k+1,k),1,b(k+1),1)
   20    continue
   30    continue
         do 40 kb = 1, n
            k = n + 1 - kb
            b(k) = b(k)/a(k,k)
            t = -b(k)
            call daxpy(k-1,t,a(1,k),1,b(1),1)
   40    continue
      go to 100
   50 continue

         do 60 k = 1, n
            t = ddot(k-1,a(1,k),1,b(1),1)
            b(k) = (b(k) - t)/a(k,k)
   60    continue

         if (nm1 .lt. 1) go to 90
         do 80 kb = 1, nm1
            k = n - kb
            b(k) = b(k) + ddot(n-k,a(k+1,k),1,b(k+1),1)
            l = ipvt(k)
            if (l .eq. k) go to 70
               t = b(l)
               b(l) = b(k)
               b(k) = t
   70       continue
   80    continue
   90    continue
  100 continue
```

```
      return
      end
c-----------------------------------------------------------------------
----
      subroutine dgbfa(abd,lda,n,ml,mu,ipvt,info)
      integer lda,n,ml,mu,ipvt(n),info
      double precision abd(lda,n)
      j0 = mu + 2
      j1 = min0(n,m) - 1
      if (j1 .lt. j0) go to 30
      do 20 jz = j0, j1
         i0 = m + 1 - jz
         do 10 i = i0, ml
            abd(i,jz) = 0.0d0
   10    continue
   20 continue
   30 continue
      jz = j1
      ju = 0

      nm1 = n - 1
      if (nm1 .lt. 1) go to 130
      do 120 k = 1, nm1
         kp1 = k + 1

         jz = jz + 1
         if (jz .gt. n) go to 50
         if (ml .lt. 1) go to 50
            do 40 i = 1, ml
               abd(i,jz) = 0.0d0
   40       continue
   50    continue
         lm = min0(ml,n-k)
         l = idamax(lm+1,abd(m,k),1) + m - 1
         ipvt(k) = l + k - m

         if (abd(l,k) .eq. 0.0d0) go to 100
            if (l .eq. m) go to 60
               t = abd(l,k)
               abd(l,k) = abd(m,k)
               abd(m,k) = t
   60       continue

            t = -1.0d0/abd(m,k)
            call dscal(lm,t,abd(m+1,k),1)
            ju = min0(max0(ju,mu+ipvt(k)),n)
            mm = m
            if (ju .lt. kp1) go to 90
            do 80 j = kp1, ju
               l = l - 1
               mm = mm - 1
               t = abd(l,j)
               if (l .eq. mm) go to 70
                  abd(l,j) = abd(mm,j)
                  abd(mm,j) = t
```

```
   70          continue
               call daxpy(lm,t,abd(m+1,k),1,abd(mm+1,j),1)
   80       continue
   90       continue
         go to 110
  100    continue
            info = k
  110    continue
  120 continue
  130 continue
      ipvt(n) = n
      if (abd(m,n) .eq. 0.0d0) info = n
      return
      end
         if (ml .eq. 0) go to 30
         if (nm1 .lt. 1) go to 30
            do 20 k = 1, nm1
               lm = min0(ml,n-k)
               l = ipvt(k)
               t = b(l)
               if (l .eq. k) go to 10
                  b(l) = b(k)
                  b(k) = t
   10          continue
               call daxpy(lm,t,abd(m+1,k),1,b(k+1),1)
   20       continue
   30    continue
c
c        now solve  u*x = y
c
         do 40 kb = 1, n
            k = n + 1 - kb
            b(k) = b(k)/abd(m,k)
            lm = min0(k,m) - 1
            la = m - lm
            lb = k - lm
            t = -b(k)
            call daxpy(lm,t,abd(la,k),1,b(lb),1)
   40    continue
      go to 100
   50 continue
         do 60 k = 1, n
            lm = min0(k,m) - 1
            la = m - lm
            lb = k - lm
            t = ddot(lm,abd(la,k),1,b(lb),1)
            b(k) = (b(k) - t)/abd(m,k)
   60    continue

         if (ml .eq. 0) go to 90
         if (nm1 .lt. 1) go to 90
            do 80 kb = 1, nm1
               k = n - kb
               lm = min0(ml,n-k)
               b(k) = b(k) + ddot(lm,abd(m+1,k),1,b(k+1),1)
```

```
               l = ipvt(k)
               if (l .eq. k) go to 70
                  t = b(l)
                  b(l) = b(k)
                  b(k) = t
   70          continue
   80       continue
   90    continue
  100 continue
      return
      end
      DOUBLE PRECISION FUNCTION D1MACH(I)
      INTEGER I
      INTEGER SMALL(2)
      INTEGER LARGE(2)
      INTEGER RIGHT(2)
      INTEGER DIVER(2)
      INTEGER LOG10(2)
      INTEGER SC, CRAY1(38), J
      COMMON /D9MACH/ CRAY1
      SAVE SMALL, LARGE, RIGHT, DIVER, LOG10, SC
      DOUBLE PRECISION DMACH(5)
      EQUIVALENCE (DMACH(1),SMALL(1))
      EQUIVALENCE (DMACH(2),LARGE(1))
      EQUIVALENCE (DMACH(3),RIGHT(1))
      EQUIVALENCE (DMACH(4),DIVER(1))
      EQUIVALENCE (DMACH(5),LOG10(1))
      IF (DMACH(4) .GE. 1.0D0) STOP 778
      IF (I .LT. 1 .OR. I .GT. 5) THEN
         WRITE(*,*) 'D1MACH(I): I =',I,' is out of bounds.'
         STOP
         END IF
      D1MACH = DMACH(I)
      RETURN
 9000 FORMAT(/' Adjust D1MACH by uncommenting data statements'/
     *' appropriate for your machine.')
* /* ANSI C source for D1MACH -- remove the * in column 1 */
*#include <stdio.h>
*#include <float.h>
*#include <math.h>
*double d1mach_(long *i)
*{
*     switch(*i){
*       case 1: return DBL_MIN;
*       case 2: return DBL_MAX;
*       case 3: return DBL_EPSILON/FLT_RADIX;
*       case 4: return DBL_EPSILON;
*       case 5: return log10(FLT_RADIX);
*       }
*     fprintf(stderr, "invalid argument: d1mach(%ld)\n", *i);
*     exit(1); return 0; /* for compilers that complain of missing
return values */
*}
      END
```

Vita

Barath Raghavan was born on February 3, 1982 in Tamil Nadu, India. He graduated from University of Madras with a Bachelors in Automobile engineering in 2003. He then attended University of Tennessee, Knoxville and graduated with a masters degree in Mechanical Engineering with an emphasis on thermal science.